

Aus dem Institut für Radiation Medicine
Helmholtz Zentrum München
German Research Center for Environmental Health (GmbH)
Neuherberg, Germany
Vorstand: Prof. Dr. med. Dr. h.c. Matthias H. Tschöp



***Characterization of BeO Optically Stimulated Luminescence
Dosimeters for External and Medical Applications***

Dissertation
zum Erwerb des Doktorgrades der Naturwissenschaften
an der Medizinischen Fakultät der
Ludwig-Maximilians-Universität München

vorgelegt von

Elif Kara

aus

Mersin, Türkei

Jahr

2024

Mit Genehmigung der Medizinischen Fakultät
der Ludwig-Maximilians-Universität München

Betreuer: Prof. Dr. Werner Rühm

Zweitgutachterin: Prof. Dr. Katia Parodi

Dekan: Prof. Dr. med. Thomas Gudermann

Tag der mündlichen Prüfung: 23 Juli 2025

Affidavit



Promotionsbüro
Medizinische Fakultät



Affidavit

Kara, Elif

Surname, first name

Ingolstädter Landstraße 1

Street

85764, Oberschleißheim, Germany

Zip code, town, country

I hereby declare, that the submitted thesis entitled:

Characterization of BeO Optically Stimulated Luminescence Dosimeters for External and Medical Applications

is my own work. I have only used the sources indicated and have not made unauthorised use of services of a third party. Where the work of others has been quoted or reproduced, the source is always given.

I further declare that the dissertation presented here has not been submitted in the same or similar form to any other institution for the purpose of obtaining an academic degree.

Munich, Germany – 08.09.2024

place, date

Elif Kara

Signature doctoral candidate

Table of content

Affidavit	3
Table of content	4
List of abbreviations.....	5
List of publications.....	6
1. Your contribution to the publications	7
1.1 Contribution to publication I	7
1.2 Contribution to publication II	7
1.3 Contribution to Appendix A.....	7
2. Introduction.....	8
2.1 Luminescence dosimetry	10
2.1.1 Theory of luminescence	10
2.1.2 The band model	11
2.2 Thermoluminescence	13
2.3 Optically stimulated luminescence	15
2.4 Optically stimulated luminescence dosimetry	17
2.5 Challenges in BeO for OSL dosimetry	20
3. Materials and Methods.....	23
3.1 BeO dosimeters.....	23
3.2 The Risoe reader.....	23
3.2.1 Stimulation and detection	24
3.2.2 Irradiation source.....	25
3.3 External irradiation sources	26
4. Major results of this thesis	28
4.1 Publication I	28
4.2 Publication II	30
5. Summary (in English)	32
6. Zusammenfassung (Deutsch)	34
7. Publication I	37
8. Publication II	46
References	58
Appendix A: CT Application	64
Acknowledgements	69
Curriculum vitae	71

List of abbreviations

Al ₂ O ₃ :C	Carbon-doped Aluminum Oxide
CB	Conduction Band
BeO	Beryllium Oxide
DT	Deep Trap
HMGU	Helmholtz Zentrum München
LED	Light Emitting Diode
LiF	Lithium Fluoride
LM-OSL	Linearly Modulated Optically Stimulated Luminescence
MDT	Main Dosimetric Trap
POSL	Pulsed Optically Stimulated Luminescence
RC	Radiative Recombination Center
OSL	Optically Stimulated Luminescence
OSLDs	Optically Stimulated Luminescence Dosimeters
PMT	Photomultiplier Tube
ST	Shallow Trap
TL	Thermoluminescence
TLDs	Thermoluminescent Dosimeters
VB	Valence Band

List of publications

Publication I – Radiation Measurements, 2023

Elif Kara, Clemens Woda. *Further characterization of BeO detectors for applications in external and medical dosimetry*, 10.1016/j.radmeas.2023.106950.

Publication II – Radiation Measurements, 2023

Elif Kara, Clemens Woda. *Correlation between thermoluminescence and optically stimulated luminescence signal in BeO*. 10.1016/j.radmeas.2023.107049

1. Your contribution to the publications

This dissertation focuses on examining the properties of Beryllium Oxide (BeO) dosimeters as optically stimulated luminescence dosimeters (OSLDs).

The first publication involves characterizing the dosimeter's luminescence properties through the utilization of the OSL technique for medical and external applications.

In the second publication, the dosimeter's luminescence mechanism was investigated by analyzing the bleaching properties of its thermoluminescence (TL) signal.

In the appendix A, use of BeO OSL dosimeters in a clinical setting is described where organ doses were measured in total CT body scans and results compared with the commercially available and widely used LiF: Mg,Ti TL dosimeters.

1.1 Contribution to Publication I

As the first author of Publication I, Elif Kara contributed by conducting a literature search, developing method, designing the study, acquiring data, analyzing and interpreting the findings, as well as preparing figures, writing the manuscript, and overseeing editing and revision processes.

1.2 Contribution to Publication II

As the first author of Publication II, Elif Kara contributed by developing the idea for the publication, designing the study, planning and executing the data analysis, as well as drafting the manuscript, submitting it for publication, and overseeing the revision process.

1.3 Contribution to Appendix A:

Elif Kara conducted measurements with BeO dosimeters and analyzed data derived from BeO OSL dosimeters and from LiF: Mg; Ti TL dosimeters obtained during total CT body scans, and drafted a manuscript in which the BeO OSL results are compared with those obtained from LiF: Mg; Ti TL dosimeters.

(Results shown in the Appendix A have not yet been published at the time of submission of the Ph.D. Thesis.)

2. Introduction

Dosimeters play a crucial role in determining the absorbed dose received by materials or tissues after exposure to ionizing radiation, and they are generally classified into two groups. Active dosimeters provide real-time direct readings of the dose, while passive dosimeters measure and record an individual's exposure to ionizing radiation over a specific period of time. However, the challenge obstructing the usage of active dosimeters such as electronic and pen dosimeters, which are the type of dosimeters often used for medical applications, is not only their bigger size as compared to that of passive dosimeters, but also the appearance of electronic equipment such as cables (which may be a source of irritation, especially for pediatric patients), making it sometimes difficult to use them on patients (Ahmed, 2007; Stabin, 2007). In contrast, passive dosimeters present some advantages in that they are smaller in size, more cost-effective, readily available, and widely used (Dhanekar and Rangra, 2021).

Passive solid-state dosimeters are extensively employed for dose monitoring, and they can be categorized into thermoluminescence dosimeters (TLDs) and optically stimulated luminescence dosimeters (OSLDs) based on the readout technique. Both of these techniques hold promise for dose monitoring in medical dosimetry. While TLDs are commonly utilized, optical readout offers distinct advantages over thermal readout. OSL readers allow for faster readout times, are more flexible and easier to be automated than TL readers (Akselrod et al., 2006; Olko, 2010; W. S. McKeever, 2002). However, the limited availability of suitable materials currently restricts the widespread adoption of the OSL technique (Akselrod et al., 2006; McKeever, 2002; W. S. McKeever and Moscovitch, 2003).

Carbon-doped Aluminum Oxide ($\text{Al}_2\text{O}_3\text{:C}$) and Beryllium Oxide (BeO) are commonly used types of OSL dosimeters (Kara and Woda, 2023a), due to their appropriate dosimetric characteristics. Although $\text{Al}_2\text{O}_3\text{:C}$ is known for its comparatively high effective atomic number ($Z_{\text{eff}} \approx 11.28$) in relation to soft tissue, extensive literature exists on its characterization and medical applications (Mrčela et al., 2011). On the other hand, the effective atomic number of BeO dosimeters ($Z_{\text{eff}} \approx 7.22$) closely matches to soft tissue ($Z_{\text{eff}} \approx 7.65$) and is highly attractive for medical use (Kara and Woda, 2023a, Trindade et al., 2018; Bos, 2001; Malthez et al., 2014).

Given the limited number of luminescence dosimeters that are tissue-equivalent with sensitivity to both direct and scattered ionizing radiation comparable to that of human tissue, together with the demonstrated promising luminescence properties of BeO OSL dosimeters, it is evident that these dosimeters may provide advantages in medical applications, particularly in clinical and radiation therapy applications. However, further research is needed to investigate the suitability of BeO OSLDs especially in such medical settings, elucidate their potential advantages, and facilitate their routine dosimetric application. For this, current gaps in understanding their luminescence mechanism must be closed and variations in reading protocols be reduced.

This study has two primary objectives. Firstly, to characterize BeO dosimeters for their suitability in medical dosimetry applications, with a specific focus on a rapid OSL reading protocol (publication I). This characterization involves of annealing and preheating in terms of temperature and time, as well as their effects on fading, energy and angular dependence of the detected signals under controlled laboratory conditions. Moreover, a new measurement protocol for BeO OSL dosimeters developed as part of this thesis, was tested. The testing involved measuring organ doses

in a Computed Tomography (CT) examination chosen as a typical medical setting, using an anthropomorphic phantom (In the Appendix).

Secondly, to gain a more comprehensive understanding of the correlation of OSL and TL signals in BeO (publication II, (Kara and Woda, 2023b)). For this, intensity measurements of R-TL glow peaks were conducted over a range of bleaching durations, at doses up to 100 Gy. Fitting procedures aimed at determining the bleaching decay rates of residual TL curves were then applied to the collected datasets along with their respective OSL decay curves. The applied fitting procedures in (Kara and Woda, 2023b) were based on exponential decay functions, exploring two models — with and without optical attenuation. The decay rates obtained from the bleaching process for each TL peak were then evaluated with the OSL components. The objective of this comparative analysis done by Kara and Woda (2023b) was to study potential correlations between OSL and TL traps. Besides, the discussion on bleaching models for TL signals was thoroughly investigated. Furthermore, the dose response of TL signals and OSL signals following various preheating was compared across a wide dose range by Kara and Woda (2023b). This comparison sought to provide additional support for potential correlations and determine the mechanism that likely accounts for the disparity observed in the step annealing tests. The obtained results were utilized to gain insights into the luminescence mechanism occurring in the BeO material.

2.1 Luminescence Dosimetry

This section provides an overview of the background theory of luminescence, including fundamental definitions and concepts. The aim is to clarify how luminescence occurs in materials exposed to radiation when they are stimulated by both heat and light.

2.1.1 Theory of luminescence

Following (McKeever and Chen, 1997), the luminescence can be described as:

“Luminescence is the emission of light from a material upon absorbing energy from an external source”.

This phenomenon can be categorized according to different mechanisms of initial excitation, including those due to ionizing radiation, chemical reactions or stress (McKeever, 1985; McKeever and Chen, 1997; Nasdala et al., n.d.; Sunta et al., 1997). Table 1 provides an overview of several luminescence phenomena.

Table 1. Luminescence emission types.

Types of luminescence	Excited by the absorption of ...
Photoluminescence	Light
Cathodoluminescence	Electrons
Radioluminescence	Nuclear energy (α , β , γ or χ -rays)
Electroluminescence	Electrical energy
Chemiluminescence	Chemical energy
Bioluminescence	Biochemical energy
Triboluminescence	Mechanical energy
Sonoluminescence	Sound waves

Luminescence, broadly categorized into two types, fluorescence and phosphorescence, is characterized by the unique atomic processes that produce the light (Thomsen, 2004). Fluorescence occurs when light is emitted as a result of an electron returning from an excited state to the ground state (Zhang et al., 2006; Randall and Wilkins, 1945a, 1945b, Thomsen, 2004). The lifetime of the excited state is defined by the delay between the absorption of energy, which results in an excited state, and the subsequent emission of light. Phosphorescence is a light emission that occurs after a delay, caused by an electron transition from an excited state to a meta-stable state before returning to its initial ground state. In this meta-stable state, relaxation to the ground state is not allowed. External energy is required to release the trapped charges back to the excited state, from where they can return to the ground state (McKinlay, 1981, Thomsen, 2004).

The distinction between fluorescence and phosphorescence is primarily based on the duration of the luminescence process. Unlike fluorescence, where the emission of light occurs predominantly during excitation, phosphorescence continues to emit light even after the excitation source has been removed. Both processes can occur during the excitation period. However, due to the temperature dependence of phosphorescence emission, fluorescence and phosphorescence can be distinguished by utilizing temperature-dependent characteristics (Aitken, 1987; McKeever, 1985). Phosphorescence offers an additional advantage as it can be induced by external energy stimulation in the form of heat or light. Thermoluminescence (TL) occurs when heat serves as the energy source (Kouroukla, 2015). Likewise, when a light source is employed for stimulation, it's termed optically stimulated luminescence (OSL) (Kouroukla, 2015). The present study specifically focused on TL and OSL of BeO material as types of luminescence of interest.

2.1.2 The band model

In a solid crystalline material, characterized by a periodic arrangement of atoms, electrons populate allowed energy states like the discrete energy levels permitted for electrons within individual atoms (Geber-Bergstrand, 2017; Kittel, 2013; Lakshmanan, 2008). The region between these energy bands, known as the band gap, is energetically prohibited, preventing electrons from occupying this space in a perfect crystal.

As depicted in Figure 1a, the valence band represents the lower band of allowed states with E_v denoting the highest energy state within the valence band, while the conduction band is the upper band of allowed states with E_c denoting the lowest possible energy state in the conduction band (Thomsen, 2004). An applied external energy of at least ($E_g = E_c - E_v$), may promote electrons into the conduction band, in this way producing electron-hole pairs. However, these excited electrons in the conduction band remain stable only for a brief duration before losing their energy and undergoing de-excitation back to the valence band.

Crystalline materials can be categorized into three classes: insulators, semiconductors, and conductors, based on the width of their band gap. Insulators possess a relatively large band gap, typically exceeding 2.5 eV ($E_v \ll E_c$), which impedes thermally induced electron transitions to the conduction band at room temperature. In contrast, conductors exhibit overlapping valence and conduction bands ($E_v = E_c$), allowing electrons to move freely across the material. Semiconductors fall between insulators and conductors, with a band gap ($E_v < E_c$) representing the energy difference between the valence and conduction bands. Electrons can transition from the valence to the conduction band upon appropriate external energy application, if energy exceeds the band gap. The Fermi level (E_f) resides midway between E_v and E_c , providing a reference point for electron energy levels within the material. Luminescent materials are classified as insulators.

In the ideal crystal lattice of an insulator, the probability of an electron transitioning from the valence to the conduction band without any external energy is negligible. In the case of the interaction of ionizing radiation with matter, energy is transferred. This energy transfer can result in an electron acquiring enough energy ($\geq E_g$) to move from the valence to the conduction band, generating charge carriers known as electron-hole pairs (Thomsen, 2004). After becoming excited, the electron remains within the conduction band for approximately 10 nanoseconds, which is its average lifetime, then recombines with a hole. Energy is emitted as a result of this process in the form of either light (known as radiative recombination) or heat (referred to as non-radiative recombination) (Thomsen, 2004).

However, the structure of crystalline materials is not perfect. Rather, they exhibit inherent defects that can be categorized as intrinsic or extrinsic. Intrinsic defects arise within the crystal lattice and can manifest themselves as vacancies (missing atoms), interstitials (extra atoms occupying interstitial positions between regular lattice sites), or other types of dislocations. Extrinsic defects, on the other hand, result from the presence of impurities, where foreign atoms replace original atoms in the crystal structure (A. M. Stoneham, 2001). For instance, in BeO, impurities such as Mg, Ca, B, Al, and Si may be present, which can act as electron traps during irradiation (Becker et al., 1970; Watanabe et al., 2010). These defects and impurity atoms, capable of creating localized energy states within the forbidden band gap, can also capture a charge carrier (electron or hole) and re-emit it back to the band from where it originated (Thomsen, 2004). They can be classified as trap centers (T and H in Figure 1a). If such an energy state captures charges of opposite signs, resulting in electron-hole recombination, it is denoted as a recombination center (RC) (Bos, 2006; Horowitz, 2014).

When ionizing radiation is applied, electrons can become trapped within electron traps with energy levels above the Fermi level, and an equal number of holes can be trapped in hole traps below the Fermi level (Figure 1b). These traps can be classified as shallow (ST), main dosimetric (MDT) and deep (DT) traps, depending on the energetic depth below the conduction band (Figure 1c). External energy is necessary to release trapped electrons back into the conduction band. A trap is termed a shallow trap when lattice vibrations in the crystal at room temperature are sufficient to release the trapped electrons into the conduction band, typically occurring within hours after irradiation. However, for dosimetry applications, traps need to be deep enough to store the dosimetric information until sufficient external energy, as heat or light, is provided for readout. Electrons trapped in the main dosimetric trap are released through either thermal or optical stimulation. For electrons trapped in deep traps, achievable readout temperatures or modes of optical stimulation do not provide sufficient energy for detrapping, thus these charge carriers remain localized once captured. During stimulation of irradiated material either by heat or light, electrons can be liberated and undergo recombination with a hole at a recombination center (Figure 1c). Luminescence light is emitted when recombination occurs radiatively (McKeever and Chen, 1997). This emitted light can be detected using a photomultiplier tube (PMT). The intensity of this detected light can be linked to the quantity of trapped charges within the crystal, which corresponds to the absorbed dose in the material. This property allows the material to be utilized as a dosimeter (G Scarpa, 1970; Mandeville and Albrecht, 1954, Geber-Bergstrand, 2017).

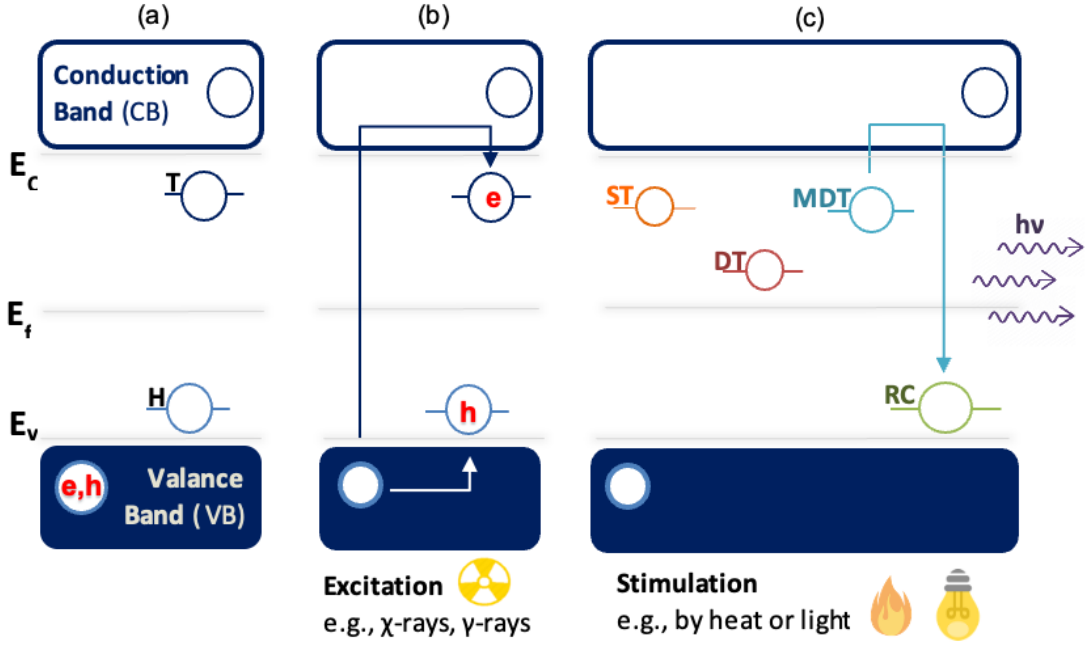


Figure 1. Band model illustrating the TL/OSL process. Before the excitation (a), ionizing radiation excites charges to move to traps, then are trapped and stable (b). Possible charges transfers producing luminescence during stimulation (c).

(e: electron, h: hole, H: hole trap, T: electron trap, ST: shallow trap, MDT: main dosimetric trap, DT: deep trap, and RC: recombination center)

2.2 Thermoluminescence

To stimulate the trapped electrons into the conduction band, a sample is subjected to linear heating from room temperature to a specific elevated temperature, such as 500 °C. During this process, the emitted luminescence light is recorded as a function of temperature, which is referred to as thermoluminescence (TL) (Murthy, 2013). The TL signal is represented by a graph known as the TL glow curve, which can exhibit a single or a series of peaks at different temperatures depending on the material. These peaks correspond to traps at different trap depths present in the sample.

The Boltzmann factor describes the probability (p) of releasing an electron from a trap (Geber-Bergstrand, 2017):

$$p = s \cdot e^{-\frac{\Delta E}{kT}} \quad (1)$$

Where s is the frequency factor (s^{-1}), ΔE is the energy depth of the trap (eV), k is the Boltzmann constant (eV/K), and T is the absolute temperature (K) (Choi J.H. et al., 2006).

Upon elevating the temperature, the intensity of luminescence exhibits an increment until reaching a maximum, after which it begins to decline as the trapped charges are depleted. Due to the presence of various trap types in different energy levels within real crystals, the TL glow curve comprises multiple peaks, each corresponding to distinct trap types. Electrons trapped in deep traps have longer lifetimes compared to those trapped in shallow traps. It should be noted that shallow traps are typically regarded as unstable at ambient temperatures and therefore deemed unsuitable for dosimetry purposes.

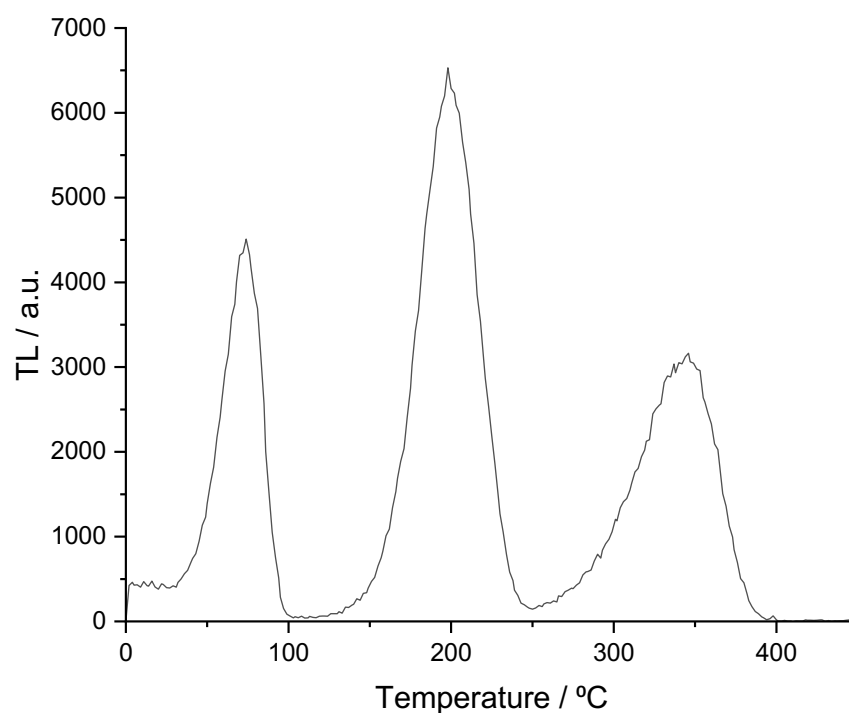


Figure 2. Thermoluminescence (TL) glow curve of a BeO dosimeter irradiated with a beta dose of 40 mGy; heating rate: 5 °C.s⁻¹; a.u. – arbitrary units.

BeO is defined with three TL peaks in its glow curve, with in the temperature range of 50-120 °C for peak 1, 150-260 °C for peak 2, and 260-400 °C for peak 3; see Figure 2 (Jahn et al., 2013; Sommer et al., 2008, 2007; Sommer and Henniger, 2006; Yukihiro et al., 2016; Kara and Woda, 2023b; Kara and Woda, 2023a). Such TL measurements were performed as part of the studies described in Publications I and II.

2.3 Optically Stimulated Luminescence

In Optically Stimulated Luminescence (OSL), trapped electrons are stimulated using light within the wavelength range from 400 nm to 700 nm. Optical stimulation offers greater flexibility compared to TL stimulation. Various modes of optical stimulation can be utilized, including continuous wave (CW-OSL), linearly modulated (LM-OSL), and pulsed OSL (POSL) (Geber-Bergstrand, 2017). Among these, CW-OSL is the most commonly employed mode in routine OSL dosimetry. In CW-OSL, the stimulation light maintains a constant intensity, and the emitted light is continuously recorded during the entire stimulation process (Kouroukla 2015; Bøtter-Jensen, 1997; Bulur, 1996; Bulur and Saraç, 2013).

The luminescence signal obtained during OSL stimulation follows an exponential decay pattern that is termed as a decay curve. In LM-OSL, the stimulation light intensity gradually rises to peak level, revealing different traps with distinct photoionization cross-sections at different time intervals, like a TL glow curve (Kouroukla 2015; Bulur, 1996). In POSL, luminescence is measured between the stimulation pulses, enabling measurements without the need for optical filters (Bøtter-Jensen, 1997; Eduardo G Yukihara, 2011; McKeever and Akselrod, 1999). For Publications I and II, only CW-OSL was employed, thus LM-OSL and POSL will not be further elucidated in this context. Figure 3 depicts a typical CW-OSL curve obtained for BeO dosimeters.

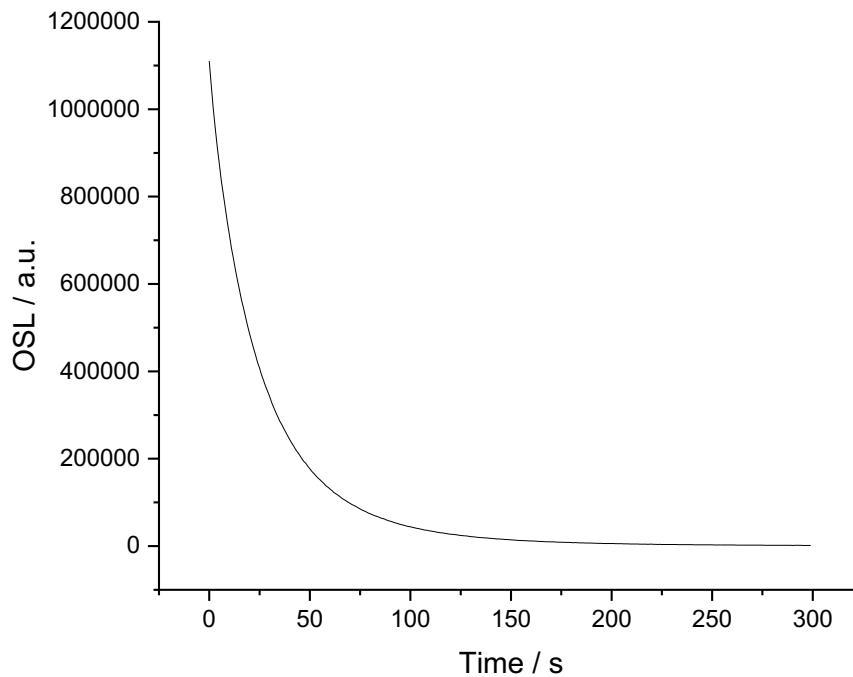


Figure 3. Optically stimulated luminescence (OSL) decay curve of BeO dosimeter irradiated with beta dose of 40 mGy; a.u. – arbitrary units.

The shape of the CW-OSL decay curve can be different depending on the material, stimulation light, and readout temperature. The simplest form of an OSL decay curve can be derived using a fundamental model, consisting of one trap and one radiative recombination center (McKeever, 2001).

When stimulating in CW-mode, the de-trapping rate of electrons decreases with stimulation time. The probability (p) of this process is defined by the product of stimulation intensity (photon fluence rate; Φ , $\text{m}^{-2}\text{s}^{-1}$) and photoionization crosssection (σ , m^2) (Geber-Bergstrand, 2017):

$$p = \Phi \cdot \sigma \quad (2)$$

After the end of irradiation and before the start of optical stimulation, the number of trapped electrons at the electron trap must be equal to the number of trapped holes at the hole trap ($n_0 = m_0$), due to conservation of charge. Therefore, charge flow during stimulation can be described by the following rate equations,

$$\frac{dn_c}{dt} = -\frac{dn}{dt} + \frac{dm}{dt} \quad (3)$$

$$I_{OSL} = -\frac{dm}{dt} = -\frac{dn}{dt} = np \quad (4)$$

where, I_{OSL} is the intensity of luminescence light and n_c represents the number of electrons in the conduction band, n is the number of trapped electrons, m is the number of the trapped holes (Geber-Bergstrand, 2017). Assuming the quasi-equilibrium condition and charge neutrality, the solution of the rate equations (equations 3 and 4) is,

$$I_{OSL} = n_0 p \cdot e^{-tp} = I_0 \cdot e^{-t/\tau} \quad (5)$$

where, I_0 is the initial OSL intensity and $\tau = \frac{1}{p}$ is the decay constant (s) (Geber-Bergstrand, 2017).

When accounting for multiple active traps (denoted as $i = 1, \dots, w$), the OSL intensity can be expressed as the cumulative sum of several exponential components.

$$I_{OSL} = \sum_{i=1}^w I_{i0} \cdot e^{-t/\tau_i} \quad (6)$$

The absorbed dose of a material can be correlated with the integral of its OSL curve. The selection of an optimal integration interval plays a crucial role in the analysis of the OSL signal. It should be noted that if the entire OSL signal is integrated, this intensity then remains independent of the stimulation power utilized.

2.4 Optically Stimulated Luminescence Dosimetry

The observation of luminescence from a diamond upon heating was initially reported by Sir Robert Boyle in the 1660s and later termed thermoluminescence (TL). TL dosimetry is based on the thermal stimulation of a dosimeter to release luminescent light proportional to the absorbed dose from an external source (Bilski et al., 2014). Optical stimulation luminescence (OSL) is a similar process that utilizes optical energy to stimulate the dosimeter (Bøtter-Jensen, 1997).

One significant advantage of optical readout, compared to thermal readouts, is the increased sensitivity of the OSL signal, particularly if the luminescence efficiency is temperature-dependent, a phenomenon known as "thermal quenching" (W. S. McKeever and Moscovitch, 2003). The OSL technique allows for partial and faster readouts of the absorbed dose using short light pulses, enabling multiple measurements. Additionally, using light sources (LEDs, laser, or lamp) for stimulation offers the flexibility and ease of control of portable OSL readers. However, the limited availability of suitable OSL materials has restricted the widespread adoption of this technique (Yukihara et al., 2014, 2010; Yukihara and McKeever, 2008).

Dosimeter materials intended for clinical applications must fulfill a comprehensive set of essential dosimetric properties to ensure accurate and reliable dose estimation (Yukihara and Kron, 2020). Dosimeters from such materials should have high sensitivity to radiation, efficient stimulation, tissue equivalence characterized by a low effective Z-number (Z_{eff}), negligible fading of the absorbed dose until measurement, linear dose response across a wide range, and simple usability (Bos, 2001; Broadhead et al., 2022; Rivera, 2012; Rivera-Montalvo, 2016).

Aluminum oxide ($\text{Al}_2\text{O}_3\text{:C}$) is the most popular OSL dosimeter because of its appropriate characteristics. Initially introduced as a TL dosimeter (Akselrod et al., 1990), it was later proposed as an OSL dosimeter, to take advantage of its light sensitivity (Markey et al., 1995). $\text{Al}_2\text{O}_3\text{:C}$ exhibits advantageous dosimetric properties, including low fading during dark storage (below 5% annually) (Reft, 2009; Akselrod et al., 1990), high reproducibility with reusability, and straightforward readout and bleaching of dose history (Azorin Nieto, 2016). Various commercially available $\text{Al}_2\text{O}_3\text{:C}$ dosimeters, such as Luxel™ and InLight™ dosimeters for personnel dosimetry, and nanoDot™ for clinical dosimetry, are manufactured by Landauer Inc. (Glenwood, IL, USA) (Bøtter-Jensen et al., 2003; Perks et al., 2006).

Tissue-equivalent dosimeters are designed to mimic the radiation response of biological tissue. In general, absorption of energy by tissue depends on factors including effective atomic number, incident photon energy, and mass density of the tissue. Tissues absorb low-energy photons more effectively than high-energy photons. Selecting tissue equivalent dosimeters, particularly in fields like medical imaging and radiation therapy dosimetry applications, is important to ensure precise and reliable dose estimations (Bos, 2001; McKeever, S. W., Moscovitch, M., & Townsend, 1995).

The $\text{Al}_2\text{O}_3\text{:C}$ OSL dosimeter's energy dependence has been presented for different types of radiation (Figure 4). However, they are considered non-tissue equivalent dosimeters, with a higher effective atomic number ($Z_{\text{eff}} \sim 11.28$), which leads to an overresponse to low-energy X-rays in the kilovoltage spectrum as compared to tissue (Kara and Woda, 2023a). It is worth noting that the use of $\text{Al}_2\text{O}_3\text{:C}$ dosimeters for a mixed radiation field, especially containing low-energy photons (< 120 keV), can ultimately result in an overestimation of the absorbed dose. This implies that radiation-quality-specific correction factors have to be introduced. Despite this limitation, $\text{Al}_2\text{O}_3\text{:C}$

dosimeters have been widely used in several dosimetry applications including medical, environmental, space, and retrospective purposes (McKeever, 2004; Yukihiro and McKeever, 2008).

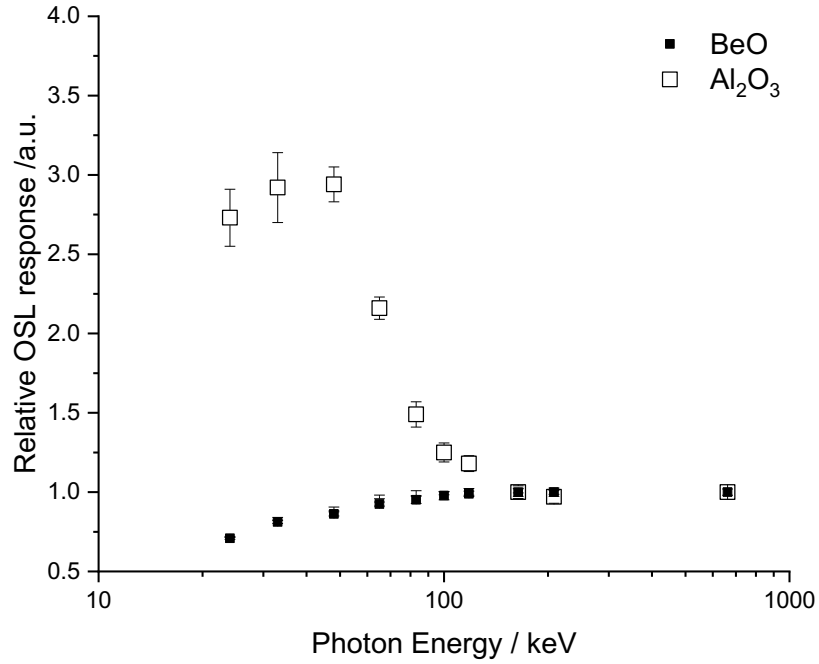


Figure 4. Relative photon energy responses of Al₂O₃:C (Gasparian et al., 2012) and BeO dosimeters (Publication I). Results are presented as the average of measurements and their standard deviation from three different samples for both BeO and Al₂O₃ dosimeters: a.u. – arbitrary units.

BeO has found extensive application in the electronics industry, particularly in metallurgy and nuclear reactors, due to its high thermal conductivity and electrical resistance (G Scarpa, 1970). Its TL properties were initially investigated by Albrecht and Mandeville in 1956. Tochilin et al. (1969) observed the light sensitivity of TL peaks, suggesting the presence of OSL features. Then the first characterization study of the OSL properties of BeO was presented by Bulur and Göksu (1998). Following studies have shown that they have promising dosimetric characteristics (Bulur and Göksu, 1998; Sommer et al., 2007; Sommer and Henniger, 2006; Kara and Woda, 2023a), with a linear dose response of the OSL signal between 5 μ Gy and 10 Gy (Broadhead et al., 2022; Polymeris et al., 2021; Sommer et al., 2007). An initial signal loss in the OSL signal by 6% taken after 30 minutes, as opposed to the OSL measured post-irradiation (Sommer et al., 2008, 2007). After this time period, the further loss in signal was reported to be about 1% over a period of up to six months if stored at ambient temperature (25°C), which makes BeO attractive for dosimetry applications (Bulur and Göksu, 1998; Sommer et al., 2007). In addition, a good reproducibility in the OSL was showed (Jahn et al., 2013; Sommer et al., 2008, 2007; Sommer and Henniger, 2006; Yukihiro et al., 2016).

Following the widespread use of Al₂O₃:C, considerable attention has been shifted towards exploring the potential applications of BeO dosimeters. Due to its effective atomic number ($Z_{\text{eff}}=7.22$) being similar to human soft tissue ($Z_{\text{eff}}=7.65$), BeO dosimeters are valuable in personal, space, environmental and especially in medical dosimetry (Aşlar et al., 2019; Bos, 2001; Mukherjee, 2015; Eduardo G. Yukihiro, 2011). In fact, BeO is currently being considered the most promising OSL material, it is superior to Al₂O₃:C in terms of tissue equivalence and competitive with cost

(Broadhead et al., 2022). BeO dosimeters for OSL applications are already commercially available by manufacturers such as Brush Wellman, Materion Corporation, and Mirion, see Figure 5.

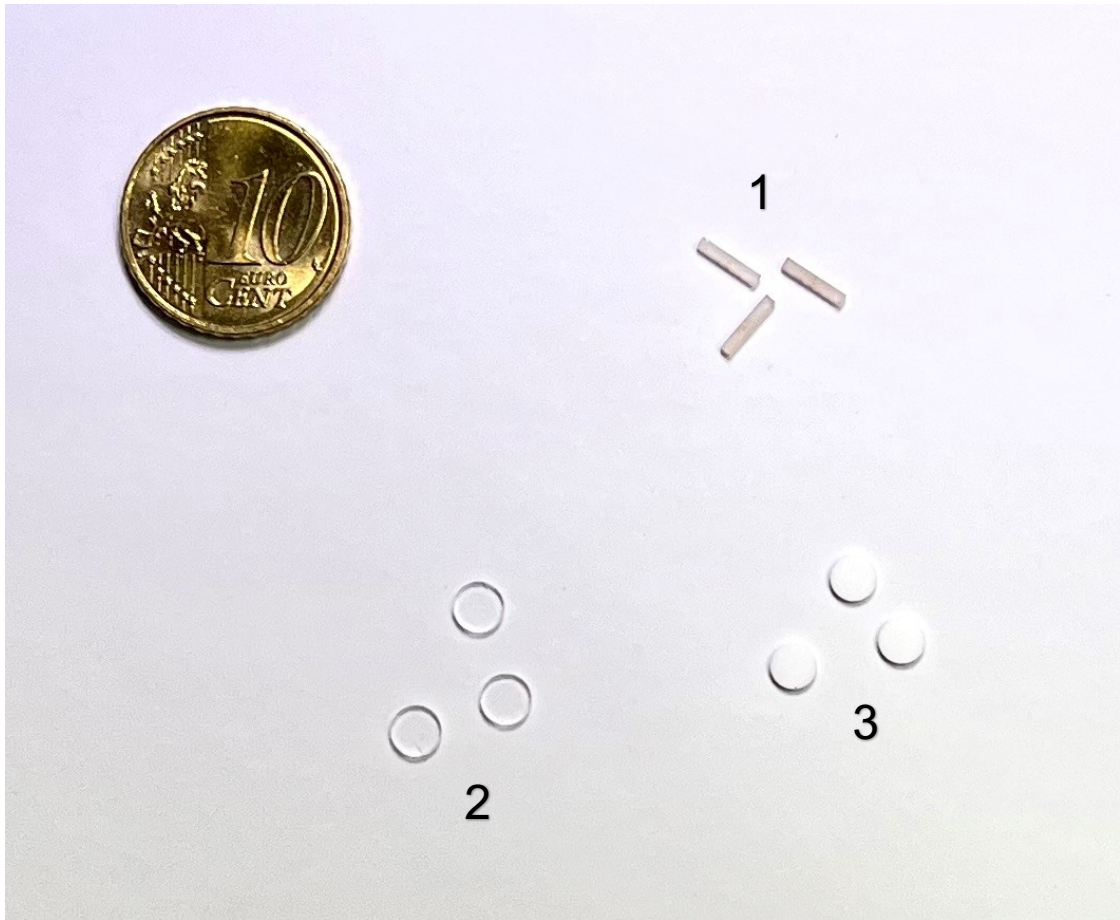


Figure 5. (1) LiF:Mg,Ti TL dosimeter; Thermofisher (in the shape of rods), (2) Al₂O₃:C; Landauer Inc., and (3) BeO;Thermalox TM 995 Brush Wellman OSL dosimeters.

2.5 Challenges in BeO for OSL Dosimetry

Due to its tissue equivalence, there is a growing interest in utilizing BeO as an OSL dosimeter, and its suitability has already been demonstrated in different medical applications. In the context of radiotherapy, BeO dosimeters have been successfully applied in electron beam breast radiotherapy, as demonstrated by Şahin et al. (2020). For brachytherapy, Santos et al. (2015) utilized optical fibers coupled with BeO OSL dosimeters for real-time medical application. In the realm of diagnostic X-ray beams, Rodriguez et al. (2012) conducted organ dose measurements in a clinical setting using BeO dosimeters. Yagui et al. (2020) reported the use of BeO dosimeters in pediatric gastrointestinal fluoroscopy applications. Moreover, Aşlar et al. (2020) presented the results of dose assessment in breast imaging. These investigations had the primary objective of demonstrating the utility of BeO as an OSL dosimeter in clinical environment. The outcomes presented that BeO OSL dosimeters exceeded expectations in performance (Kara and Woda, 2023a). However, the adoption of BeO OSLDs in medical dosimetry and recent advancements are still limited compared to $\text{Al}_2\text{O}_3\text{:C}$ OSL dosimeters. Kara and Woda (2023a) emphasized that the studies mentioned above varied in the employed readout protocols and exhibited discrepancies in annealing temperature, stimulation duration, and preheating temperature. Reading parameters, especially annealing and preheating temperatures, are important for dose assessment: Selecting incorrect values for these parameters can adversely affect dose evaluation, leading to inaccuracies. Additionally, any gaps in understanding the luminescence mechanisms in TL and OSL processes may result in missing any trapping centers, potentially reducing the efficiency of dosimeters. Therefore, a standardized reading protocol is indispensable to ensure accuracy, repeatability, and reliable dose assessment. Consequently, the use of BeO dosimeters in dosimetric applications requires further in-depth investigations into its characterization and a deeper understanding of its luminescence mechanisms (Bulur, 2007).

To be more specific, the first challenge is the lack of a systematic characterization of dosimeters to minimize uncertainty in the measured absorbed dose (Kara and Woda, 2023a). Yukihiro et al. (2016) demonstrated that the sensitivity of the BeO dosimeter changes when subjected to successive usage of irradiation and readout. Therefore, suitable annealing in between measurements to restore the radiation response of the material is needed. Moreover, when using the available stimulation power in the Risø TL DA15 readers (approximately $30\text{--}36 \text{ mW.cm}^{-2}$), measurement times ranging from 120 to 300 seconds are needed for full OSL readout of the dosimeter. However, this results in large time durations when reading many detectors in various applications as emphasized by Kara and Woda (2023a). Instead of utilizing the entire OSL signal, dose assessment can be accomplished using only a small fraction of it, resulting in shorter reading times. In principle, it is possible if combined with appropriate subsequent thermal annealing. However, systematic investigations of characterization of dosimeters are yet to be conducted (Kara and Woda, 2023a).

The literature presents varying recommendations on preheat treatment, which was also addressed by (Kara and Woda, 2023a). Sommer and Henninger (2006) demonstrated that the OSL signal fades by approximately 5% during the initial hours following irradiation, and no additional fading was observed during storage periods exceeding 200 days. On the other hand, Yukihiro et al. (2016) observed a rapid OSL component that thermally decayed in just 10 minutes. Bulur and Göksu (1998) recommended a preheating at 125°C for 125 seconds to eliminate the unstable component of the OSL when employing green light for stimulation. In their later work, Bulur and

Yeltik (2010) utilized a preheating at 160°C for 10 seconds for LM-OSL measurements with blue light stimulation, although they did not provide further details as stated by (Kara and Woda, 2023a).

In the studies by Sommer and Henninger (2006) as well as by Sommer et al. (2007), measured energy response of BeO was found to agree with the calculated one, based on mass-energy absorption coefficients. However, Jahn et al. (2014) discovered that for BeO within packaging, measured energy response was considerably lower than what was expected from Monte Carlo simulations. The angular dependence of BeO dosimeters at varying energy levels has not been reported in the literature.

Furthermore, the occurrence of a TL signal induced by room light has been reported in BeO dosimeters, emphasizing the need to protect the dosimeters from light exposure even after thermal cleaning of residual dose, especially for environmental applications at low doses (Crane and Gamble, 1975; Henaish et al., 1979; Yukihiro et al., 2016; Kara and Woda, 2023a). Moreover, Yukihiro et al. (2016) documented the presence of an OSL signal induced by room light. However, the mechanism behind these phenomena has not been explained. Therefore, the establishment of measurement protocols for applications becomes highly challenging.

The second challenge is that a controversy exists regarding the possible association of TL peaks with the OSL signal of BeO dosimeters (Aşlar et al., 2019; Bulur and Göksu, 1998; Bulur and Saraç, 2013; Bulur and Yeltik, 2010; Yukihiro et al., 2016). The correlations between TL and OSL properties of BeO was investigated by using bleaching and step annealing experiments. The results of the bleaching experiments revealed that TL peak 1 and 2 of BeO were strongly influenced by light, while the peak 3 remained relatively unchanged (Altun et al., 2022). This observation suggested that the traps responsible for TL peaks 1 and 2 may also be responsible for the OSL. In contrast, step annealing experiments presented that the OSL signal is unaffected by preheating up to 250 °C. Consequently, it has been proposed that the source of the OSL signal may originate solely from traps responsible for TL peak 3 (located around 340 °C) (Bulur and Göksu, 1998; Bulur and Yeltik, 2010; Yukihiro, 2011). Furthermore, Bulur and Saraç (2013) and Aşlar et al. (2019) observed an OSL signal that potentially correlates with TL peak 2 at higher doses using step-annealing experiments.

Another issue is understanding the differences and similarities between TL and OSL emission spectra of BeO. In previous studies, it was reported that the TL emission spectrum of BeO peaks around 335 nm with a shoulder between 400 to 450 nm (McKeever, S. W., Moscovitch, M., & Townsend, 1995). While it was initially assumed that TL and OSL emissions occur in the same region due to the high efficiency of OSL measurements in the UV region below 370 nm (Sommer et al., 2008; Tochilin et al., 1969), recent studies have suggested that OSL emission spectra exhibit two peaks at 370 nm ('brighter') and 310 nm ('weaker') (Bulur and Saraç, 2013; Yukihiro, 2011). These results indicate that the luminescence mechanism possibly involves different TL and OSL emission processes. Still, more studies are needed to clarify the details of the BeO luminescence mechanism and to determine whether these processes are correlated.

The dosimetric characterization of BeO dosimeters and mechanism behind the room-light-induced OSL signal were extensively investigated in Publication I (Kara and Woda, 2023a), and a measurement protocol was established. In Publication II (Kara and Woda, 2023b), the correlation between TL and OSL over the entire dose range is discussed in detail, and optical attenuation is considered in describing the bleaching curves for the two stimulation modes. Besides, the

mechanism behind the luminescence phenomenon in BeO was evaluated according to models defined by (McKeever, 1994). In the Appendix, the developed protocol was tested in a CT examination using an anthropomorphic phantom.

3. Materials and Methods

3.1 BeO Dosimeters

For publication I (Kara and Woda, 2023a), BeO dosimeters (Thermalox TM 995) accessible on the market, which had a 4 mm in diameter and with a thickness about ~0.5 mm were used.

In publication II (Kara and Woda, 2023b), square-shaped BeO dosimeters, supplied by Dosimetrix GmbH (Mirion Technologies GmbH), were employed, with dimensions ~4.7 mm x ~4.7 mm with a thickness around ~0.5 mm.

3.2 The Risø Reader

The Risø TL and OSL reader (Technical University of Denmark, Risø Campus, Roskilde, Denmark) is one of several available OSL reader options (Geber-Bergstrand, 2017) and was employed in this thesis.

All TL and OSL measurements were conducted at the Luminescence Laboratory of the Institute of Radiation Medicine of Helmholtz Munich, utilizing the Risø TL/OSL Luminescence reader (model DA-15) developed at Risø DTU National Laboratory, Denmark, as shown in Figure 6.



Figure 6. Risø TL and OSL luminescence reader (model TL/DA-15), www.nutech.dtu.dk, (Kouroukla, 2015; *Guide to the “Risø TL/OSL reader”*, 2013).

The Risø reader includes different components, including a stimulation unit for thermal and/or optical stimulation, a light detection system (e.g., a photomultiplier tube), and a radioactive source (Kouroukla, 2015; Bøtter-Jensen, 1997; Bøtter-Jensen et al., 2003, 2000; *Guide to the “Risø TL/OSL reader”*, 2013). Figure 7 provides a schematic representation of the reader configuration.

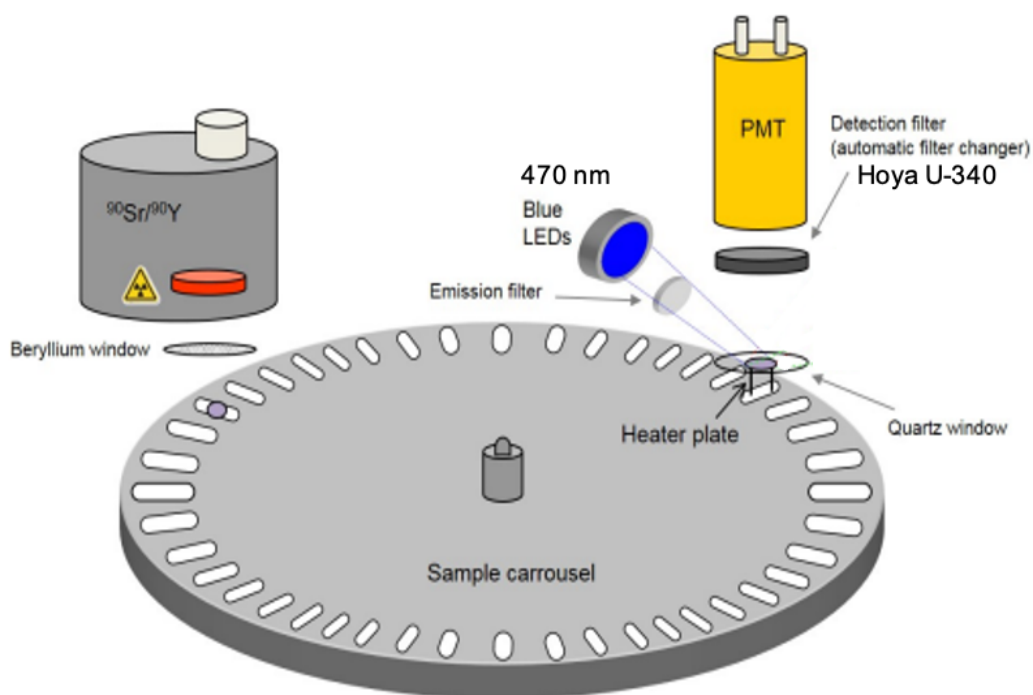


Figure 7. Schematic representation of the Risø TL and OSL reader. (Picture adapted from the “Risø TL/OSL reader”, 2013, www.nutech.dtu.dk).

The Risø reader incorporates a motor-driven rotating carousel capable of holding up to 24 samples, which can be placed in stainless steel or nickel discs with a diameter of 11.65 mm. Once the samples are positioned in the sample chamber, reading parameters can be configured using the sequence program. When performing the read-out process, the samples can be stimulated using either light or heat, within a nitrogen atmosphere. This versatility allows the equipment to function as both an OSL and TL reader.

3.2.1 Stimulation and detection

The Risø reader provides stimulation capabilities through both a heating unit for thermoluminescence measurements and an optical setup including LEDs and filters for optically stimulated luminescence measurements (Geber-Bergstrand, 2017). These functionalities can be employed separately or in conjunction. The heating unit allows samples to be heated up to 700 °C, heating rates are adaptable starting at 0.01 to 10 K.s⁻¹ (Kouroukla, 2015). For OSL stimulation, the reader utilizes blue light emitting diodes (LEDs) emitting light at around 470 nm.

To detect the emitted luminescence light, a 9235QB bialkali photomultiplier tube (PMT) from ET Enterprises is employed along with appropriate optical filters. The PMT has a maximum detection efficiency in the ultraviolet region (200-400 nm). The optical filters function as shields, to block scattered light from reaching the PMT (Geber-Bergstrand, 2017). Different combinations of filters can be used depending on the wavelength of the stimulating light. In this study, a Hoya U-340 (7.5 mm) filter was utilized in luminescence readings. This filter has a transmission range of approximately 250-390 nm. The transmission characteristics of the filter are illustrated in Figure 8.

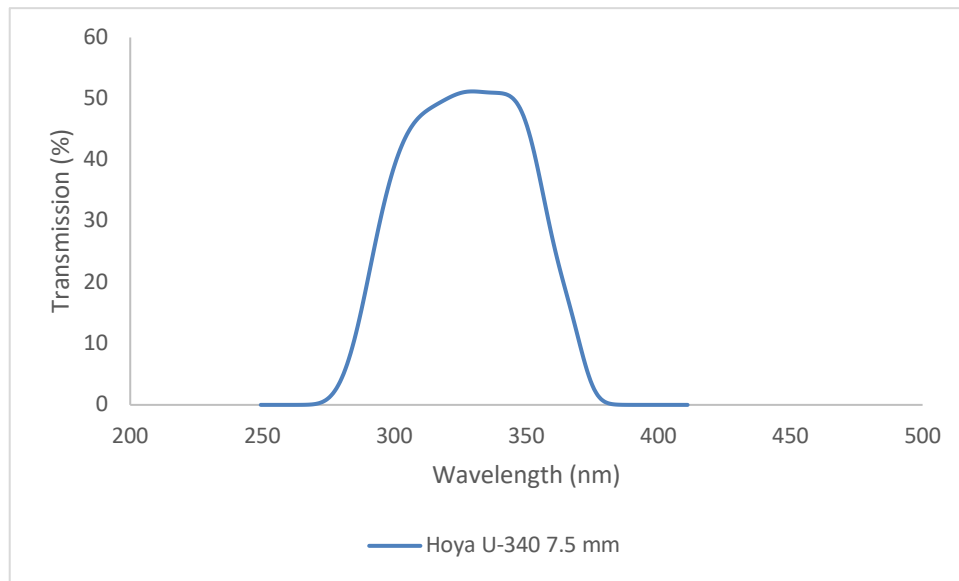


Figure 8. Transmission curve of the Hoya U-340 (7.5 mm) filter accompanying the Risø TL/OSL reader (www.hoyaoptics.com).

3.2.2 Irradiation source

The Risø TL/OSL reader used in this study is equipped with a beta source. A $^{90}\text{Sr}/^{90}\text{Y}$ source is located ~5 mm above the sample emits beta particles, with an activity of 465 MBq (Reference date: 01.06.2023), (Kouroukla, 2015). A beryllium window (0.125 mm) is used as protective barrier to separate the sample chamber from the source (Kouroukla, 2015; Bøtter-Jensen et al., 2003; Guide to the Risø TL/OSL reader, 2013).

The BeO OSL dosimeters used in publications I and II, and in the Appendix, were calibrated in terms of ^{137}Cs at the radiation facilities at Helmholtz Zentrum München (HMGU) in München, Germany.

3.3 External Irradiation Sources

For the dosimetric measurements, various radiation sources including X-rays and gamma rays available at the HMGU radiation facilities were used to irradiate the BeO dosimeters. In Publication I, the energy and angular dependence of the dosimeters were assessed using different X-ray qualities ranging from N30 to N250 (Yxlon MG420 with PTW calibration bench; Figure 9) as well as ^{137}Cs (Buchler Gammakalibrator OB20; Figure 10). For the gamma source, available calibration values for the air kerma rate at a given distance could be used. During calibration process, a polymethyl methacrylate platter (thickness of 3 millimeters) was used as the buildup material. The X-ray source was calibrated individually for each radiation quality at the same irradiation distance using the combination of an ionization chamber and a high precision electrometer, both traceable to the primary standard at the Physikalisch-Technische Bundesanstalt (PTB) in Braunschweig, Germany. The accumulated charge over one-minute intervals was measured in Helmholtz Zentrum München, from which the air kerma rate could be calculated after applying correction factors for radiation quality, ambient air pressure and temperature in Helmholtz Zentrum München (Greiter, Denk, & Hoedlmoser, 2016).

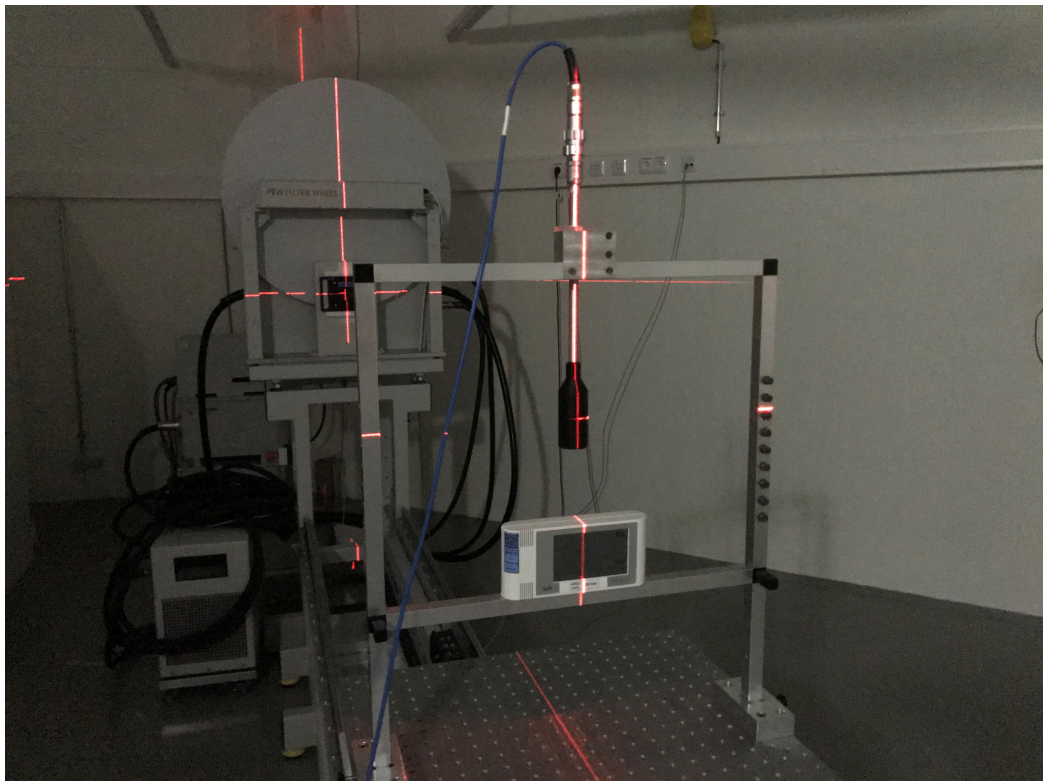


Figure 9. X-ray source MG320 at the Helmholtz Zentrum München (back), with calibration bench. An ionization chamber is mounted for calibration (front), at the same position where the BeO dosimeters were later irradiated. Below the chamber is a precision temperature, humidity and pressure logger (OPUS 20, OTT HydroMet Fellbach GmbH). The laser crosshairs locate the center of the irradiation field.

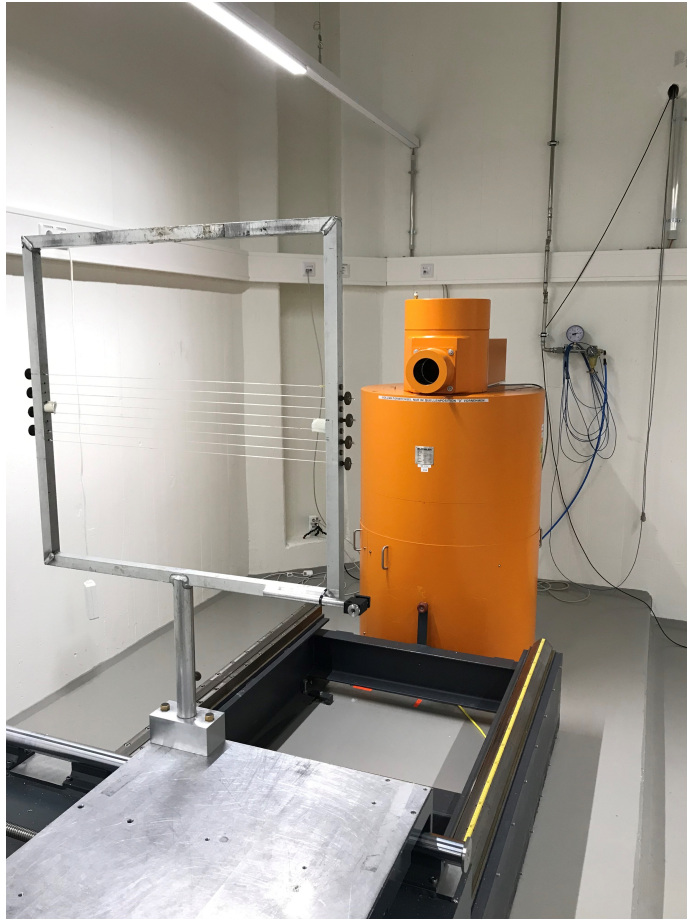


Figure 10. ^{137}Cs gamma source at the Helmholtz Zentrum München. The BeO dosimeter, wrapped in lighttight aluminum foil, can be affixed to the sample harp with adhesive tape.

4. Major results of this thesis

Considering the increasing interest in OSL dosimetry and the promising prospects of BeO dosimeters in medical applications, this thesis aimed to elucidate the dosimetric and luminescence properties of these types of dosimeters and to assess their capability to accurately measure absorbed doses in medical scenarios.

4.1 Publication I

The first publication analyzes the dosimetric characterization of BeO dosimeters by evaluating their performance and reliability when used in the clinical environments, with a particular focus on implementing a fast OSL readout protocol. The dosimetric characterization includes annealing characteristics (temperature and time duration), short-term fading and preheat temperature, stimulation time, energy, and angular dependence to assess the useability of the dosimeters in medical applications. Determining these parameters is important for reliable dose estimation, to ensure accuracy.

To achieve reliable and repeatable dose measurements using luminescence dosimeters multiple times, it is necessary to anneal those dosimeters and, in this way, to delete the dose history from previous exposures. This involves heating the dosimeter to a specific temperature for a set duration, followed by cooling it down to room temperature. The annealing temperature can affect the characteristics of the dosimeter material by influencing crystal defects, while the duration of annealing may be (too) time-consuming during clinical routines, particularly when handling numerous dosimeters. Using annealing temperatures that do not delete the dose history completely can lead to inaccurate results. Hence these parameters (annealing temperature and annealing duration) were investigated.

Fading, characterized by the decrease in luminescence output with time after irradiation, is also crucial for a dosimeter's suitability in clinical dosimetry. The main reason for fading is the presence of electrons within traps of varying depths: Shallow traps, i.e. those with lower energy levels, will fade more rapidly at room temperature compared to deeper traps, owing to the increased likelihood of transition. To prevent significant errors in the dose assessment, it is crucial to account for the influence of fading. The dosimeter can be heated to a specific temperature to remove shallow traps (preheating process) or implementing an appropriate time delay between irradiation and reading can help to overcome the effect of fading. Since insufficient preheating protocols were applied to the dosimeter in previous studies, the fading of OSL signal in short term and an appropriate preheating temperature were evaluated for BeO OSL dosimeters, in the present study.

In previous studies optimization of the optimal optical stimulation time to speed up the measurements has often been overlooked. In principle, this optimization can be established by assessing the gain obtained from dosimetric traps at different reading time intervals, which depends not only on the dosimeter material but also on the light sources employed in the OSL reader.

BeO demonstrates tissue-equivalent properties, a characteristic that is desired for an ideal dosimeter, and especially important when measurements are taken under radiation conditions where the photon energy is difficult to be determined. The photon energy dependence of OSLDs may be influenced by the selection of reading parameters (e.g. initial or total OSL intensity), due to the number of defects in the investigated material. This has not yet been investigated for BeO OSLDs.

Moreover, in many applications, the angular dependence of dosimeters is crucial because it determines how accurately the dosimeter measures radiation exposure across various angles of incidence. Testing of the angular dependence for the investigated BeO OSLDs was also necessary, as this aspect has also not yet been studied in the literature.

Exposure of dosimeters to room light, especially for long durations or high light intensities, can generate an OSL signal resembling ionizing radiation, if those dosimeters are sensitive to non-ionizing radiation like visible and UV light. This can lead to inaccurate dosimeter readings. It is noted that while the presence of TL and OSL signals induced by room light have been reported for BeO dosimeters in previous studies, the mechanism behind has not yet been investigated. Consequently, this phenomenon was explained in publication I.

In conclusion, the dosimetric characterization of BeO dosimeters, particularly focusing on a fast readout protocol for medical applications, has been thoroughly investigated in this study. Specifically, the annealing characteristics, fading, preheating temperature, stimulation time, energy and angular dependence have been examined to ensure accurate dose estimation. Overall, this comprehensive investigation provided valuable insights that allowed for optimizing the use of BeO dosimeters in clinical dosimetry, with enhanced accuracy and reliability in radiation measurements.

Key finding I: The phototransferred OSL signal are related with traps beyond 700°C may cause a light-induced signal after annealing.

Key finding II: The degree of fading of the initial OSL signals of BeO dosimeters depends on both the applied dose and the integration interval. To avoid dose underestimation, dosimeters should undergo preheat treatment.

Key finding III: In order to ensure accurate and precise dose measurements in clinical applications, special attention should be given to angular response of lower photon energies (< 60 keV) which exhibit substantial variations in dosimeter response. This could significantly impact accurate dose measurements, particularly in medical diagnostics.

Key finding IV: The relative detector response is nearly independent of the photon energy and has a uniform angular dependence for energies above 60 keV.

Key finding V: When properly annealed and preheated, BeO dosimeters exhibit high reproducibility in the laboratory and results hold promise for medical dosimetry applications.

4.2 Publication II

The second publication focuses on investigating the TL and OSL luminescence mechanisms by conducting step annealing test on the OSL signal and bleaching test of the TL signal in BeO dosimeters. This exploration aims to uncover the correlation between these signals. Additionally, the publication reported dose response of each TL peak with corresponding OSL signals and discusses the existing bleaching models for BeO.

The study involved measuring the residual TL (R-TL) glow peak intensities at various bleaching times and fitting of exponential decay functions to investigate possible correlations of OSL signals with bleaching time. Additionally, the publication discusses the bleaching luminescence models for BeO. These correlation studies allowed understanding the BeO luminescence mechanism, and thereby enhancing dosimetry techniques and opening a variety of practical applications. In particular, correlation between OSL and TL signals allowed identification of common traps under optical and thermal stimulations. These traps facilitated development of reading protocols for measuring radiation doses absorbed by the investigated materials. Furthermore, by defining the characteristics of luminescent light, luminescence readers can be designed in the future more effectively with suitable LEDs and optical filters to enhance their performance. The bleaching of TL signals with optical stimulation (using the same light source as for OSL) and conducting step annealing tests of OSL signals were used for the above-mentioned correlation studies.

Optical bleaching of TL involves application of stimulation light before TL measurement. In this manner, the trapped charges that contribute to the OSL signal are evicted. As a result, the subsequently measured TL signal intensity will decrease. Exponential decay functions can be fitted to the measured residual TL (R-TL) glow peak intensities at various bleaching times and to the OSL decay curve, to investigate possible correlations between them.

The step annealing test is a method used to evaluate the thermal stability of the OSL signal in dosimeters. After irradiation, dosimeters undergo thermal readings at specific temperatures to erase a part of luminescence signals before performing the OSL reading. In the test, the annealing temperature is raised in discrete steps. The intensity of the OSL signal measured after each temperature step indicates the thermal stability of the dosimeters and provides insights into common trap parameters with its thermoluminescence signal.

Determining the dose response of OSL and TL signals is important in terms of dosimetry and is essential for both quality assurance and calibration purposes. Along with this, the dose response of each peak of the thermoluminescence signal and its relationship with the OSL signal establishes how the luminescence signals are correlated in response to varying doses of radiation.

As reported by Kara and Woda (2023b), various studies (Aşlar et al., 2019; Bulur and Saraç, 2013; Yukihiro, 2011) have explored the luminescence mechanism responsible for generating TL peaks and its relationship with the OSL signal in BeO dosimeters. Results of bleaching tests showed that TL peaks 1 and 2 exhibit strong bleachability, suggesting a connection to the OSL signal, while step annealing tests after irradiation with 200 mGy (lower dose) indicate that TL peak 3 contributes significantly to the OSL signal despite being poorly bleachable (Yukihiro, 2020). In contrast, at higher doses around 10 Gy, the thermal stability test revealed a two-step decrease in the OSL signal, with the first decrease occurring in the temperature range of the second TL peak (Bulur and Saraç, 2013). This indicates that the second TL peak indeed contributes to the OSL signal. To address those discussions, Yukihiro (2020) suggested that optically active traps reach

saturation at lower doses, thereby allowing the contribution of TL peak 2 to become visible at higher doses. Conversely, Bulur and Yeltik (2011) proposed the formation of new traps due to radiation damage. However, it is important to note that previous studies did not provide direct experimental evidence to confirm their explanation. For this reason, in the present study step annealing tests were conducted and bleaching rates of R-TL curves and optical components were quantified at different doses using fitting functions to find possible correlations between OSL and TL signals (Publication II). Additionally, dose-response tests were conducted for further clarification, along with step annealing and bleaching tests.

Levy (1982) proposed a model with multiple electron traps causing re-trapping or recombination with holes, resulting in decreased TL intensity after bleaching (optical stimulation). Chen et al. (1990) introduced a model with a single electron trap and recombination center. In this model, bleaching (optical stimulation) removes electrons from both the electron trap and the recombination center, leading to increased hole number at recombination centers and causing a residual TL signal that remains unaffected by the initial trap population (Kara and Woda, 2023b). McKeever (1994) proposed another model with optically inactive TL traps and deep thermally disconnected traps. In this model, bleaching doesn't affect TL traps but removes electrons from deep traps, causing radiative recombination and resulting a residual TL signal resistant to bleaching dependent on the initial trap distribution (McKeever and Chen, 1997b; Kara and Woda, 2023b).

In Publication II, the suitability of these models for each TL peak of BeO dosimeters is also discussed, with emphasis on McKeever's and Chen's models. To gain a better understanding, the remaining TL signals were measured following bleaching at various applied doses. The proportion of the unbleachable residual signal compared to the total TL signal, as well as how this signal varies with dose, were investigated by Kara and Woda (2023b).

To assess the potential relation between thermoluminescence and optically luminescence of dosimeters bleaching test was employed to TL, and step annealing tests were conducted for OSL at varying doses. The results obtained provided valuable insights into both thermal stability and luminescent properties, with the identification of common traps under optical and thermal stimulations. Furthermore, the study enhanced the understanding the dose response of OSL and individual TL peaks, as well as how their relations contribute to elucidating luminescence signal behavior under varying radiation doses. Discussion of the bleaching models for TL peaks shed some light on about the luminescence mechanisms responsible for those peaks.

Key finding I: There are two types of bleachable traps for TL peaks 2 and 3 and for OSL. At low doses, the OSL originates from the trap related to TL peak 3, while at higher doses there is an increasing contribution to the OSL signal from the trap related to TL peak 2.

Key finding II: TL peaks 2 and 3 show a different bleaching behavior which implies different luminescence mechanisms are taking place.

Key finding III: Direct experimental evidence is provided on the correlation of TL peaks and OSL at different doses, with the observation that the bleaching behavior of various TL peaks compared to OSL components exhibit overlapping values.

5. Summary (in English)

This doctoral thesis highlights the potential of BeO as an OSL dosimeter for accurate dose measurements in medical applications. This study aimed to (1) characterizing the dosimetric properties of BeO and in this way establish a fast readout protocol while maintaining dose estimation accuracy, (2) to investigate the luminescence mechanisms in BeO through the study of the bleaching behavior at varying doses, and (3) evaluation of BeO as a medical dosimeter under clinical irradiation conditions.

Publication I, as reported by Kara and Woda (2023a), focuses on characterizing BeO OSL dosimeters as an alternative dosimeter for dose estimation in the medical field. A detailed characterization of BeO dosimeters and the establishment of a measurement protocol was needed, since luminescence mechanism of the dosimeter is complex, and existing knowledge did not yet meet the requirements for applications in terms of characterization approaches. In addition, additional considerations when employing BeO dosimeters for rapid clinical applications were addressed. Furthermore, an experimental investigation of the light-induced luminescence signal was conducted, along with theoretical explanations.

In Kara and Woda (2023a) it is suggested that “shorter annealing and readout times are possible compared to those reported in previous studies, allowing for faster dose assessment, particularly when using equipment with moderate OSL stimulation power ($\sim 30 \text{ mW/cm}^2$)”. The fading in dosimeters was reported to be dose-dependent, especially noticeable at shorter readout times following storage. Therefore, to preserve dose information, particularly in clinical applications, an appropriate preheating temperature before conducting OSL measurements was investigated. Kara and Woda (2023a) demonstrated that in such cases, preheating is indeed necessary to avoid underestimation of the dose when using BeO OSL dosimeters. The results of the energy dependence as reported by Kara and Woda (2023a) were compared to published results, and some differences were found. These differences indicate the necessity for either a batch-dependent assessment of the energy response or for a precise alignment between the calibration setup and the dose measurement setup, to prevent systematic errors. It was also shown that – in contrast to $\text{Al}_2\text{O}_3\text{:C}$ dosimeters – the relative dosimeter response is independent of photon energy, except for low X-ray energies of about 60 keV, indicating that energy corrections are not needed. Furthermore, the angular dependence of the BeO dosimeter response was investigated for the first time by Kara and Woda (2023a). The results indicated that at energies below 60 keV the angular dependence must be corrected for, which is particularly relevant for X-ray energies used in medical diagnostics. For photon energies above $\sim 60 \text{ keV}$, it was shown here that the angular dependence of the dosimeter response does not significantly contribute to the overall dose uncertainty. However, for photon energies below 60 keV, the angular dependence leads to a relative response variation that can increase by up to 30%, which requires further investigations of the energy dependence of dosimeter response in clinical settings. A readout protocol was developed based on the obtained dosimetric characteristics of BeO OSL dosimeters by Kara and Woda (2023a), enabling both a faster measurement cycle than before, and accounting for uncertainties in dose measurement. Repositioning with the developed protocol resulted in a reproducibility of $\pm 1.1\%$. It is concluded that this study indicated that, despite the identified issues, BeO dosimeters offer favorable dosimetric properties enabling short reading times with reduced uncertainty and meeting clinical demands effectively.

Moreover, Kara and Woda (2023a) stated that “adopting BeO dosimeters in dosimetric applications requires a precise understanding of the luminescence mechanism behind. However, the relation between TL and OSL signals is not yet fully understood, potentially complicating their use in dosimetric applications”. Consequently, Publication II (Kara and Woda (2023b)) includes a comprehensive correlation study on TL and OSL signals in BeO dosimeters by using bleaching, step annealing, and dose-response tests. Bleaching models were also examined to assess appropriate luminescence mechanisms for individual TL peaks.

This was complemented in Kara and Woda (2023b) by: “Previous observations reported in the literature indicate that in BeO and at doses in the mGy range the OSL signal is strongly correlated with TL traps associated with peak 3. However, at doses of 10 Gy and higher, there is an increasing contribution of TL peak 2 traps to the OSL signal, which becomes dominant at very high doses.” However, in previous studies this relationship was not directly investigated. Results of step annealing and bleaching tests performed as part of this thesis revealed that TL and OSL traps were found more consistent than previously reported.

The BeO dose-response of each TL peak and corresponding OSL signals was reported for the first time by Kara and Woda (2023b). Specifically, the OSL signal’s dose response was observed to maintain linearity to 100 Gy. This linearity could be attributed to the combined dose response behaviors of TL peak 2 and 3. The TL peak 2 demonstrates a supra-linear dose-response, while the dose-response of the bleachable part within TL peak 3 exhibits saturation up to 40 Gy. Subsequently, higher doses elicited a linear dose-response for both peaks (Kara and Woda, 2023b).

To further elucidate the luminescence mechanism, Kara and Woda (2023b) evaluated bleaching models for each TL peak after optical bleaching. The results revealed that TL peaks 2 and 3 have distinct luminescence mechanisms. Moreover, the study indicated that that TL and OSL luminescence mechanisms appear to be more consistent than previously assumed.

To conclude, the results obtained by Kara and Woda (2023b) significantly contribute to the existing knowledge on the luminescence mechanisms in BeO at different doses and at thermal treatments. The relationship between TL peaks 2 and 3 and the OSL signals was established. This provided valuable insights into the luminescent properties and bleaching mechanisms of BeO. In general, understanding the thermoluminescence and optically stimulated luminescence behavior of BeO and their relationship enhances our fundamental understanding of the material's properties, providing useful insights for its practical applications. Thus, this study significantly advanced the understanding of the luminescence behavior of BeO, paving the way for further exploration and utilization of this material in various applications.

In the Appendix, it is described how the developed OSL measurement protocol for BeO was applied to a computer tomography setting by measuring the absorbed organ doses in a one-year-old anthropomorphic phantom for total body scan. Results are compared with those obtained with LiF:Mg,Ti TLDs in the same experiment. Based on the results obtained it is concluded that BeO dosimeters are capable of accurately measuring absorbed doses in clinical applications.

6. Zusammenfassung (deutsch)

Diese Dissertation beleuchtet das Potenzial von BeO als OSL-Dosimeter für Dosismessungen bei medizinischen Anwendungen. Die Forschungsziele dieser Studie waren (1) die Charakterisierung der dosimetrischen Eigenschaften von BeO und insbesondere die Etablierung eines schnellen Ausleseprotokolls unter Beibehaltung der Genauigkeit der Dosismessung, (2) die Aufklärung der Lumineszenz-Mechanismen in BeO durch die Untersuchung des Bleichverhaltens und des Verhaltens von TL- und OSL-Signalen bei Bestrahlung und (3) die Prüfung der Anwendbarkeit von BeO als medizinisches Dosimeter unter klinischen Bestrahlungsbedingungen.

Publikation I konzentriert sich auf die Charakterisierung von BeO-OSL-Dosimetern als alternative Dosimeter für die Dosismessung im medizinischen Bereich (Kara und Woda, 2023a). Eine detaillierte Charakterisierung von BeO-Dosimetern und die Erstellung eines Messprotokolls war aufgrund des komplexen Lumineszenzmechanismus des Materials notwendig, insbesondere weil das vorhandene Wissen dazu für bestimmte Anwendungen noch nicht ausgereicht hatte. Dieser Teil der Arbeit befasst sich mit den dosimetrischen Eigenschaften von BeO OSLDs sowie mit weiteren Aspekten, die bei der Verwendung von BeO-Dosimetern bei klinischen Anwendungen berücksichtigt werden müssen. Dazu wurden das optimale Ausglühverfahren, das kurzfristige Fading mit und ohne Vorwärmung, die Reproduzierbarkeit sowie die Energie- und Winkelabhängigkeit von BeO-Dosimetern untersucht und das lichtinduzierte Lumineszenzsignal ermittelt.

Die erzielten Ergebnisse deuten darauf hin, dass im Gegensatz zu Ergebnissen früherer Studien kürzere Glüh- und Auslesezeiten möglich sind, was eine schnellere Dosisbestimmung ermöglicht, insbesondere bei Verwendung von Geräten mit moderater OSL-Stimulationsleistung ($\sim 30 \text{ mW/cm}^2$) (Kara und Woda, 2023a). Es wurde im Rahmen dieser Arbeit beobachtet, dass das Fading in BeO-Dosimetern dosisabhängig ist, insbesondere bei kürzeren Auslesezeiten. Außerdem wurde beobachtet, dass die Wahl einer geeigneten Vorwärmtemperatur nach der Lagerung der OSL-Dosimeter, jedoch vor der Durchführung von OSL-Messungen, erforderlich ist, um Dosismessungen durchführen zu können, insbesondere bei klinischen Anwendungen. In solchen Fällen ist eine Vorwärmung erforderlich, um eine Unterschätzung der Dosis zu vermeiden. In Abhängigkeit von der Photonenenergie wurden Abweichungen im Vergleich zu in der Literatur veröffentlichten Ergebnissen festgestellt. Das deutet darauf hin, dass es wichtig ist, entweder die individuelle Abhängigkeit der Nachweisempfindlichkeit des Detektors von der Photonenenergie zu berücksichtigen oder eine genaue Anpassung zwischen dem Kalibrierungsaufbau und dem Dosismessaufbau vor-zunehmen, um systematische Fehler zu vermeiden. Es konnte zudem gezeigt werden, dass die relative Dosimeter-Antwort auf Bestrahlung unabhängig von der Photonenenergie ist, außer bei niedrigen Röntgenenergien, so dass keine Energiekorrekturen erforderlich sind, wie dies z. B. bei $\text{Al}_2\text{O}_3\text{:C}$ -Dosimetern der Fall ist. Allerdings zeigten die Ergebnisse der vorliegenden Arbeit auch, dass bei Expositionsenergien unter 60 keV für eine genaue Dosisabschätzung Energiekorrekturen berücksichtigt werden müssen, insbesondere bei der Anwendung von Röntgenstrahlung in der medizinischen Diagnostik. Bei Photonenenergien über $\sim 60 \text{ keV}$ trägt die Winkelabhängigkeit der Dosimeter-Antwort nicht wesentlich zur Gesamtdosisunsicherheit bei. Bei niedrigeren Photonenenergien kann die relative Unsicherheit bei der Dosisbestimmung jedoch um bis zu 30 % zunehmen, was weitere Untersuchungen der Energieabhängigkeit bei klinischen Anwendungen erfordert. Die entwickelten schnellen Messprotokolle lassen genügend Zeit für einen Messzyklus, wobei die Unsicherheit der berechneten Dosis berücksichtigt wird. Die Reproduzierbarkeit der Dosismessungen, wenn die Dosimeter in der Anlage neu positioniert

werden, betrug bei Anwendung des entwickelten Protokolls etwa $\pm 1,1$ %. Diese Studie zeigte, dass BeO-Dosimeter trotz der festgestellten Verbesserungsmöglichkeiten günstige dosimetrische Eigenschaften aufweisen, die kürzere Ablesezeiten bei geringerer Unsicherheit ermöglichen, und somit Anforderungen bei klinischen Anwendungen gerecht werden.

Darüber hinaus ist für den Einsatz eines BeO-Dosimeters ein genaues Verständnis des zugrundeliegenden Lumineszenzmechanismus erforderlich. Die Beziehung zwischen TL- und OSL-Signalen in BeO ist jedoch noch nicht vollständig geklärt, was ihren Einsatz bei dosimetrischen Anwendungen erschwert. In Publikation II werden daher Ergebnisse einer umfassende Korrelationsstudie zu TL- und OSL-Signalen von BeO-Dosimetern unter Verwendung von Bleich-, Stufenglüh- und Dosis-Wirkungs-Tests beschrieben, die im Rahmen dieser Arbeit erzielt wurden (Kara und Woda, 2023b). Zudem wurden Bleichmodelle untersucht, um die Lumineszenzmechanismen für einzelne TL-Peaks zu ermitteln. Die bisherigen Beobachtungen, dass bei Energiedosen im mGy-Bereich das OSL-Signal von BeO stark mit TL-Peak 3-Fallen korreliert ist, wurden bestätigt. Bei Energiedosen von 10 Gy und höher ist jedoch ein zunehmender Beitrag von TL-Peak-2-Fallen zum OSL-Signal zu beobachten, der bei sehr hohen Dosen dominiert. In den bisherigen Studien wurde dieser Zusammenhang jedoch noch nicht direkt untersucht. Es wurden daher im Rahmen dieser Arbeit auch Bleichmodelle untersucht, um geeignete Lumineszenzmechanismen für einzelne TL-Peaks zu bewerten. Die Ergebnisse der durchgeführten Stufenglüh- und Bleichtests zeigten, dass TL- und OSL-Fallen korreliert sind, anders als bisher berichtet.

Die Dosisabhängigkeit der einzelnen TL-Peaks und der entsprechenden OSL-Signale wurde im Rahmen dieser Arbeit zum ersten Mal beschrieben. Die Dosisabhängigkeit des OSL-Signals erwies sich bis zu 100 Gy als linear. Diese Linearität könnte auf die Überlagerung von Sättigungseffekten der bleichbaren Fallen von TL-Peak 3 und einer supralinearen Dosisabhängigkeit der Fallen von TL-Peak 2 bis zu einer Dosis von etwa 40 Gy zurückgeführt werden, gefolgt von der anschließenden linearen Dosisabhängigkeit beider Peaks für höhere Dosen.

Zur weiteren Aufklärung des Lumineszenzmechanismus wurden für BeO Bleichmodelle für jeden TL-Peak nach dem optischen Bleichen bewertet. Dieser Teil der Studie verdeutlichte die Existenz unterschiedlicher Lumineszenzmechanismen in Verbindung mit den TL-Peaks 2 und 3, insbesondere in Bezug auf ihre Reaktion auf das Bleichen.

Darüber hinaus ergab die hier beschriebene Studie, dass die Mechanismen der TL- und OSL-Lumineszenz möglicherweise stärker miteinander korrelieren könnten als bisher angenommen. Zusammenfassend lässt sich daher sagen, dass diese Studie einen wichtigen Beitrag zum bestehenden Wissen über die Lumineszenzmechanismen von BeO bei verschiedenen Energiedosen und thermischen Behandlungen leistet. Sie verdeutlicht die komplizierte Beziehung zwischen den TL-Peaks 2 und 3 und dem OSL-Signal und liefert Einblicke in die Lumineszenzeigenschaften und Bleichmechanismen von BeO. Das erreichte verbesserte Verständnis des Lumineszenzverhaltens von BeO und der Korrelation zwischen TL- und OSL-Signalen verbessert nicht nur unser grundlegendes Verständnis der Materialeigenschaften von BeO, sondern liefert auch Erkenntnisse für seine praktischen Anwendungen. Somit trägt diese Studie zu unserem Verständnis des Lumineszenzverhaltens von BeO bei und ebnet den Weg für die weitere Erforschung und Nutzung dieses Materials bei verschiedenen Anwendungen.

Schließlich wurde, wie im Anhang beschrieben, das in dieser Arbeit entwickelte OSL-Messprotokoll für BeO in einer Computertomografie-Studie durch Messung der Organenergiedosen in einem einjährigen anthropomorphen Phantom getestet. Die Ergebnisse wurden mit denen von

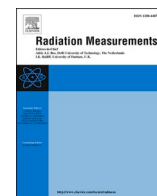
LiF:Mg,Ti TLDs verglichen. Dabei zeigte sich, dass BeO-Dosimeter es in der Tat erlauben, Strahlendosen bei klinischen Anwendungen genau zu messen.

7. Publication I

Further characterization of BeO detectors for applications in external and medical dosimetry, Kara and Woda (2023a).

Elif Kara, Clemens Woda.

10.1016/j.radmeas.2023.106950.



Further characterization of BeO detectors for applications in external and medical dosimetry

Elif Kara^{a,b,*}, Clemens Woda^a

^a Helmholtz Zentrum München-German Research Center for Environmental Health, Institute of Radiation Medicine, Neuherberg, Germany

^b Faculty of Medicine, Ludwig Maximilian University (LMU) Munich, Munich, Germany

ARTICLE INFO

Keywords:

Optically stimulated luminescence (OSL)

Beryllium oxide (BeO)

Luminescence dosimetry

ABSTRACT

Measuring absorbed doses with high precision and accuracy for clinical applications using Optically Stimulated Luminescence (OSL) dosimeters can help to optimize treatment to patients. Beryllium Oxide (BeO) is a nearly tissue-equivalent material that has the potential to increase the applicability of OSL dosimetry in medical dosimetry, but there has been limited research into its characterization. We present here the characterization of BeO dosimeters in terms of annealing temperature and duration, the effect of preheat treatment on short-term fading, energy and angular dependence, and discuss possible errors in laboratory conditions by using the OSL technique. Shorter readout of 30 s when using stimulation power of $\sim 30 \text{ mW cm}^{-2}$ is feasible but preheating then becomes necessary. The fading behavior of BeO was found to be dose-dependent in this case. Reproducibility of an OSL measurement with repositioning of the dosimeter in the reader and for the short readout times was found to be $\sim 1\%$. Energy response was close to the theoretical values, which agrees with some but differs from other published studies, indicating that the OSL efficiency might vary. The angular dependence presented the greatest uncertainty factor. In summary, BeO dosimeters have the potential to be used in clinical applications for dose evaluation. However, care should be taken while handling and applying an optimized measurement procedure is necessary due to the complex luminescence mechanism of the material.

1. Introduction

The Optically stimulated luminescence (OSL) technique has recently received noticeable attention to be applied in medical dosimetry owing to the flexible automation of OSL readers and fast readout times. However, one of the major challenges in the spread of this technique for use in dosimetry applications is the lack of suitable materials that can directly reflect absorbed doses in such materials (Souza et al., 2019; Yukihiro et al., 2010). Dosimeters based on carbon-doped Aluminum Oxide ($\text{Al}_2\text{O}_3\text{:C}$) and BeO are the most common OSL dosimeters because these are readily available and have appropriate dosimetric characteristics. However, the major drawback of $\text{Al}_2\text{O}_3\text{:C}$ is the high effective atomic number ($Z_{\text{eff}} \approx 11.28$) which causes an over response to low energy X-rays in the keV range (Bos, 2001). In contrast, BeO dosimeters have a similar effective atomic number ($Z_{\text{eff}} \approx 7.2$) as soft tissue ($Z_{\text{eff}} \approx 7.65$) which makes them an attractive choice for OSL applications, particularly in medical dosimetry (Bos, 2001; Malthes et al., 2014). However, investigations of BeO dosimeters are still limited (Yukihiro and Kron, 2020), as compared to the plentiful literature on $\text{Al}_2\text{O}_3\text{:C}$

applied in medical dosimetry.

Earlier studies have indicated that BeO OSL dosimeters have characteristics especially valuable for use in the clinical environment, such as wide dose response range along with good linearity (Bulur and Göksu, 1998; Sommer et al., 2007; Sommer and Henniger, 2006), reproducibility (Sommer and Henniger, 2006; Yukihiro et al., 2016) and low fading (Bulur and Göksu, 1998; Sommer et al., 2007). Besides, it has already been used for medical applications, for example in radiotherapy by Şahin et al. (2020) and has demonstrated its utility in electron beam breast radiotherapy. Furthermore, Santos et al. (2015) used BeO coupled optical fibers for OSL dosimetry in brachytherapy. Rodriguez et al. (2012) studied its application in clinical organ dose measurements for diagnostic X-ray beams, while Yagui et al. (2020) applied it to pediatric gastrointestinal fluoroscopy. In recent work, Aşlar et al. (2020) demonstrated the potential of BeO OSL dosimeters in mammography. All these studies aimed at demonstrating the benefits and feasibility of BeO OSL dosimeters in various medical applications, and the results demonstrated that the benefits of BeO dosimeters are even more pronounced than predicted. However, these studies differed in the used

* Corresponding author. Helmholtz Zentrum München-German Research Center for Environmental Health, Institute of Radiation Medicine, Neuherberg, Germany.
E-mail addresses: elif.kara@helmholtz-munich.de (E. Kara), cwoda@bfs.de (C. Woda).

readout protocols. Moreover, on the one hand BeO can be manufactured cost-effectively in batches, but on the other hand this may cause variability in the OSL response. Therefore, characterization of dosimeters should be examined systematically to reduce uncertainty in the measurement of absorbed dose in clinical research.

In Yukihiro et al. (2016) it is shown that sensitivity changes occur for BeO dosimeter in repeated cycles of dosing and pure optical measurements. The authors recommend thermal annealing after each dose measurement to restore the initial sensitivity of the detector. A full optical readout of the detector with the stimulation power available in the Risø TL DA15 readers ($\sim 30\text{--}36\text{ mW cm}^{-2}$) takes between 120 and 300 s. This results in long measurement times, if a large number of detectors has to be readout e.g. after a phantom irradiation. If, on the other hand, thermal annealing is necessary anyway, shorter readings, with only part of the OSL signal being readout, should be possible. As a large number of detectors could then be simultaneously thermally annealed in an external furnace, this could significantly shorten the time needed for dose assessment. However, systematic investigations on such an approach is lacking.

Another issue is the necessity of preheating. In Sommer and Henniger (2006) it is shown that fading of the OSL signal of about 5% occurs within the first hours after irradiation, with no further fading then taking place over storage periods over 200 days. In Yukihiro et al. (2016) a fast OSL component, that decays within 10 min is observed. For readout times of 120 s it contributes to less than 1% to the total signal, so that no preheating should be necessary. This relative contribution might be different for shorter readout times. On the other hand, Bulur and Göksu (1998) suggested a preheat of 125 °C for 125 s to remove the instable part of the OSL signal in case of green light stimulation. In Bulur and Yeltik (2010), a preheat of 160 °C for 10 s was used for LM-OSL measurements with blue light stimulation of the Risø DA15 reader, without further details. Overall, there seem to be different recommendations on preheat treatment.

In Sommer and Henniger (2006) and Sommer et al. (2007), there is an agreement between measured and calculated energy response for BeO but in Jahn et al. (2014), the measured energy response is significantly smaller than expected (simulated), which was explained by a reduced OSL efficiency for photons and secondary electrons in the material. Furthermore, in Malthiez et al. (2014), it was observed that the choice of integration interval (initial signal or total OSL decay curve) has only a small influence on the energy response.

This study aims at the characterization of BeO dosimeters for use in medical dosimetry applications by focussing on a fast OSL reading protocol. Consequently, annealing temperature and duration, the effect of preheat treatment on short-term fading, energy and angular dependence were examined in laboratory conditions, addressing the issues mentioned above. The results obtained were used to assess the luminescence mechanism that takes place in the BeO material.

2. Material and Methods

2.1. Detectors and irradiations

Commercially available disk-shaped BeO ceramics (Thermalox TM 995, Brush Wellman Inc., USA) with a diameter of 4 mm and a thickness of ~ 0.5 mm were used in this study. A total of 30 randomly selected BeO dosimeters were used in this study. For measurement of the energy and angular dependence, irradiations were carried out with calibrated ^{137}Cs and X-ray sources at the Radiation Facilities of the Helmholtz Zentrum München, Germany. For the X-ray irradiations, ISO narrow spectrum qualities from N-30 to N-300 were used (ISO, 1996). All irradiations were done in terms of air kerma free in air, with a dose of 5 mGy. Dosimeters were wrapped in a thin layer of aluminum foil for this purpose. The kerma in air was determined using an ionization chamber traceable to the primary standard at the Physikalisch-Technische Bundesanstalt (PTB), Germany.

2.2. TL and OSL readouts

Luminescence irradiations and readings were performed on an automated luminescence reader (model Risø TL/OSL-DA-15) equipped with a $^{90}\text{Sr}/^{90}\text{Y}$ beta source (1.48 GBq). Optical stimulation was provided by using blue light emitting diodes (LEDs) at 470 nm with an intensity of 36 mW cm^{-2} at the sample position. OSL read-out was performed at room temperature with 90% power of blue LEDs at different stimulation times. The reader includes a 9235QB bialkali photomultiplier tube (PMT) from ET Enterprises and Hoya U-340 filter for the detection of the luminescence signal. For OSL measurements of BeO dosimeters irradiated with 2 Gy, a black cardboard with a pinhole was additionally inserted between optical filter and detector to avoid over-exposure of the PMT. TL measurements were carried out in an N_2 atmosphere and recorded up to 450 °C with a heating rate was 5 °C.s^{-1} . The built-in beta source of the reader was calibrated against the above mentioned ^{137}Cs source using the same BeO dosimeters. Thermal annealing at temperatures of 700 °C or above were performed in an external muffle furnace.

2.3. Data analysis

For OSL, signal intensity was determined for two different integration intervals: the first 30 s and 300s. The net OSL signal was calculated by subtracting the average of the last 5 s or 50 s of OSL counts from each data point (1 s per channel) of the first 30 s or 300 s of the integrated OSL counts, respectively. The TL glow curve of BeO consists of three peaks (Bulur and Göksu 1998). For the analysis in this work, Peak 1 was integrated between 50 and 120 °C and Peak 3 between 250 °C and 450 °C.

The mass energy absorption coefficients of BeO were calculated based on data for beryllium and oxygen using the following expression:

$$\left(\frac{\mu_{\text{en}}}{\rho}\right)_{\text{BeO}} = f_{\text{Be}} \left(\frac{\mu_{\text{en}}}{\rho}\right)_{\text{Be}} + f_{\text{O}} \left(\frac{\mu_{\text{en}}}{\rho}\right)_{\text{O}}$$

where $f_{\text{Be}} \cong 0.360$ and $f_{\text{O}} \cong 0.640$ are the weight fraction for beryllium and oxygen in BeO, respectively.

The mass energy absorption coefficient for Be, O and air were taken from the National Institute of Standards and Technology (NIST) database (<https://www.nist.gov/pml/x-ray-mass-attenuation-coefficients>).

3. Results

3.1. Annealing temperature and time

Yukihiro et al. (2016) suggested to anneal BeO dosimeters at 700 °C for 15 min for thermal resetting and to erase any pre-existing dose history. In line with this recommendation, BeO dosimeters were first irradiated with 20 Gy beta dose, annealed at 700 °C for 15 min and then the residual OSL signals measured. Since a fast readout protocol can be beneficial for medical applications to save time, the annealing temperature was tested with additionally a 5 min annealing time at the same temperature was also applied and the results then compared to the reading of a blank disc. The results are shown in Fig. 1.

The OSL signal reaches the background value obtained from the blank disc for both annealing times. Having ascertained that 5 min annealing time at 700 °C is enough to reset the OSL signal even after a high dose irradiation, we next tested whether annealing time affects the sensitivity of the OSL signal. Five BeO dosimeters were annealed for 5, 10 and 15 min at 700 °C and then irradiated to a beta dose of 40 mGy before OSL readout for 300 s. The results of the annealing time at 10 and 15 min were normalized to that of 5 min annealing time and the OSL integration time was 300 s, in Fig. 2.

The effect of annealing temperature on the sensitivity of the OSL response of BeO was investigated by Yukihiro et al. (2016), who suggested that 700 °C annealing for 15 min is enough to eliminate photo-transferred signal from deep traps that are responsible for the glow peak

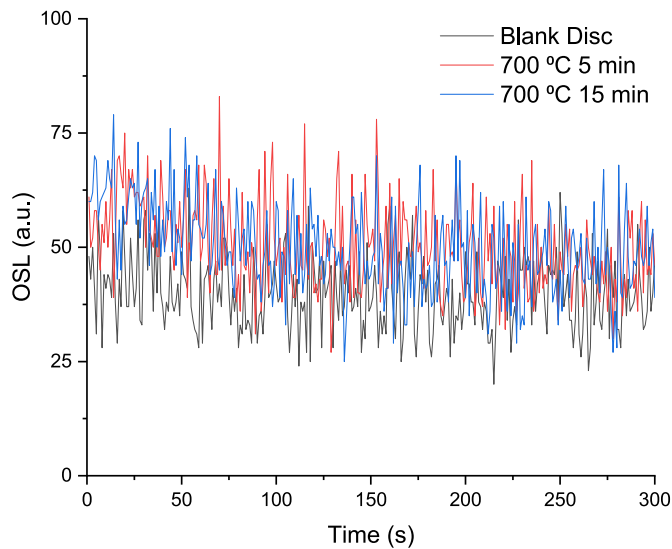


Fig. 1. Residual OSL signal of BeO after annealing at 700 °C for 5 and 15 min following irradiation with 20 Gy of beta dose, together with reading from a blank disk.

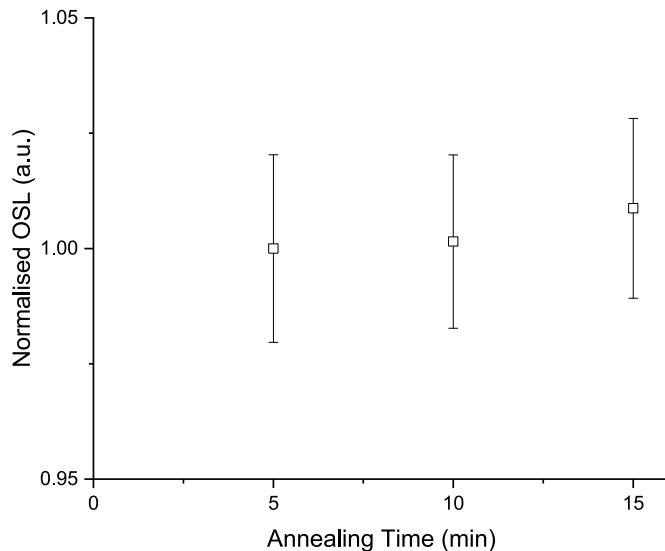


Fig. 2. Sensitivity changes of the OSL signal as a function of the annealing time of 40 mGy irradiated BeO dosimeters. Error bars represent the standard deviation between the response of same five dosimeter, which is $\sim 1.9\%$ on average.

in the 400–625 °C region of the TL glow curve of BeO (Bulur, 2007). As seen in Fig. 2, the differently pretreated dosimeters have almost identical OSL responses, there are no changes in sensitivity at 700 °C regardless of annealing time. The error bars represent the standard deviation between the OSL response of the five dosimeters per annealing time, which amounts to $\sim 1.9\%$ on average. For the present study, the annealing time was selected at 5 min at 700 °C and used throughout.

Previous works on the room light-induced luminescence signal of BeO argued that samples should be protected from light after annealing, particularly for low-dose measurements (Crane and Gammage, 1975; Henaish et al., 1979; Yukihiro et al., 2016). Having determined the annealing conditions, we thus examined the room light-induced OSL signal, concordantly with the previous study of Yukihiro et al. (2016). BeO dosimeters were irradiated with 40 mGy and 400 mGy of beta dose before annealing at 700 °C and 900 °C for 5 min. Room light-induced OSL signal from BeO dosimeters was investigated by exposing the

detectors to room fluorescent light in the laboratory for 20 and 40 min between removal from the furnace and OSL readout (300 s). The measured signals were converted into dose by calibrating the dosimeters after readouts. The same three dosimeters were used during this part of the study and the error bars represent the standard deviation between the dosimeters. Results can be seen in Fig. 3.

The room light-induced OSL signal is dose-dependent, increasing with increasing doses and is also dependent on the exposure time to light. Chen et al. (1990) proposed a model to explain the optical bleaching of the TL signal, in which optical exposure can remove charges from the recombination centers that are near the Fermi level into the conduction band. The same mechanism could potentially cause a light-induced luminescence signal in virgin samples, which were exposed to light of the same wavelength (McKeever, 1994): removed charges from recombination centers by light exposure may be trapped at empty trapping levels with subsequent optical stimulation then leading to radiative or non-radiative recombination. However, an OSL signal was not observed from BeO dosimeters which were exposed to only blue light for 300 s after being irradiated with 20 Gy and annealed at 700 °C for 5 min, as can be seen in Fig. 1. Alternatively, McKeever (2001) proposed the production of free charges from pre-existing defects by optical exposure to explain optically induced TL from a virgin sample. Those free charges can become trapped at empty traps, which again can lead to a luminescence signal in a later measurement. On the other hand, there is no room light-induced signal after annealing at 900 °C for 5 min and this significant drop in the OSL signal compared to annealing at 700 °C can also imply that the mechanism may be a photo-transferred luminescence signal associated with deep traps beyond 700 °C.

Looking at the apparent dose values in Fig. 3, the maximum apparent dose measured for a predose of 400 mGy and duration of fluorescent room light exposure of 40 min is ~ 30 μ Gy. A similar value was reported in Yukihiro et al. (2016) for 10 min light exposure after irradiation with 3.5 Gy and annealing at 700 °C for 15 min. It thus seems that extra care in dosimeter handling after annealing is mostly relevant when measuring low doses, which is relevant for environmental and individual monitoring but less for medical applications. Nevertheless, our results indicate that an annealing temperature of 900 °C might make any precautions after annealing unnecessary. This could be further investigated in future studies.

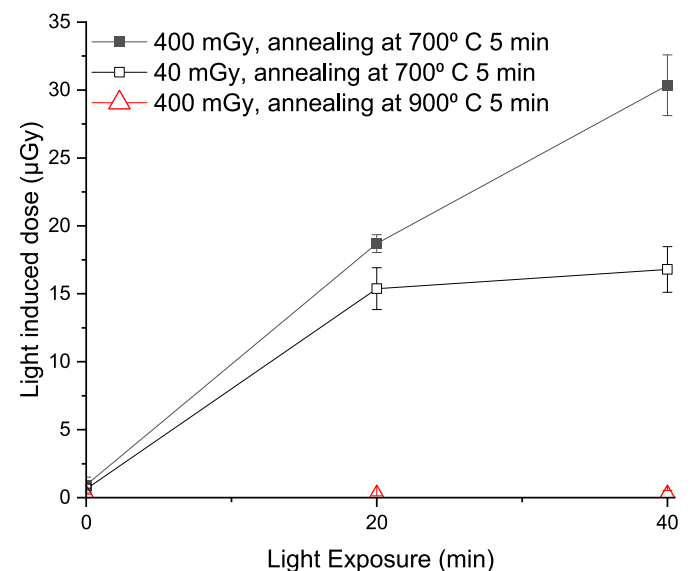


Fig. 3. Room light-induced OSL signal after annealing at different exposure times. Room light-induced OSL signals were measured for 300 s, and then were converted into an apparent dose by calibration. Each point represents the mean with a standard deviation of three BeO dosimeters.

3.2. Choice of CW-OSL stimulation time

Depopulating the OSL traps strongly depends on the optical stimulation equipments of readers, so it could be time-consuming for readers with moderate available stimulation power. For the luminescence reader used in this study, 300 s are necessary for a readout of the OSL signal to less than 1% of the initial intensity (in the first second of stimulation). As described in the introduction, shorter measurement times would be preferable and should also be feasible due to the necessity of thermal resetting when measuring higher doses. The exact value of the shorter readout time is somewhat arbitrary, it should ensure a suitable degree of sensitivity while noticeably reducing the time for dose assessment at the same time. Since TL peak 3 (250 °C - 400 °C) is known to be strongly related to the OSL signal at doses of tens of mGy (Bulur and Yeltik, 2010), the comparison of optical bleaching of this TL peak with the corresponding gain in OSL signal was used to choose the optical stimulation time for the BeO dosimeter. The OSL signals were recorded after 40 mGy irradiation in 30-s increments from the initial signal to 300 s. The average of the last 50 s was subtracted from each channel as background. The residual TL (R-TL) signal of TL peak 3, as shown in Fig. 4a, was measured immediately after each OSL measurement.

Fig. 4b shows the integrated OSL intensities together with integrated R-TL intensities of TL peak 3 after each OSL readout as a function of optical stimulation times. While the OSL signal is increasing, the corresponding residual TL signal has a sharp ~25% decrease in the first 30 s then continues to decrease at a slower rate and then stays almost stable at an intensity level of ~60% for illumination times larger than 100 s. This suggests that the optical stimulation time may be determined as 30 s, as a compromise between sufficient contribution from the main dosimetric trap and maximum gain in readout speed.

3.3. Short-term fading, preheating and readout protocol

The reduction in the OSL signal with time after irradiation due to the diminishing contribution of unstable shallow traps is interpreted as fading. These unstable signals can introduce uncertainty or dose underestimation, potential lowering the precision and accuracy of a dose assessment, hence effects on the OSL signal should be removed by a suitable preheating or time delay before readout.

The short-term fading of BeO dosimeters was investigated in laboratory conditions for different time intervals up to 1800 s as well as its dependence on preheating temperature. Five randomly selected BeO dosimeters were annealed at 700 °C for 5 min before irradiations at 40 mGy and 2 Gy and then stored for different time periods in the reader (dark conditions) before readout. OSL signals were measured with and without preheating at 160 °C for 10 s. The OSL signal of each dosimeter was then normalized to its initial OSL signal intensity and the average and standard deviation of the five normalized OSL signals from the five dosimeters calculated for each time interval.

After a storage time of 10 min, the integrated OSL intensity measured at short readout (30 s) and without preheating drops by ~3.4% for 40 mGy and ~31% for 2 Gy and then remains stable (Fig. 5). On the other hand, the preheat treatment significantly improves the results for both given doses for this readout time. When using the long OSL readings (300 s), more stable results on fading are obtained for both applied doses and preheating only has little influence. The standard deviation of the average OSL intensity after different storage times is 0.2% for 40 mGy and 0.8% for 2 Gy, for 30 s readouts after preheating. In addition, the preheat treatment also leads to a reduced standard deviation of the OSL response between dosimeters for a given storage time ("error bars" in Fig. 5) and the 30 s OSL readouts, which can lead to a more precise measurements among dosimeters. The mean standard deviation decreased from ~4.0% to ~1.9% for 40 mGy and from ~7.4% to ~2.9% for 2 Gy, after preheating at 160 °C. The large standard deviation for the 30 s WO PH data in Fig. 5 (b) is thus an indication of the large variability

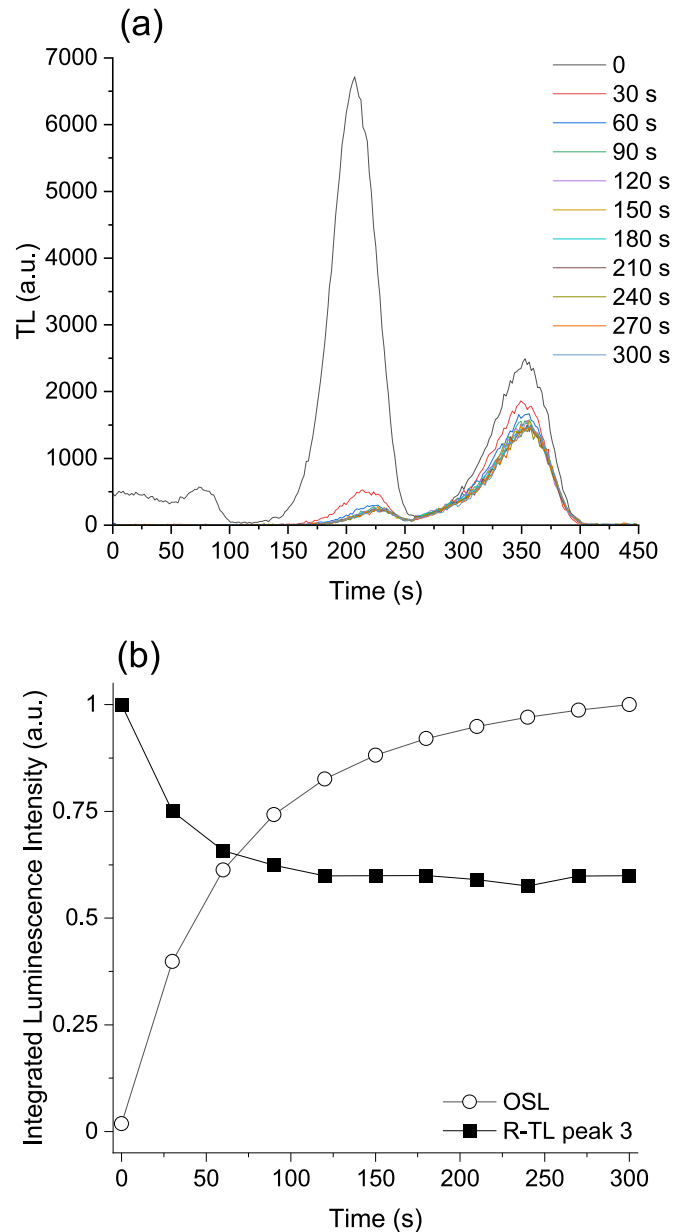


Fig. 4. (a): TL glow curve of a BeO dosimeter after optical bleaching. The time durations of optical stimulation are given in the legend. (b): integrated optically stimulated luminescence (OSL) and residual thermoluminescence intensities of TL peak 3 ("R-TL peak 3") as a function of stimulation time. The dosimeter was irradiated to a dose of 40 mGy.

in the degree of short-term fading of the OSL signal of the five dosimeters measured per data point and likely related to different defect concentrations of the electron trap involved in the different dosimeters. The time dependence of the signal fading, on the other hand, is the same for all dosimeters, leading to the high reproducibility of the average of the OSL signal in the same dataset (open circle symbols). Preheating thus removes the variability in the degree of fading between detectors and in this way leads to the reduced mean standard deviation mentioned above.

Fading of the fast OSL component of BeO within 10 min at room temperature was observed by Yukihiro et al. (2016) who reasonably argued that this is caused by shallow trapping centers but did not explicitly try to correlate this to the low temperature TL peak. In order to investigate this, the relationship between the TL peak 1 of the TL glow curve and the initial OSL signal was studied, using a BeO dosimeter

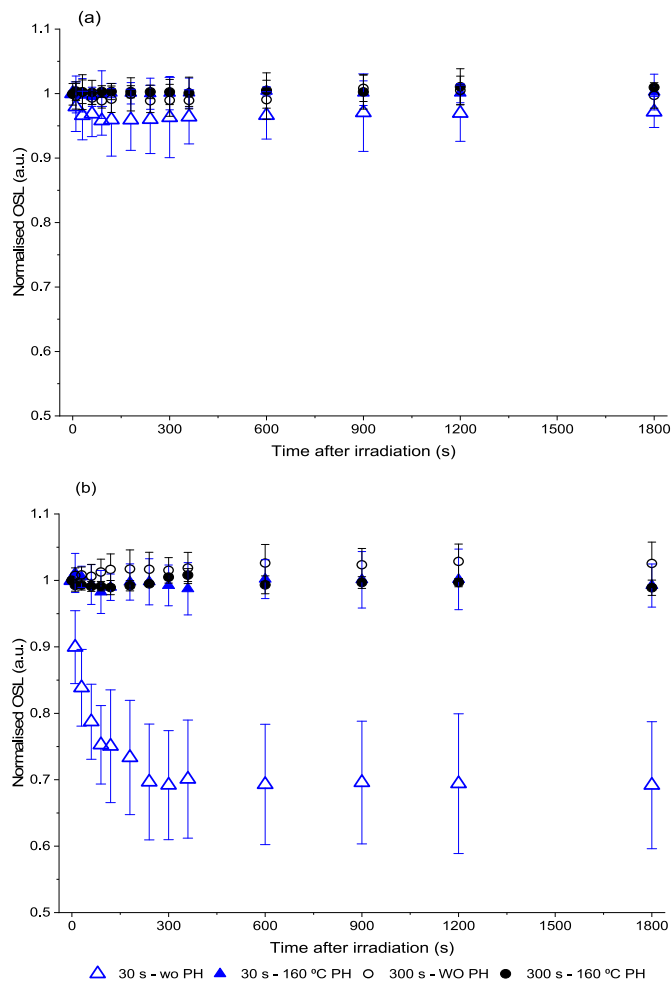


Fig. 5. Short-term fading of BeO dosimeters for short (30 s) and long (300 s) OSL readouts and for measurements carried out with and without preheating at 160 °C. Each data point represents the mean and standard deviation of five BeO dosimeters. Abbreviations describe the preheat treatment, WO PH: without preheating PH: with preheating at the given temperature. Panel (a) shows the results for a dose of 40 mGy, panel (b) for 2 Gy. The same five dosimeters were used for all measurements.

irradiated with a 40 mGy of beta dose. Then, OSL and TL signals were measured after different storage times, ranging from 0 to 30 min. OSL measurements were performed for 300 s with 0.1 s per channel for higher resolution, with and without preheating at 120 °C for 10 s. This lower preheat is sufficient to eliminate the possible contribution of TL peak 1. For data analysis, the OSL signal was integrated over the first 0.5 s for each delay time and the background (same integration interval but for the OSL signal after a delay time of 30 min) was subtracted.

Fig. 6a shows the effect of the different time delays on the TL glow curve of the BeO dosimeter. While TL peak 1 (0–120 °C) quickly fades almost completely within 10 min, TL peak 2 (120–250 °C) shows only a small but noticeable decrease in intensity. TL peak 3 (250–400 °C) stays almost unaffected. The net OSL signal of the BeO dosimeter which was not preheated (Fig. 6c) then was plotted against the peak areas of TL peak 1 for corresponding delay times. A value of $R^2 \sim 0.99$ indicates that a regression line fits the data well as an indicator of a good correlation between the thermal decay of TL peak 1 and the initial OSL signal (Fig. 6b). When additionally considering that TL peak 1 completely bleaches upon optical stimulation within less than a second (Fig. 6c), it seems likely that this TL peak and the fast initial OSL signal originate from the same trap.

To eliminate this unstable part of the OSL signal depicted in Fig. 6c,

preheating at 120 °C can be considered to be appropriate. However, choosing a higher preheat temperatures is necessary because of the minor decay of the unstable parts of TL peak 2, which seems to correlate with the minor decrease of the OSL signal after preheating at 120 °C with increasing time delay, as can be seen in Fig. 6a and d, respectively. The dose-response of TL peaks following beta irradiation was reported previously by Bulur (2007). TL peak 1 grows linearly up to a few hundred mGy and then saturates, while TL peak 2 shows a supralinear behavior after this range. At 40 mGy, the OSL signal beyond a stimulation time of 0.5 s almost completely originates from the trap responsible for TL Peak 3, the contribution from TL peak 2 is almost negligible. The small contribution from TL peak 1 in the first 0.5 s is already “diluted” for a signal integration time of 30 s and even more so for 300s. At 2 Gy, however, TL peak 2 has grown overproportionally with respect to TL peak 3, resulting in a noticeable contribution to the OSL signal. As TL peak 2 has a higher bleaching rate than TL Peak 3 (Fig. 4), the short-term fading of parts of TL Peak 2 is then more prominent for short OSL readout (30 s) and will be again “diluted” for longer readout times (300 s, Fig. 5 (b)). These suggested associations could explain why the fading of the OSL signal of BeO is both dose-dependent and dependent on the signal integration interval.

In summary, we conclude that the relative contribution of shallow (or instable) traps to the fast OSL component may increase with increasing doses while its contribution to total signal decreases if the OSL readout time is increased. Our results indicate that short-term fading of BeO for short OSL readings is dose-dependent. Consequently, to overcome instable results, dosimeters should undergo preheat treatment, in the present study we propose preheating for 10 s at 160 °C. This is consistent with previous notions that this can become a problem for very fast readings, particularly in medical applications (Sommer and Henniger, 2006; Yukihiro et al., 2016). It is concluded that fading in the first 10 min should be taken into account when calibrating the dosimeters for short reading, and a time delay or preheating should be applied.

Having established the time optimized thermal resetting procedure, the short readout times for OSL combined with the necessary preheating, this results in the measurement protocol illustrated in Table 1.

3.4. Reproducibility of BeO OSL dosimeters

Reproducibility can be dependent on degree of purity between dosimeters, and orientation of dosimeters in the planchet. To assess this, ten randomly selected dosimeters were irradiated with a beta dose of 40 mGy, followed by preheating at 160 °C and OSL read-out for 30 s. This sequence was repeated ten times while the dosimeters were staying in the reader, without being replaced. TL reading up to 450 °C (5°C.s^{-1}) was performed before each measurement for thermal resetting. The same reproducibility test was done by removing the dosimeters from the reader after OSL measurement and annealing them in the furnace at 700 °C for 5 min instead of the TL measurement, to evaluate any additional positioning error caused by replacing the dosimeters into the reader. This was done for doses of 40 mGy and 2 Gy (Fig. 7).

The dosimeter reproducibility does not appear to be dependent on the applied dose, but on the repositioning of the dosimeter as well as the annealing procedure. For both datasets with repositioning, the decrease in intensity in the first four to five cycles seems to be systematic rather than random, and then it stays almost constant with high reproducibility. For the dosimeters that stayed and were annealed in the reader, no such systematic effect is observed. This difference in behavior may be related to the difference in thermal treatment after each cycle, although there is no similar effect for the storage experiment in Fig. 5. More research is required to fully understand this issue. For the full datasets in Fig. 7, a relative standard deviation of the average OSL signal of $\sim 0.60\%$, $\sim 1.04\%$ and $\sim 1.13\%$ is calculated for the 40 mGy without repositioning, 40 mGy with repositioning and 2 Gy with repositioning datasets, respectively. The standard deviations of the ten dosimeters used per reading are illustrated by the “error bars” in Fig. 7 and are on average

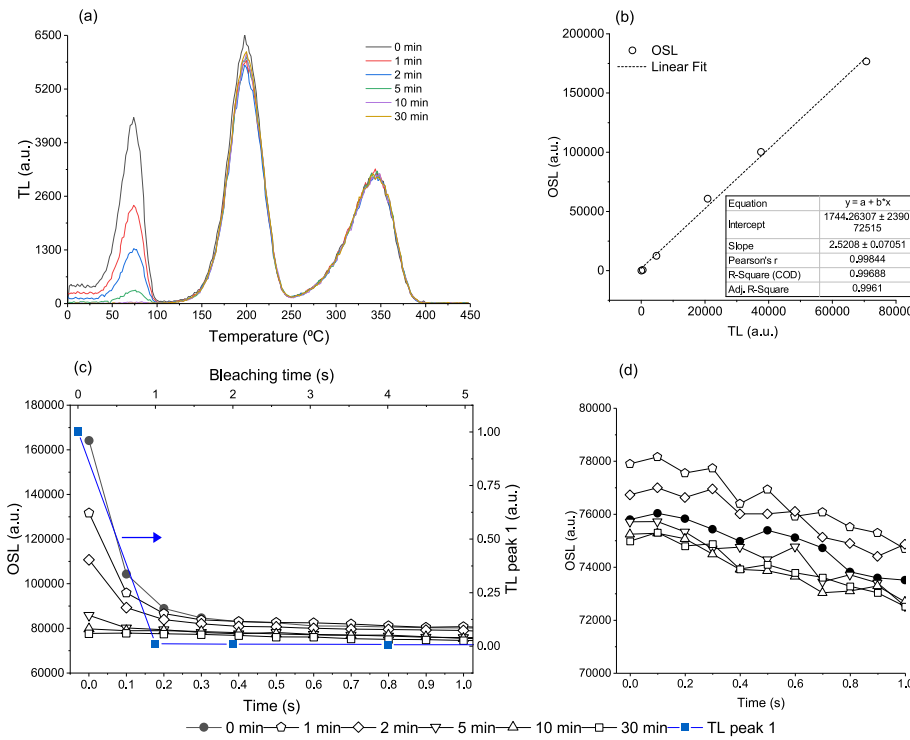


Fig. 6. (a): The effect of storage times on the TL glow curve of BeO; (b): correlation between the thermal decay of TL peak 1 and thermal decay of the OSL intensity of the initial, fast component (0–0.5 s), the dashed line is a linear regression model fitted to the data, the difference of the intercept to zero is statistically not significant; (c): OSL decay curves of BeO in the first second of optical stimulation, added is the optical bleaching of TL peak 1 (solid blue square symbols) over the same time period; (d) OSL decay curves in the first second of optical stimulation after preheating at 120 °C. Irradiations were performed with beta dose of 40 mGy.

Table 1
A read-out protocol for BeO.

1	Annealing at 700 °C for 5 min
2	Irradiation dose
3	Preheating at 160 °C for 10 s
4	OSL 30 s

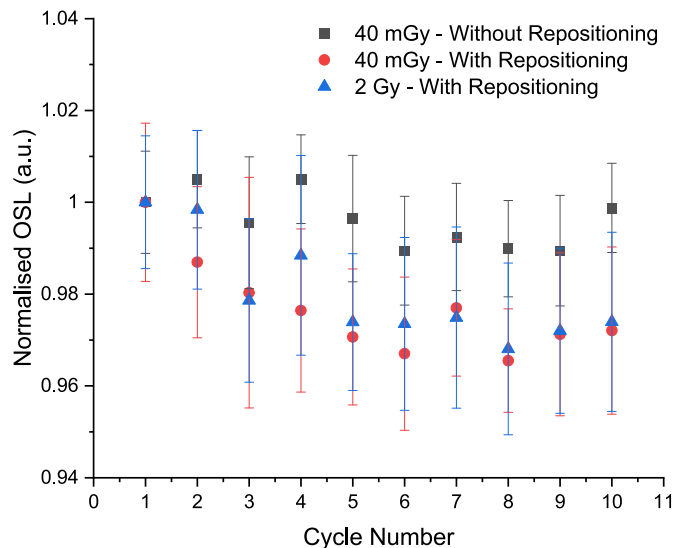


Fig. 7. Average OSL response from ten BeO dosimeters per cycle of thermal resetting, irradiation, preheating and measurement. Results are given for two doses and for cycles carried out completely in the equipment, with no removal of dosimeters in between (“without repositioning”) and for cycles with external thermal resetting and repositioning of dosimeters (“with repositioning”). Error bars represent the standard deviation between the dosimeters. For each dataset OSL responses were normalized to the respective value of the first cycle.

1.1%, 1.7%, and 1.8%, respectively. Handling of the dosimeters outside the equipment and repositioning thus increases the uncertainty from about 0.6 to 1.1%.

3.5. Energy and angular dependency

Knowledge of the energy dependence and the angular response of dosimeters is important for accurate dose measurements in medical applications by using the OSL technique. As described in the introduction, different results have been published in the literature concerning the energy dependence of BeO, measured using discrete photon energies and beams, and the agreement with theoretical values (Jahn et al., 2014; Malthez et al., 2014; Sommer and Henniger, 2006). We thus reinvestigated this issue with the BeO dosimeters from our production batch.

Three BeO dosimeters were annealed at 700 °C for 5 min before 5 mGy irradiation with different X-ray qualities and ^{137}Cs (see Material and Methods section). OSL measurements were performed for 300 s after preheating at 160 °C for 10 s. Results are given for three different integration times of the OSL signal: 1, 30 and 300 s. The responses of the dosimeters were normalized to the response at an energy of 662 keV (^{137}Cs). The experimental data were compared to the calculated energy dependence based on the ratio of the mass energy absorption coefficients of BeO and air. Results are shown in Fig. 8.

One can see that that the general trend known from the literature is reproduced, namely that there is a minor underresponse for lower photon energies. Except for the lowest photon energy (24 keV), the measured OSL response is on average somewhat higher than the calculated values, but the difference is small: The measured OSL response for 300 s OSL integration time is on average 1.1% higher and for 30 s and 1 s integration times on average 3.0% and 3.1% than calculated, respectively. Maximum deviation is observed for N-80 (65 keV), where the measured response for 30 s and 1 s integration intervals is about 8% higher than the theoretical value. This is markedly different from the results reported in Jahn et al. (2014), where for photon energies of 100 keV and lower, an OSL response was measured that was on average 25% lower than simulated. Also in Malthez et al. (2014), one can roughly estimate from their Fig. 2 an underresponse at 40–50 keV of

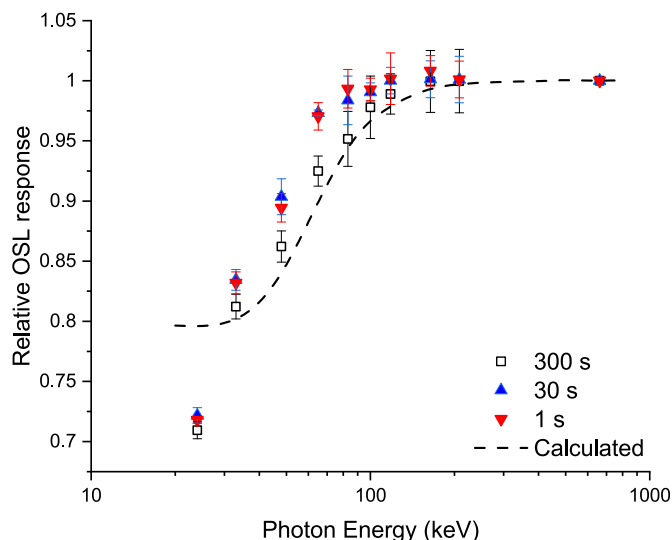


Fig. 8. Measured energy dependence of BeO dosimeters for three different integration intervals, given in the legend. Error bars represent the standard deviation of three dosimeters for each energy measurement. Irradiations were performed with dose of 5 mGy (air kerma). The dashed line is the ratio between the mass-energy absorption coefficients μ_{en}/ρ for BeO and air, normalized at 1250 keV (see Section 2.3).

around 0.7, which is significantly smaller than here. On the other hand, our results agree with the results in Sommer et al. (2007) and in Sommer and Henniger (2006) and this indicates that the actual photon energy dependence of BeO may vary according to the production batch used. In Jahn et al. (2104), the discrepancy between measured and simulated energy dependence was explained and successfully modeled by a reduced OSL efficiency due to local saturation effects. One may thus speculate that the differences in energy response are related to differences in defect concentration, which should manifest itself in differences in sensitivity (when using the same equipment). From a practical point of view, it seems advisable to either measure the energy dependence of one's sample set before applications or to use the same radiation quality and setup for calibrating the dosimeters that is then used for monitoring the actual dose (if feasible). The low standard deviation between dosimeters in this and the cited works indicate that the energy response for frontal irradiation is homogeneous within one production batch, therefore it is sufficient to measure a small sample set.

As mentioned above, there is a minor but noticeable difference in energy response in Fig. 8 for the shorter readouts (1 and 30 s), compared to the long readout time of 300 s, which is somewhat more pronounced than the one observed in Malthez et al. (2014). If the suggestion in Sommer et al. (2008) is adopted, that the OSL decay curve is a result of optical attenuation of stimulated and emitted light, then shorter OSL readout will predominantly measure the nearer surface layer and the longer readout times more the bulk of the dosimeter. In this case, the dependence of the energy response on the stimulation time might be explained by non-homogeneous defect concentration within the material. Again from a practical point of view, the shorter readout in our case has the additional advantage of reducing, albeit on a small scale, the underresponse of BeO for lower photon energies.

Further studies should address the variations in energy response as a function of scan parameters in clinical applications.

The angular dependence of BeO dosimeters was investigated by irradiating the dosimeters with 5 mGy at different X-ray qualities between N30 to N250 and at different angles of incidence. Dosimeters were read out with preheating at 160 °C before OSL for 30 s. Relative OSL responses at angles of -60°, -30°, 0°, 30° and 60° were normalized to the one at 0°. In Fig. 9, each data point represents the mean of the response of five BeO OSL dosimeters. For the sake of clarity, error bars

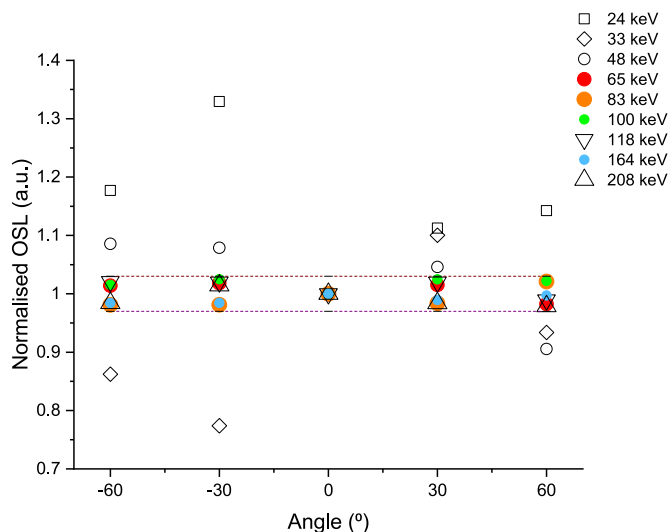


Fig. 9. Angular response of BeO dosimeters, normalized to the response at 0° (frontal irradiation). Irradiations were performed with dose of 5 mGy. Each data point is the average of the response of five dosimeters, standard deviations were omitted for the sake of clarity. The dotted lines indicate the range of $\pm 3\%$ around unity.

are not shown in the graph. The data shown in Fig. 9 demonstrate that the BeO dosimeters show a small angular dependence of only $\sim 3\%$ for the investigated angles and energies from 208 keV (N-250) down to 65 keV (N-80). The relative standard deviations of the angular responses for a given energy in this energy range range from 0.8% to 1.7%, with an average value of 1.3%. These values are close to the values of the reproducibility of an OSL measurement for irradiations with a fixed calibration source (here the in-built beta source of the reader; section 3.4), therefore the angular dependence is not expected to add significant uncertainty to an actual dose measurement in this case. For lower photon energies however, the scatter can increase up to around 30% and could become the dominating source of uncertainty. This can have implications for the achievable precision for applications in diagnostics. The reasons for this behavior are at present not fully clear but might again be found in the combination of local saturation effects for lower LET and differences in defect concentration throughout the material. It will be important to see in future studies, if similar effects occur for BeO dosimeters from other production batches and whether the experimental data can be successfully reproduced by an appropriate model for a better understanding of the underlying mechanism.

4. Conclusion

In this work, several prominent dosimetric properties have been discussed for BeO and were characterized by investigating its annealing temperature and duration, the effect of preheat treatment on short-term fading, energy, and angular dependence. Our results indicate that shorter annealing and readout times are possible, enabling faster dose assessment, especially when using equipment with moderate OSL stimulation power ($\sim 30 \text{ mW cm}^{-2}$), but in this case preheating is necessary to avoid dose underestimation. Reproducibility when dosimeters are repositioned in the equipment was found to be around 1.1% when using the developed protocol. A variation was observed between the measured energy response in this work and published results, indicating that either a batch-dependent assessment of the energy response or an exact correspondence between calibration setup and dose measurement setup is necessary to avoid systematic errors. For photon energies above $\sim 60 \text{ keV}$, the angular dependence will not substantially add to the overall dose uncertainty budget but for lower photon energies, the variation in relative response can increase up to 30%. This

needs to be further investigated with respect to application in medical diagnostics. Despite some of the issues found it can still be concluded that BeO is convenient for dosimetry applications, also in the medical field and has practical features which are comparable to those of other OSL materials.

Declaration of competing interest

The authors declare that they have no known competing financial interests or personal relationships that could have appeared to influence the work reported in this paper.

Data availability

Data will be made available on request.

Acknowledgements

EK especially would like to thank Prof. Dr. Werner Ruehm for valuable advice and his guidance.

EK gratefully acknowledges the financial support of the Study Abroad Postgraduate Education Scholarship (YLSY) awarded by the Republic of Türkiye Ministry of National Education.

References

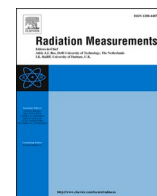
- Aşlar, E., Şahiner, E., Polymeris, G.S., Meriç, N., 2020. Feasibility of determining Entrance Surface Dose (ESD) and mean glandular dose (MGD) using OSL signal from BeO dosimeters in mammography. *Radiat. Phys. Chem.* 177, 109151. <https://doi.org/10.1016/J.RADPHYSCH.2020.109151>.
- Bos, A.J.J., 2001. High sensitivity thermoluminescence dosimetry. *Nucl. Instrum. Methods Phys. Res. Sect. B Beam Interact. Mater. Atoms* 184, 3–28. [https://doi.org/10.1016/S0168-583X\(01\)00717-0](https://doi.org/10.1016/S0168-583X(01)00717-0).
- Bulur, E., 2007. Photo-transferred luminescence from BeO ceramics. *Radiat. Meas.* 42, 334–340. <https://doi.org/10.1016/j.radmeas.2007.02.065>.
- Bulur, E., Göksu, H.Y., 1998. OSL from BeO ceramics: new observations from an old material. *Radiat. Meas.* 29, 639–650. [https://doi.org/10.1016/S1350-4487\(98\)00084-5](https://doi.org/10.1016/S1350-4487(98)00084-5).
- Bulur, E., Yeltik, A., 2010. Optically stimulated luminescence from BeO ceramics: an LM-OSL study. *Radiat. Meas.* 45, 29–34. <https://doi.org/10.1016/j.radmeas.2009.08.007>.
- Chen, R., Hornyak, W.F., Mathur, V.K., 1990. Competition between excitation and bleaching of thermoluminescence. *J. Phys. D Appl. Phys.* 23, 724–728. <https://doi.org/10.1088/0022-3727/23/6/015>.
- Crase, K.W., Gammage, R.B., 1975. Improvements in the use of ceramic BeO for TLD. *Health Phys.* 29, 739–746. <https://doi.org/10.1097/00004032-197511000-00014>.
- Henaish, B.A., Sayed, A.M., Morsy, S.M., 1979. Light influence on thermoluminescent BeO and other TL-phosphors. *Nucl. Instrum. Methods* 163, 511–517. [https://doi.org/10.1016/0029-554X\(79\)90140-X](https://doi.org/10.1016/0029-554X(79)90140-X).
- International Organization for Standardization (ISO), 1996. X and Gamma Reference Radiation for Calibrating Dosimeters and Doserate Meters and for Determining Their Response as a Function of Photon Energy/Part 1: Radiation Characteristics and Production Methods. ISO, Geneva, 4037-1.
- Jahn, A., Sommer, M., Henniger, J., 2014. OSL efficiency for BeO OSL dosimeters. *Radiat. Meas.* 71, 104–107. <https://doi.org/10.1016/J.RADMEAS.2014.03.024>.
- Malthez, A.L.M.C., Freitas, M.B., Yoshimura, E.M., Button, V.L.S.N., 2014. Experimental photon energy response of different dosimetric materials for a dual detector system combining thermoluminescence and optically stimulated luminescence. *Radiat. Meas.* 71, 133–138. <https://doi.org/10.1016/J.RADMEAS.2014.07.018>.
- McKeever, S.W.S., 2001. Optically stimulated luminescence dosimetry. *Nucl. Instrum. Methods Phys. Res. Sect. B Beam Interact. Mater. Atoms* 184, 29–54. [https://doi.org/10.1016/S0168-583X\(01\)00588-2](https://doi.org/10.1016/S0168-583X(01)00588-2).
- McKeever, S.W.S., 1994. Models for optical bleaching of thermoluminescence in sediments. *Radiat. Meas.* 23, 267–275. [https://doi.org/10.1016/1350-4487\(94\)90051-5](https://doi.org/10.1016/1350-4487(94)90051-5).
- Rodriguez, M., Yukihiro, E., Ahmad, S., Ruan, C., 2012. MO-F-213CD-04: characterization of optically stimulated luminescence detectors for organ dose phantom measurement in diagnostic radiology. *Med. Phys.* 39. <https://doi.org/10.1118/1.4735829>, 3877–3877.
- Şahin, S., Şahiner, E., Göksel, F., Meriç, N., 2020. Comprehensive evaluation of electron radiation dose using beryllium oxide dosimeters at breast radiotherapy. *J. Radiother. Pract.* 19, 38–44. <https://doi.org/10.1017/S1460396919000190>.
- Santos, A.M.C., Mohammadi, M., Afshar, V.S., 2015. Evaluation of a real-time BeO ceramic fiber-coupled luminescence dosimetry system for dose verification of high dose rate brachytherapy. *Med. Phys.* 42, 6349–6356. <https://doi.org/10.1118/1.4931968>.
- Sommer, M., Jahn, A., Henniger, J., 2008. Beryllium oxide as optically stimulated luminescence dosimeter. *Radiat. Meas.* 43, 353–356. <https://doi.org/10.1016/j.radmeas.2007.11.018>.
- Sommer, M., Freudenberg, R., Henniger, J., 2007. New aspects of a BeO-based optically stimulated luminescence dosimeter. *Radiat. Meas.* 42, 617–620. <https://doi.org/10.1016/j.radmeas.2007.01.052>.
- Sommer, M., Henniger, J., 2006. Investigation of a BeO-based optically stimulated luminescence dosimeter. *Radiat. Protect. Dosim.* 119, 394–397. <https://doi.org/10.1093/rpd/nci626>.
- Souza, L.F., Novais, A.L.F., Antonio, P.L., Caldas, L.V.E., Souza, D.N., 2019. Luminescent properties of MgB4O7:Ce, Li to be applied in radiation dosimetry. *Radiat. Phys. Chem.* 164, 108353. <https://doi.org/10.1016/j.radphyschem.2019.108353>.
- Yagui, A., Malthez, A.L.M.C., Filipov, D., 2020. Dose evaluation in pediatric gastrointestinal fluoroscopy. *Radiat. Phys. Chem.* 167, 108384. <https://doi.org/10.1016/J.RADPHYSCH.2019.108384>.
- Yukihiro, E.G., Andrade, A.B., Eller, S., 2016. BeO optically stimulated luminescence dosimetry using automated research readers. *Radiat. Meas.* 94, 27–34. <https://doi.org/10.1016/j.radmeas.2016.08.008>.
- Yukihiro, E.G., Gasparian, P.B.R., Sawakuchi, G.O., Ruan, C., Ahmad, S., Kalavagunta, C., Clouse, W.J., Sahoo, N., Titt, U., 2010. Medical applications of optically stimulated luminescence dosimeters (OSLDs). *Radiat. Meas.* 45, 658–662. <https://doi.org/10.1016/J.RADMEAS.2009.12.034>.
- Yukihiro, E.G., Kron, T., 2020. Applications of optically stimulated luminescence in medical dosimetry. *Radiat. Protect. Dosim.* 192, 122–138. <https://doi.org/10.1093/rpd/ncaa213>.

9. Publication II

Correlation between thermoluminescence and optically stimulated luminescence signal in BeO, Kara and Woda (2023b).

Elif Kara, Clemens Woda.

10.1016/j.radmeas.2023.107049.



Correlation between thermoluminescence and optically stimulated luminescence signal in BeO

Elif Kara^{a,*}, Clemens Woda^b

^a Helmholtz Zentrum München-German Research Center for Environmental Health, Institute of Radiation Medicine, Neuherberg, Germany

^b Federal Office for Radiation Protection (BfS), Neuherberg, Germany

ARTICLE INFO

Keywords:

Beryllium oxide (BeO)
Optically stimulated luminescence (OSL)
Thermoluminescence (TL)
Residual thermoluminescence (R-TL)
Bleaching
Decay constant

ABSTRACT

Beryllium Oxide (BeO) is a promising dosimetric material that is rapidly becoming an essential instrument in Optically Stimulated Luminescence (OSL) dosimetry applications. Despite the potential of BeO as a luminescence dosimeter, gaps remain in understanding how its Thermoluminescence (TL) and Optically Stimulated Luminescence (OSL) signals are connected. Our study aimed at examining Residual Thermoluminescence (R-TL) glow curves after various bleaching times to find an association between TL traps and OSL components across a wide range of doses, at 40 mGy and from 10 to 100 Gy. OSL decay curves and intensities of R-TL glow curves were fitted to either pure exponential decay functions or to stretched exponential decay functions, due to optical attenuation, to determine the OSL components and the bleaching decay rates of each TL peak, respectively. A good correlation between the decay rates of the OSL components and bleaching decay rates of each TL peak for both high and low-dose irradiations was found only for the model functions considering optical attenuation in the material. Taken together, this qualitative method helped to identify various traps, and results revealed a more consistent luminescence mechanism between TL and OSL signals than was previously assumed. Further support for the correlation between TL and OSL was derived from thermal stability studies of the OSL signal and from the dose response of the TL peaks and the OSL signal after different thermal pretreatments. Different bleaching models were discussed to define the appropriate one for BeO. These results may enhance our understanding of BeO as a dosimeter.

1. Introduction

BeO has been suggested as a luminescence dosimeter as early as 1969/1970 (Rhyner and Miller, 1970; Tochilin et al., 1969), however it was not until the rediscovery of this material as potential OSL dosimeter with modern equipment (Bulur and Göksu 1998) that BeO received attention as serious candidate for dosimetric applications by the scientific community. The TL glow curve of BeO consists of three distinct peaks, which are located between 50 and 120 °C (peak 1), 150–260 °C (peak 2), and 260–400 °C (peak 3). The light sensitivity of the TL glow curve has implied the potential use of BeO as an OSL dosimeter. Moreover, it has increasingly drawn attention in OSL applications due to its favorable characteristics, particularly its nearly tissue-equivalence (Bos, 2001; Sommer et al., 2007; Watanabe et al., 2010). However, the luminescence mechanism for TL and OSL signals are not fully understood and this can potentially complicate its adoption in dosimetry applications (Bulur, 2007).

The possible correlation between the traps responsible for the individual TL peaks and those for the OSL signal in BeO has been investigated by (Polymeris et al., 2021; Aşlar et al., 2019; Bulur and Göksu, 1998; Bulur and Saraç, 2013; Yukihiro, 2011). The strong bleachability of TL peaks 1 and 2 suggested that these peaks might be associated with the OSL signal. However thermal stability studies of the OSL signal after irradiation with 200 mGy demonstrated that the signal is unaffected by preheating up to 250 °C, implying that TL peak 3, despite being only poorly bleachable, carries a major contribution to the OSL signal (Yukihiro, 2020). At a dose of 50 Gy, however, the same thermal stability test for the OSL signal showed a two-step profile in signal decrease, with a first drop in OSL intensity starting at a preheat temperature of 150 °C and lasting until 220 °C, which is the temperature region in which TL peak 2 is located (Bulur and Saraç, 2013). To resolve this apparent discrepancy, Yukihiro (2020) proposed that optically active traps located in TL peak 3 region saturate at lower doses, and thus the contribution of the optically active traps of TL peak 2 (located between

* Corresponding author.

E-mail address: kara.elifk@gmail.com (E. Kara).

<https://doi.org/10.1016/j.radmeas.2023.107049>

Received 12 July 2023; Received in revised form 2 December 2023; Accepted 11 December 2023

Available online 15 December 2023

1350-4487/© 2023 Elsevier Ltd. All rights reserved.

150 °C and 220 °C) to the OSL signal becomes visible at higher doses. Experimental evidence to confirm this hypothesis has so far not been produced.

Aşlar et al. (2019) studied the correlation between unbleached and bleached TL peaks (after 400s of optical stimulation), the OSL signal and ESR centers of the BeO dosimeter at 30 Gy by using a step annealing test. The OSL signal was fitted by a sum of two main components, denoted as C1 and C2. The authors inferred that TL peak 2 could be correlated with the OSL component C1 and TL peak 3 with C2. Moreover, TL peak 2 was considered as to be more relevant to the OSL signal at this dose. In the study of Polymeris et al. (2021), the dose-response of TL and OSL signals was investigated up to 4 Gy for varying irradiation temperatures for TL, and different measurement temperatures and preheating conditions for OSL. Intense supralinearity was observed for TL peak 2, whereas TL peak 3 displayed linearity only at an irradiation temperature of 200 °C. From the analysis of the dose-response of the component-resolved OSL signal, it was suggested that TL peak 3 serves as the origin for the charge of the first OSL component, C1. The supralinearity was ascribed to the competition for free electrons by electron traps, which occurs during both irradiation and stimulation.

Bulur and Yeltik (2010) fitted both the CW-OSL and LM-OSL curve of BeO for doses in the mGy range to the sum of two first order components but at the same time questioned the validity of this approach, as BeO is known to be a strong optical diffusor (Lembo et al., 1990). The latter aspect was considered by Sommer et al. (2008), who showed that in this case an extended exponential decay function for the OSL signal of a single trap is obtained. Since the emphasis in that work was on medical applications, the relevance of this result for investigating the correlation between TL and OSL was not explored. Generally, to date, correlation studies between the luminescence mechanisms of TL and OSL in BeO are still scarce. One approach to investigate possible correlations is to fit the Residual Thermoluminescence (R-TL) glow curves remaining after bleaching of the TL signal as a function of various bleaching times to obtain the bleaching decay rates for each TL peak. If the same approach is applied to the OSL decay curve, OSL components that are associated with bleaching decay rates of each TL peak may yield valuable insights into the traps, as investigated in the correlation studies of KMgF3:Ce+3 by Dallas et al. (2010).

In the present study, to better understand the relationship between OSL and TL signals of BeO, R-TL glow peak intensities were measured at different bleaching times for doses of 40 mGy and 10 Gy–100 Gy. These data sets and the corresponding OSL decay curves were fitted to exponential decay functions, based on models with and without optical attenuation. For the latter, the approach described in Sommer et al. (2008) for OSL was adapted to the experimental setup used in this work and also expanded to TL. The obtained bleaching decay rates of the individual TL peaks were then compared to those of the OSL components, to investigate possible correlations and to decide which model might be more appropriate. Different bleaching models were also discussed in this context. In addition, the dose response of the TL signals and of OSL signals after different pretreatments were compared over the same wide dose range to further corroborate possible correlations and to decide, which mechanism most likely explains the difference in OSL step annealing tests at 40 mGy and high doses.

2. Materials and methods

2.1. BeO dosimeter

Square-shaped BeO dosimeters, provided by Dosimetrix GmbH (now Mirion Technologies (AWST) GmbH), were used in this study, with dimensions ~4.7 mm x ~4.7 mm and a thickness of ~0.5 mm. The same dosimeter chip was used throughout the study, except for the results for 40 mGy, which were obtained on a number of dosimeters (from the same production batch).

2.2. OSL and TL readings

Luminescence readings and irradiations were performed on an automated luminescence reader (model Risø TL/OSL-DA-15) equipped with a $^{90}\text{Sr}/^{90}\text{Y}$ beta source (1.48 GBq). Calibration of the beta source of the reader for the BeO dosimeters was performed with a ^{137}Cs source at the Radiation Facilities of the Helmholtz Zentrum München, Germany (~20 mGy s⁻¹). Optical stimulation was provided by using blue light emitting diodes (LEDs) at 470 nm with an intensity of 45 mW cm⁻² at the sample position. The reader includes a 9235QB bialkali photomultiplier tube (PMT) from ET Enterprises and Hoya U-340 filter for the detection of the luminescence signal. OSL readings were performed at room temperature with 90% power intensity of LEDs. TL readings were recorded up to 450 °C in the N₂ atmosphere and the heating rate was 5 °C.s⁻¹. For doses of 10 Gy and higher, a cardboard with a pinhole was placed in front of the PM tube to avoid overexposure during luminescence measurement. The residual TL glow curve was recorded after OSL stimulation for different periods of time, which is referred to as bleaching times throughout this study. For the analysis in this work, Peak 1 was integrated between 50 and 120 °C, Peak 2 from 120 °C to 260 °C and Peak 3 between 320 °C and 400 °C.

2.3. Experimental protocol

The sequence used to obtain R-TL glow curves after various bleaching times can be seen in Table 1. All irradiations were performed in the Risø reader. For doses of 10 Gy and larger, the BeO dosimeter was annealed in a muffle furnace at 700 °C for 5 min to eliminate dose history and to restore the initial sensitivity before each measurement. For a dose of 40 mGy, thermal resetting in the Risø reader by using TL readings up to 450 °C at 5 °C.s⁻¹ was sufficient.

The bleaching to obtain the R-TL glow curve was applied at 2-s intervals up to the first 10 s to have more data points in the fitting process. After 20 s, the measurements were taken at 20-s intervals up to 300 s. The same bleaching times were applied to the BeO chip after irradiation with different doses, varying from 10 to 100 Gy.

2.4. Definition of the bleaching decay rates

Comparing bleaching decay rates of each TL peaks with OSL components can be a simple way to capture underlying information about the luminescence characteristics of the material.

In order to be able to study the bleaching decay rates, the areas under the different peaks in the R-TL curves were plotted as a function of various bleaching times. For the one trap and one recombination center model the rate equation for the trapped charge concentration under optical stimulation (bleaching), assuming negligible retrapping (first order kinetics), is the following:

$$\frac{dn}{dt} = -nf(\lambda). \quad (1)$$

The bleaching rate is given by the inverse of the characteristic time τ (in s):

Table 1

Sequence used to measure the R-TL glow curves.

Steps	Applied sequence
1	Annealing
2	Irradiation
3	TL
4	Annealing
5	Irradiation
6	Bleaching by OSL reading
7	R-TL
8	Annealing
9	Repeat of steps 5–8 with increment in the bleaching time

$$\tau^{-1} = f(\lambda) = \sigma(\lambda)\varphi(\lambda), \quad (2)$$

where φ is the photon fluence ($\text{m}^2 \cdot \text{s}^{-1}$), σ the photoionization cross section (m^2) and n the concentration of the trapped charges (m^3). For both R-TL and OSL, the solution of equation (1) leads to an exponential function of the form:

$$I(t) = I_0 e^{-t/\tau} + y_0, \quad (3)$$

where I_t is the intensity of either the OSL signal or the integrated TL peak at time t , I_0 the intensity at $t = 0$ and y_0 a constant that is added here to consider instrumental background and hard-to-bleach or unbleachable components. For several non-interacting bleachable traps with different cross sections, equation (3) will change to the sum of several exponential functions, one for each trap (component). In the case of the OSL measurements, τ was considered as the characteristic time of one OSL component, whereas τ^{-1} was interpreted as the bleaching decay rate for Residual TL readings. The OriginLab 2022 software was used for fitting exponential functions to the different data sets.

2.5. Attenuation of light by the material

A known problem concerning the luminescence of BeO is attenuation of both stimulation and luminescence light (Lembo et al., 1990; Sommer et al., 2007, 2008). For rock surface dating using quartz, (Sohbati et al., 2011; Gray and Mahan, 2015) considered attenuation of bleaching sunlight into the rock using the Lambert-Beer law, while OSL measurements were done on extracted grains. For BeO, depending upon thickness of the dosimeter, part of the emitted luminescence light may additionally be absorbed by the material itself. Sommer et al. (2008) gave an equation for the OSL signal in this case for the specific experimental setup used (e.g. stimulation from one side of the chip and measurement from the other). Here, a similar simplified approach is derived for the measurement setup of the Risø reader, where the dosimeter is stimulated and measured from the same side. The methodology is then also expanded to TL measurements.

Lambert-Beer law describes the absorption of light in a solid according to:

$$I(\lambda, x) = I_0(\lambda) e^{-\mu x} \quad (4)$$

where $I_0(\lambda)$ is the intensity of the incident light at the surface, $I(\lambda, x)$ the intensity at depth x (mm) in the solid and μ (mm^{-1}) the absorption coefficient. The stimulating photon flux φ varies with depth x into the BeO dosimeter by applying the Lambert-Beer law:

$$\varphi(\lambda, x) = \varphi_0(\lambda) e^{-\mu_s x}, \quad (5)$$

where μ_s refers to the absorption coefficient for the wavelength region of the stimulating light. The bleaching rate at depth x in the detector can then be expressed as:

$$f(\lambda, x) = \sigma(\lambda)\varphi_0(\lambda) e^{-\mu_s x}. \quad (6)$$

The solution of equation (1) is now:

$$n(t, x) = n_0(x) \bullet e^{-f(\lambda, x)t}. \quad (7)$$

The initial trap concentration $n_0(x)$ is given here as a function of depth to consider possible dose gradients in the sample. The OSL signal emitted from the infinitesimally thin layer at depth x is:

$$I_{OSL}(t, x) = -\frac{\partial n}{\partial t} = n(t, x)f(\lambda, x). \quad (8)$$

At the surface of the chip dosimeter, the attenuated OSL intensity $I_{OSL}^S(t, x)$ is recorded:

$$I_{OSL}^S(t, x) = I_{OSL}(t, x) \bullet e^{-\mu_E x} = (n_0(x) \bullet e^{-\sigma(\lambda)\varphi_0(\lambda)e^{-\mu_s x}t}) (\sigma(\lambda)\varphi_0(\lambda)e^{-\mu_s x})(e^{-\mu_E x}) \quad (9)$$

where μ_E refers to the absorption coefficient of the emitted light for the wavelength region transmitted through the optical filter in front of the PMT. The total OSL signal recorded from the sample is then:

$$I_{OSL}(t) = \frac{1}{d} \bullet \tau^{-1} \bullet \int_0^d n_0(x) \bullet e^{-(\mu_E + \mu_s)x} e^{-\frac{(\sigma(\lambda)\varphi_0(\lambda))t}{\tau}} dx, \quad (10)$$

where d is the thickness of the dosimeter, and $\sigma(\lambda)\varphi_0(\lambda)$ was set as τ^{-1} (see equation (2)). It can be directly seen, that if dose gradients and optical attenuation are negligible ($\mu_s = \mu_E = 0$), equation (10) reduces to equation (3) (setting $I_0 = n_0 / \tau$), as should be.

By measuring the attenuation of transmitted light through a thin (0.225 mm) BeO chip, (Lembo et al., 1990) showed that at 350 nm the light intensity was reduced to 36% and at 450 nm to 44% of the initial intensity. The transmission can be expressed as $I(d)/I(0)$, where $I(d)$ is the intensity of light after traversing through the chip of thickness d . The connection between transmission and the optical attenuation coefficient it then simply given by,

$$T = I(d)/I_0 = e^{-\mu d} \quad (11)$$

The ratio $\frac{\mu_s}{\mu_E}$ can thus be estimated from the transmission data as approximately 0.8, so a 20% lower value for μ_s compared to μ_E . Using the value of $(2.69 \pm 0.15) \text{ mm}^{-1}$ for μ_E , determined in Lembo et al. (1990), a value of approximately 2.2 mm^{-1} for μ_s was estimated.

In case of TL, the glow curve is not measured during bleaching but after a certain optical stimulation time t . The number of filled traps remaining in an infinitesimally thin slice at depth x after this optical stimulation time is the same as for OSL and is given by equations (6) and (7). In contrast to OSL, all horizontal slices in the dosimeter will be stimulated with the same efficiency in TL, if thermal gradients within the dosimeter can be neglected. The light emitted by thermal stimulation from each of these slices on the other hand will be attenuated in the same way as for OSL:

$$S_{TL}(T, x) = S_{TL,u}(T) \bullet e^{-\mu_E x}, \quad (12)$$

Where $S_{TL}(T, x)$ is the signal of the glow curve due to the slice at depth x , and $S_{TL,u}(T)$ the signal of the unattenuated glow curve at temperature T . Since for data analysis the glow curve is integrated and since the area under the unattenuated glow curve is equal to the number of filled traps before thermal stimulation, the result for the integrated TL intensity from the slice at depth x is:

$$I_{TL}(t, x) = \int S_{TL}(T, x) dT = \int S_{TL,u}(T) dT \bullet e^{-\mu_E x} = n_0(x) \bullet e^{-\mu_E x} e^{-\Phi_0 \bullet e^{-\mu_s x} \sigma t}. \quad (13)$$

The total integrated TL intensity of the sample after optical stimulation time t is then:

$$I_{TL}(t) = \frac{1}{d} \int_0^d n_0(x) \bullet e^{-\mu_E x} e^{-\frac{(\sigma(\lambda)\varphi_0(\lambda))t}{\tau}} dx, \quad (14)$$

where again $\sigma\varphi_0 = \tau^{-1}$ was used.

The integrals in equations (10) and (14) can only be solved numerically. This was implemented in the fitting algorithm of the OriginLab 2022 software (assuming that n_0 is independent of the depth in the detector and thus can be treated as a constant) and then applied to the experimental results. The uncertainty in μ_E (and correspondingly in μ_s) was not considered. Similar to the model without optical attenuation, the results can be expanded to the case of two types of traps with different photoionization cross sections and a constant to consider hard-to-bleach or unbleachable components plus instrumental background can be added.

2.6. Background for bleaching models

A comprehensive review of three bleaching models that evaluate the residual TL intensities as a function of bleaching time was undertaken by [McKeever \(1994\)](#) to examine the luminescence behavior of sediments. First, [Levy \(1982\)](#) used the assumption of the presence of several electron traps which may cause retrapping of charges in these traps or recombination with holes in the recombination center during excitation to explain the decrease in the TL intensity after bleaching. In this model, the TL peak can be represented by non-first-order kinetics and decays to zero for sufficiently long bleaching times. The model proposed by [Chen et al. \(1990\)](#) introduces a single electron trap and a single recombination center, where optical stimulation, or bleaching, can remove electrons from both entities. The optical stimulation can remove electrons not only from electron traps but also from recombination centers situated near the valance band, thus the concentration of holes at recombination centers increases during illumination. As a consequence, the subsequent residual thermoluminescence (R-TL) signal is unaffected by the initial trap population and cannot be reduced to non-zero intensity. Besides, a single electron trap and single recombination center are assumed in this model therefore peak position changes are not expected. [McKeever \(1994\)](#) suggested another model, in which illumination does not bleach the TL trap but removes electrons from the deep thermally disconnected trap(s). These electrons radiatively recombine with the holes in the recombination centers and cause an unbleachable residual TL signal, which depends on the initial trap population, unlike Levy's and Chen's models. In addition, the ratio between the residual signal and the applied dose is expected to vary based on two factors: (1) the relative contribution of the unbleachable residual signal to the total TL signal, and (2) the dose dependence of the unbleachable residual TL signal. The TL peak is considered first-order due to no shift in the peak position with time.

3. Results and discussions

3.1. Bleaching of TL and thermal stability of OSL at 40 mGy

Bleaching of TL and thermal stability of OSL signals of the BeO dosimeter that were obtained at 40 mGy beta dose are shown in [Figs. 1 and 2](#), respectively. Only selected R-TL glow curves are shown in the graphs for the sake of clarity.

The OSL curves of the BeO dosimeter at 40 mGy and 20 Gy are shown in [Figs. 2 and 4](#) together with preheated OSL curves, respectively. Additionally, preheated OSL curves are shown for both cases. To eliminate the contributions of TL peaks 1 and 2 from the OSL signal, the BeO

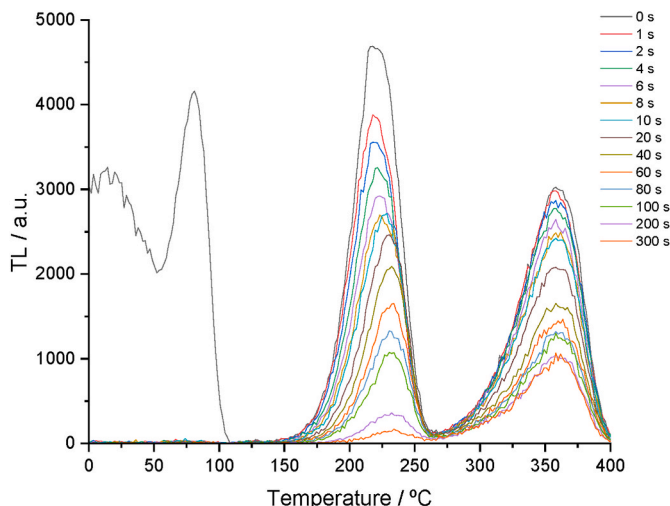


Fig. 1. R-TL glow-curves of BeO after irradiation at 40 mGy beta dose.

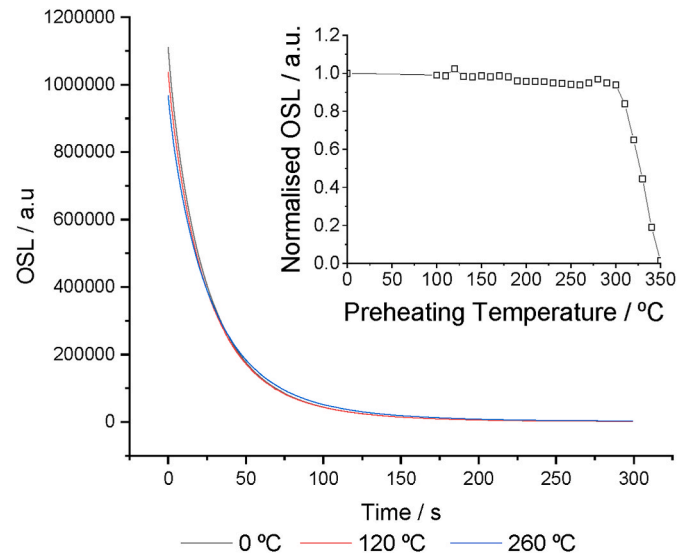


Fig. 2. OSL curves of BeO without preheating, thermal cleaning of the TL Peak 1 (preheating at 120 °C, 10 s) and thermal cleaning of the TL Peak 2 (preheating at 260 °C, 10 s) for BeO dosimeter irradiated with 40 mGy. The inset shows the normalized step annealing test for this dose.

dosimeter was preheated at 120 °C and 260 °C for 10 s.

At the selected heating rate, BeO exhibits a TL glow curve with three distinct peaks. These peaks occur at approximately 75 °C (peak 1), 220 °C (peak 2), and 350 °C (peak 3), as shown in [Figs. 1 and 2](#) for a dose of 40 mGy and 20 Gy, respectively. Consistent with previous bleaching studies on BeO from Thermalox, all TL peaks are affected by bleaching but at varying rates ([Aşlar et al., 2019](#); [Bulur and Göksu, 1998](#); [Yukihara, 2020](#)). TL peak 1 undergoes nearly complete bleaching within 1 s for both doses, making it challenging to analyze its bleaching behavior. Therefore, it was not further investigated in this study.

After 10 s of bleaching for a dose of 40 mGy, the intensity of TL peak 2 reduces by approximately 45%. After 300 s, the intensity remaining in TL peak 2 relative to its initial intensity is roughly 2.8% for the same dose. For TL peak 3, there is only a minor decline of just 9% after 10 s of bleaching. However, this decline steadily continues to reach nearly 65% by the end of the 300-s optical stimulation period.

The inset in [Fig. 2](#) illustrates the results of the step-annealing test, where the BeO dosimeter was preheated in increments of 10 °C from 100 °C to 350 °C before the OSL measurement (300 s). Results were then normalized to the OSL signal measured without preheating. The bleachable TL glow peaks can be associated with traps responsible for the OSL signal. Considering that TL peak 2 bleaches more significantly than TL peak 3, the former could be regarded as the primary source of charge carriers for the OSL signal. However, at a dose of 40 mGy, the OSL signal intensity and shape are not affected by the step annealing up to 260 °C, which completely removes TL peak 2 ([Fig. 1](#)). This characteristic is consistent with the observations made by [Bulur and Göksu \(1998\)](#) and [Yukihara \(2020\)](#), where the OSL signal shape of BeO remains unchanged after the removal of TL peaks 1 and 2 through preheating.

3.2. Bleaching of TL and thermal stability of OSL at 20 Gy

As [Fig. 3](#) indicates, at 20 Gy, the intensity of TL peak 2 is reduced by approximately 28% after 10 s of bleaching. Following 300 s, the residual intensity of TL peak 2 amounts to about 2.6%, relative to its initial intensity. TL peak 3 reduces by 20% after a 10-s bleaching time, and this decline continues to nearly 55% at the end of the 300 s of optical bleaching. In contrast to the findings of [Aşlar et al. \(2019\)](#), TL peak 3 shows a significant degree of bleaching throughout the entire bleaching process for both applied doses.

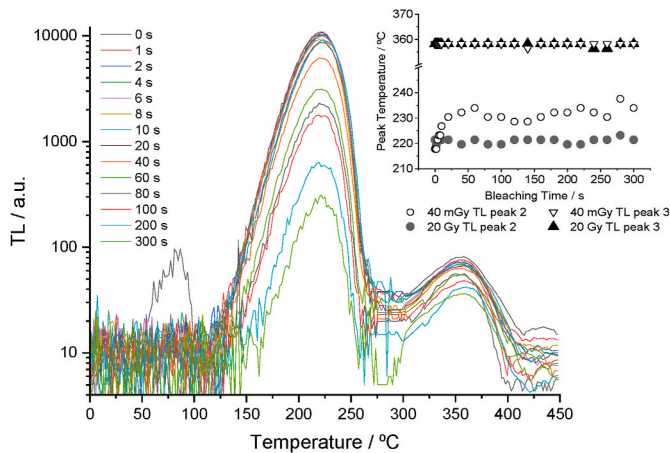


Fig. 3. R-TL glow-curves of BeO after irradiation at 20 Gy beta dose. The inset shows the maximum peak positions of the TL peaks at the two given doses as a function of bleaching times. This measurement was done using the cardboard with pinhole in front of the PMT, therefore relative intensities are not comparable to Fig. 2.

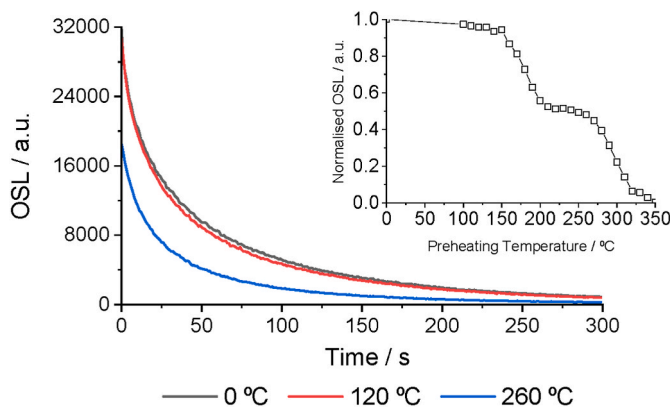


Fig. 4. OSL curves of BeO without preheating, thermal cleaning of the TL Peak 1 (preheating at 120 °C, 10 s) and thermal cleaning of the TL Peak 2 (preheating at 260 °C, 10 s) after irradiation with 20 Gy. The inset shows the normalized step annealing test for this dose.

The inset of Fig. 3 displays the maximum peak position of TL peaks 2 and 3 at given doses as a function of bleaching time. No noticeable shift in the peak position is observed for TL peak 3 at any of the given doses. Similarly, TL peak 2 at 20 Gy does not exhibit a clear shift. However, a distinct shift in the peak position can be observed for TL peak 2 at 40 mGy, with a magnitude of up to 15 °C within the first 50 s of bleaching. This indicates that TL peak 2 may consist of a single peak at higher doses.

Comparing the step annealing results at 20 Gy (Fig. 4, inset), to the same experiment at 40 mGy (Fig. 2, inset), we now see a noticeable initial drop in signal intensity of around 50% within the temperature range of approximately 150 °C–220 °C. This is followed by second decrease in the same temperature range as in the 40 mGy experiment. A similar observation has been made by (Bulur and Saraç, 2013) in a step-annealing experiment on a 50 Gy irradiated BeO dosimeter. The first signal decrease clearly indicates that in the temperature region of TL peak 2, there is an additional contribution to the OSL signal.

The results of the step annealing experiment at 40 mGy (Fig. 2) have for many years supported the notion that the OSL signal is derived exclusively from traps responsible for TL peak 3 (Bulur and Göksu 1998). The step annealing experiment at higher doses (Fig. 4) was then interpreted as the creation of new traps that contribute to the OSL signal at this dose (Bulur and Saraç, 2013). Recently, Yukihiro (2020) used the

additional property of strong thermal quenching of the luminescence emission in BeO to suggest that at low dose the contribution of TL peak 2 to the OSL signal is negligible compared to TL peak 3, contrary to what Fig. 1 implies. At higher doses, the contribution from TL peak 2 to OSL becomes noticeable due to saturation of TL peak 3 at a lower dose than TL peak 2. This suggestion has so far not been confirmed experimentally. It will be addressed in the following subsection.

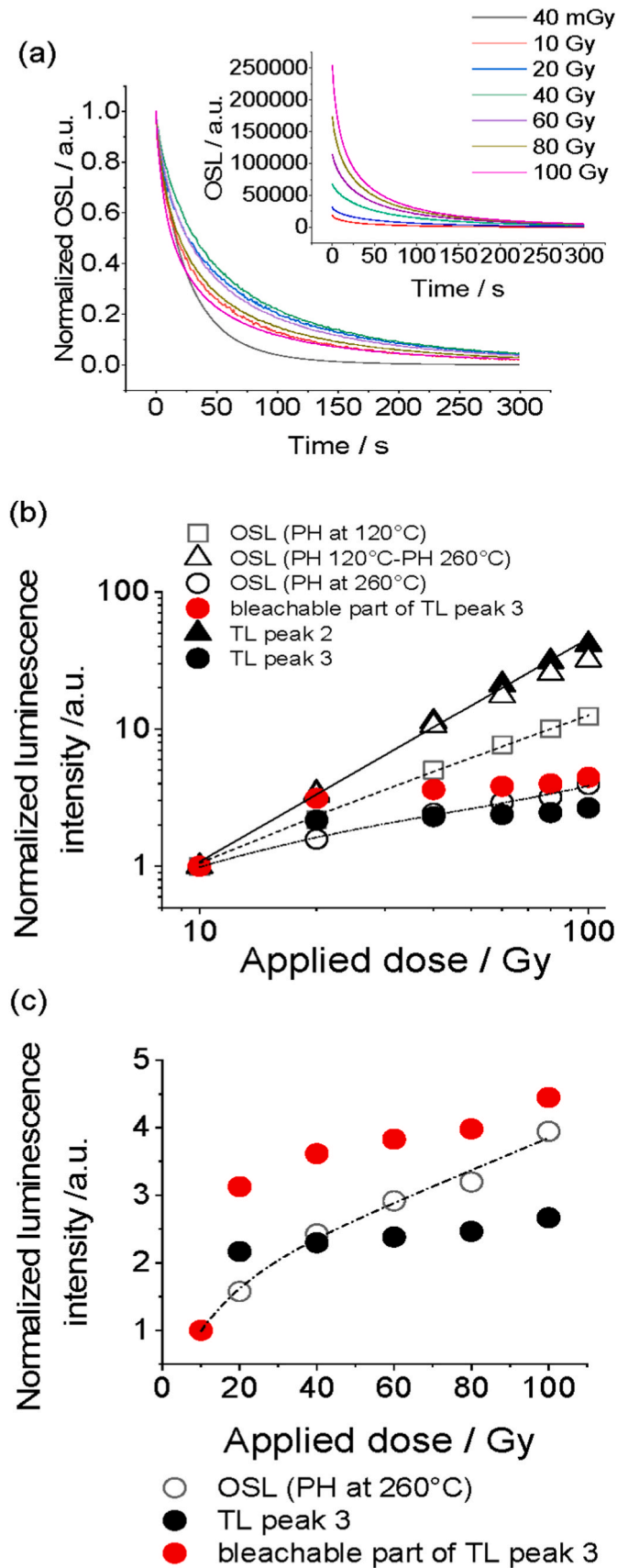
3.3. Dose response

The normalized OSL decay curves of the BeO dosimeter that was irradiated at 40 mGy and 10 mGy to 100 Gy are shown in Fig. 5a and the inset displays the OSL decay curves between 10 and 100 Gy.

The strongest difference in relative OSL curve shape can be seen between the lowest dose (40 mGy) and the set of doses starting at more than order of magnitude higher. However, between 10 and 100 Gy there is also a systematic change in OSL curve shape, with the overall rate of signal decrease first decreasing up to 40 Gy and then increasing again up to 100 Gy. In Fig. 5b, the dose-response of TL peak 2, TL peak 3, and the OSL signal are depicted (the 40 mGy data were measured with a different experimental setup and cannot be included here). Also shown is the fraction of the TL peak 3 intensity that can be bleached by light, inferred from Fig. 6 b (see below). The results were then normalized to the respective dose response values obtained at 10 Gy. To evaluate the contribution of the OSL trap(s), that become thermally unstable between 150 °C and ~220 °C (Fig. 4) to the total OSL signal, the integrated OSL signal intensity after preheating at 260 °C was subtracted from the one after preheating at 120 °C. The OSL signal measured after preheating at 260 °C should in principle be attributable to the traps responsible for TL peak 3.

Notably, TL peak 2 and the difference in OSL signal (PH 120 °C – PH 260 °C) both show a very similar dose response, with only slight discrepancies observable at higher doses. The data points of TL peak 2 were fitted by a power function of the form $I = a \times D^k$, where I denotes the (integrated) signal intensity, D the dose, a the proportionality coefficient and k the linearity index (Nikiforov et al., 2017; McKeever and Chen, 1997). A linear dose response is characterized by $k = 1$, supralinearity by $k > 1$ and a sublinear dose response by $k < 1$ (ibid.). Here a value for k of 1.63 was obtained, demonstrating the dose response is supralinear. This is consistent with the literature, where it has been reported that TL peak 2 exhibits supralinear dose-response behavior (Bulur, 2007; Crase and Gammage, 1975; Polymeris et al., 2021; Tochilin et al., 1969). Furthermore, Polymeris et al. (2021) suggested, based on their experimental data, that the supralinear dose response is due to competition effects taking place at both the irradiation and heating stage. The similarity in dose-response and in thermal stability between TL peak 2 and the OSL signal (PH 120 °C – PH 260 °C) gives direct experimental evidence, that, as proposed by Yukihiro (2020), TL peak 2 traps indeed contribute to the OSL signal and that it is those kind of traps that are responsible for the initial signal drop depicted in Fig. 4, rather than the creation of new traps. It is further noteworthy that in the dose range of 40–100 Gy, the dose response of both TL peak 2 and the related OSL signal can also be approximated by a linear function (although naturally not passing through origin). This could imply a decrease in competition effects in this dose range.

For TL peak 3 and more importantly, the bleachable part of the same peak, the dose response lies in a similar range as the OSL signal after preheating at 260 °C, but the level of agreement is not nearly as close as for TL peak 2 and the OSL signal (PH 120 °C – PH 260 °C). Obviously, there are additional different mechanisms during thermal or optical readout that lead to some degree of deviation between both stimulation modes in this case. The dose response of OSL signal after 260 °C preheating was fitted to a combination of an exponential saturation function plus linear term of the form: $y = 1.6 \times (1 - e^{-D/13 \text{ Gy}}) + 0.02 \text{ 1/Gy} \times D$. Such a phenomenological functional behavior has frequently been used for fitting the dose response of quartz or feldspar at higher doses



(caption on next column)

Fig. 5. (a): Normalized OSL curves of BeO dosimeter at different doses between 10 and 100 Gy, the original OSL decay curves are shown in the inset. (b): Dose response of OSL after 120 °C preheating, after 260 °C preheating, of the difference in OSL signal after the two preheats and of TL peak 2 and 3 of BeO dosimeter for the same doses. Abbreviation 'PH' defines the preheating treatment before luminescence measurements. For dose response curve, each measurement was normalized to its respective response at 10 Gy. The solid line is a power function fitted to the TL peak 2 data, the dashed line a linear function fitted to the OSL (PH at 120 °C) data and the dash-dotted line the sum of an exponential saturation function and a linear term fitted to the OSL (PH at 260 °C) data. (c): Data for TL peak 3 (total and bleachable part) and OSL after preheat at 260 °C on a linear scale. For details see text.

(hundreds of Gy to several kGy) in TL and OSL dating (see Berger (2010) and references therein) and could be seen as the approximation of the sum of two exponential saturation functions, with one component being far from saturation. This could be thus interpreted as the existence of two charge traps with different saturation doses (Berger and Chen, 2011). Saturation of the first component would thus occur at a dose of around 50 Gy, a dose similar to the threshold dose for TL peak 2 and the related OSL signal, above which the dose response of the latter two becomes increasingly linear. On the other hand, Berger and Chen (2011) gave a numerical and Pagonis et al. (2020) an analytical solution of the model assuming only a single trap and recombination center, that was also able to produce a double saturating exponential or a saturating plus linear dose response. Berger and Chen (2011) connected the two saturation doses of the fitting function with the transition coefficients for electron capture in traps and hole capture in recombination centers in this case. Although the exact nature of the dose response might not be resolvable, for the purpose of the present study it is sufficient to note that qualitatively the dose response of the bleachable part of TL peak 3 has in principle a similar shape than the preheated OSL signal but with a likely higher relative intensity of the saturating component and a lower slope value of the linear term. This can still be seen as an indication of a possible correlation between TL peak 3 and the OSL signal after 260 °C preheating, as the thermal stability study at 40 mGy also suggests (Fig. 2).

Concerning the overall OSL signal, its dose-response demonstrates linearity throughout the entire dose range (10–100 Gy), which differs somewhat from the reported onset of saturation at doses of 5–10 Gy in the literature (Bulur and Göksu, 1998; Sommer et al., 2007, 2008; Sommer and Henniger, 2006). In the light of the results and interpretations thereof mentioned above, this dose linearity likely arises from the combined effects of the opposing dose-response trends of TL peak 2 (supralinearity) and the OSL part linked to TL peak 3 (saturation) up to a dose of around 40 Gy and the further linear dose response of both components for higher doses.

3.4. Evaluating bleaching models for TL peak 2 and 3

The (relative) residual TL intensities of TL peaks 2 and 3 after different bleaching times for given doses between 40 mGy and 100 Gy are shown in Fig. 6. The bleaching behavior of TL 2 peak is very similar for all doses, with almost the same residual level reached after the maximum bleaching time of 300 s, independent of the initial concentration of trapped electrons. Only for the lowest dose in the mGy range there is a faster initial signal decay than at higher doses. In contrast, TL peak 3 shows a clear evolution of the bleaching curves over the entire dose range, with an increasing relative contribution of an initial rapid decay in peak intensity, a lowest residual level of below 40% at 40 mGy followed by an increase to ~65% at 10 Gy, with a subsequent decrease to around 40% for doses of 40 Gy and higher.

As seen from Fig. 6a, TL peak 2 reduces to the same residual level, independent of the irradiation dose. As stated in Fig. 3 inset, after optical stimulation the peak position of residual TL peak 2 at 20 Gy stays nearly constant. These findings are in line with the model proposed by (Chen

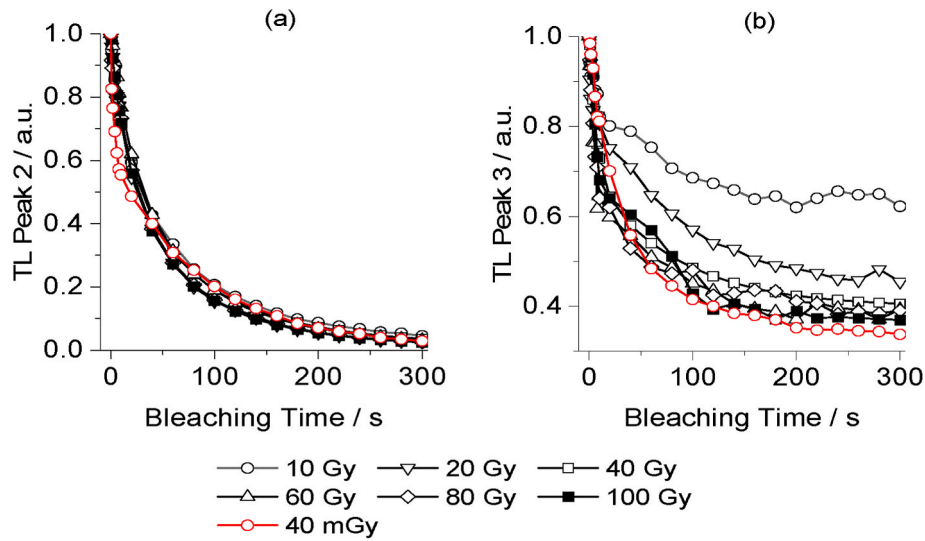


Fig. 6. R-TL peak intensities of TL peak 2 (a), and peak 3 (b) as a function of bleaching times. The dosimeter was irradiated between 40 mGy and 100 Gy.

et al., 1990). In the case of TL peak 3 (Fig. 6b), different residual levels were obtained after irradiation at different doses besides there are no shifts in the peak positions for both applied doses as a function of

bleaching time (Fig. 3 Inset). These observations are in line with the model suggested by McKeever (1994) and are in agreement with the results from Yukihiro (2019) and (2020). The evolution of the residual

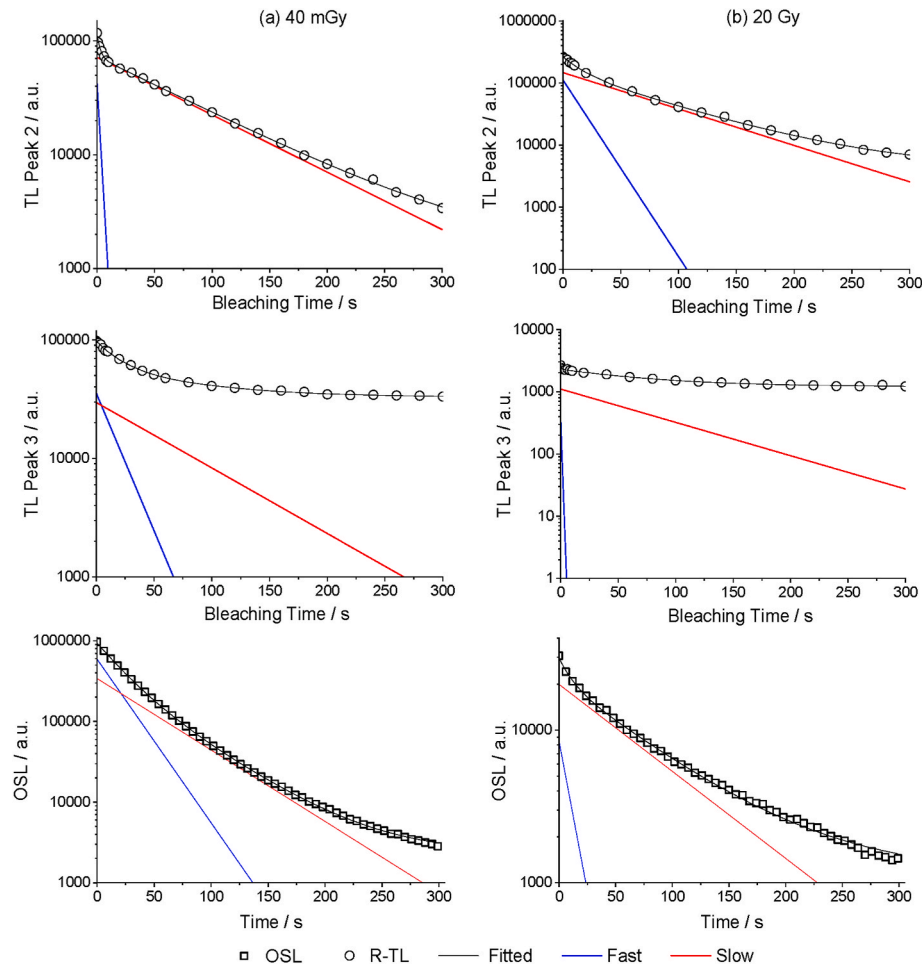


Fig. 7. Residual TL peak intensities of the BeO dosimeter as a function of bleaching times at 40 mGy (left panel) and 20 Gy beta dose (right panel). The graphic displays TL peak 2 at the top and TL peak 3 in the middle side, while the bottom panel shows the CW-OSL decay curves of BeO, for both applied doses. The black lines in all graphs indicate the fitted function (including a constant), the red and blue lines the respective two components (without the constant), according to equation (3).

level with dose for TL peak 3 could also imply that there are (at least) two components for this TL peak in the system under study: a hard-to-bleach component and an optically active component. The hard to bleach component saturates at lower doses, while the optically active component continues to grow with dose, leading to the decrease of the relative residual level with dose (see also Fig. 5 c).

3.5. Bleaching rates without optical attenuation

The R-TL intensities remaining after various bleaching times and the OSL decay curves of BeO at 40 mGy and between 10 and 100 Gy were first fitted using the model without optical attenuation, examples for doses of 40 mGy and 20 Gy are shown in the left and right panels of Fig. 7a and b. The sum of two exponential decay functions (plus constant) was needed to fit the R-TL peak 2 and peak 3 data and the OSL decay curves for all applied doses. This was based on the fact that, on the one hand, a large reduced χ^2 value and large residual values were obtained when only a single exponential decay function was used and that, on the other hand, a significantly smaller χ^2 value and generally a good agreement between measured data points and fitted function was observed when using the sum of two exponential decay functions, as illustrated in Fig. 6. No major systematic deviations could be identified that would have justified the introduction of a third component.

The results for the obtained characteristic times τ_i , which are the inverse of the bleaching rates (equations (2) and (3)), for both TL glow peaks and OSL for all doses are given in Table 2. The bleaching rate is, by definition, the rate of eviction of charges by bleaching and can be classified as fast and slow. A lower value for the bleaching rate characterizes a trap that is harder to bleach than the fast component. The presence of several bleaching rates may indicate that there are different types of traps that may have different photoionization cross-sections. The fitting results give two different bleaching decay rates per TL peak for applied doses. This may indicate different traps located in the TL peaks.

Depending on the dose dependent contribution of the TL peaks to the OSL signal (Figs. 2 and 4), bleaching decay rates in TL are expected to be connected to OSL components. At 40 mGy, we expect the OSL signal to originate almost entirely from the trap responsible for TL peak 3 (Fig. 2). The characteristic time of the fast component in OSL indeed seems to match with the characteristic time of the fast bleaching decay rate of TL

peak 3 at this dose but the values for the slow components are markedly different. In addition, no match is found between OSL components and the bleaching decay rates of TL peak 2 at this dose. The model would thus imply that at 40 mGy, no correlation exists between any of the TL peaks and the OSL signal, contrary to what other experimental data suggest (Fig. 1). With increasing dose, the contribution of the TL traps to the OSL signal gradually shifts from TL peak 3 to TL peak 2, with an expected 50:50 contribution of both peaks to the OSL signal at 20 Gy (Fig. 4). Since the characteristic time of the slow component in OSL and the characteristic times of the slow bleaching rate of both TL peaks in Table 2 for this dose are very similar (this is in fact the case for all doses of 10 Gy and above) and since a two component fit was used for the OSL data, we expect the value of the fast component in OSL to lie in between the values for the fast bleaching decay rates of TL peaks 2 and 3, and this indeed the case. For doses of 40 Gy and above, the values for the two components in OSL are close to the characteristic times of the respective bleaching decay rates (fast and slow) for TL peak 2, whereas the values for the fast bleaching decay rates of TL peak 3 are consistently lower than the fast component in OSL. This is generally in line with the expected increasing dominant contribution of TL peak 2 to the OSL signal with increasing dose (compare Fig. 5 b). It thus seems that for doses above 20 Gy, the simple model without optical attenuation produces consistent results and supports the correlation between TL peaks and the OSL signal. Nevertheless, the model fails to reproduce the same correlation at 40 mGy.

3.6. Bleaching rates with optical attenuation

The expressions for the OSL decay curve and the TL bleaching data considering optical attenuation (equations (10) and (14)) were applied to experimental data to estimate characteristic times. The fitted curves are shown in Fig. 8 and parameters are presented in Table 3. To have fewer iteration steps, attenuation equations were applied to normalized data of TL and OSL. Results were compared to values found in Table 2. The most striking feature of Table 3 is that at 40 mGy, both the bleaching data of TL peak 3 and the OSL decay curve can be described by a single component, with very similar values for the characteristic times of the respective decay rates. This is a much more consistent result than the one obtained for the model without optical attenuation and supports the correlation between TL peak 3 and OSL also at this dose. For doses of 10 Gy and higher, two components are needed for a good fit of each TL peak data and OSL data, respectively and the values of the two components in OSL are generally closer to the characteristic times of the respective decay rates of TL peak 2 than to the ones of TL peak 3. This again supports the correlation between TL and OSL also in this dose range. As the consideration of optical attenuation leads to stretched exponential functions, the obtained bleaching decay rates and lifetimes of the OSL components are generally lower than the ones obtained using the model without optical attenuation (Table 2), for those cases where the same number of fitted components have been used (e.g. two components).

When using a strong optical diffusor as detector such as BeO, it thus seems advisable to consider optical attenuation properties when interpreting the results of bleaching characteristics in TL and OSL. Generally, the observations made here confirm that the OSL decay curve of BeO is a multi-component signal as described previously (Bulur and Sarac, 2013; Yukihiro, 2020) and likely originates from several trapping centers.

3.7. Comparison with other correlation studies for BeO

All fit functions used to analyze the bleaching rates (with and without optical attenuation) were derived using the a-priori assumption of negligible retrapping and thus first order kinetics. A different approach was followed by Aşlar et al. (2019) and Polymeris et al. (2021), who used the analytical solution of the one-trap-one-center model for optical stimulation, developed by Kitis and Vlachos (2013), to fit the OSL decay curve. Although two components were used to fit the

Table 2

Bleaching decay rates, given by the inverse values of the characteristic times τ_i , of TL peaks and OSL components of BeO using the model without optical attenuation (equation (3)).

Dose/Gy	TL Peak or OSL	Characteristic times/s	
		τ_1 (fast)	τ_2 (slow)
0.04	2	2.5 ± 0.2	86.2 ± 4.0
	3	18.6 ± 2.5	78.5 ± 11.4
	OSL	21.0 ± 0.3	49.0 ± 0.3
10	2	9.3 ± 0.9	75.4 ± 2.2
	3	2.7 ± 1.2	70.0 ± 11.7
	OSL	14.2 ± 0.3	75.3 ± 0.9
20	2	15.3 ± 1.4	74.0 ± 3.6
	3	0.8 ± 0.2	81.2 ± 4.8
	OSL	11 ± 0.4	76.2 ± 0.8
40	2	17.9 ± 2.8	86.7 ± 15.0
	3	7.2 ± 0.4	87.6 ± 6.6
	OSL	17.9 ± 0.3	87.9 ± 1
60	2	17.5 ± 2.1	79.5 ± 2.1
	3	4.4 ± 1.2	82.8 ± 28.7
	OSL	14.5 ± 0.2	79.9 ± 0.8
80	2	11.1 ± 2.5	70.2 ± 5.3
	3	5.4 ± 0.7	83.9 ± 18.0
	OSL	11.7 ± 0.2	83.1 ± 0.8
100	2	18.6 ± 2.5	76.4 ± 6.5
	3	5.8 ± 2.1	74.3 ± 23.3
	OSL	12.0 ± 0.2	75.4 ± 0.7

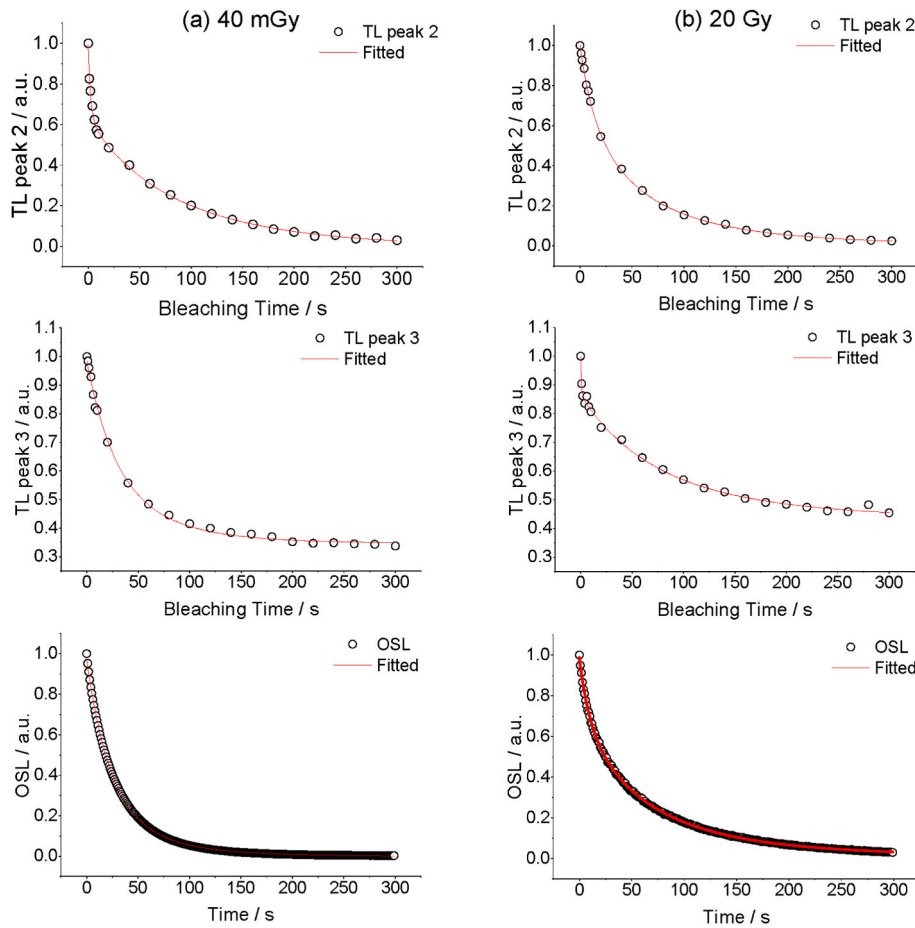


Fig. 8. Fitting results of the R-TL intensities and OSL decay curves using equation 10 (OSL) and 15 (TL) in case of a single component or sums thereof in case of two components. Left column (a) 40 mGy, right column (b) 20 Gy.

OSL data, the second component was essentially constant over the measurement time, carrying less than 10% of the total OSL signal, therefore for the purpose of comparison with the results here, the first component (C1) seems more relevant. For the step annealing experiment, carried out in Aşlar et al. (2019) for a dose of 30 Gy, the evolution of the integrated signal intensity for C1 with preheat temperature, with a first signal drop beginning around 180 °C and a second one around 275 °C, is very similar to the one shown in Fig. 4 (where the deconvoluted integrated OSL signal minus background is plotted for a dose of 20 Gy), and to the one shown in Bulur and Saraç (2013). The difference is however that for the lower temperature range beginning at ~180 °C the signal drops by about an order of magnitude in Aşlar et al. (2019), compared to a signal drop of only a factor of two for the present study (at 20 Gy) and a factor of three in Bulur and Saraç (at 50 Gy). In Aşlar et al. (2019) the component C1 was correlated to TL peak 2, whereas in the present work the total OSL signal was interpreted to carry approximately equal contributions from both TL peaks 2 (first signal drop) and TL peak 3 (second signal drop). As the OSL signal in Aşlar et al. (2019) was completely dominated by the contribution of TL peak 2 already at the given dose of 30 Gy, however, the correlations suggested in that work and in this study are actually consistent. In Polymeris et al. (2021) on the other hand, the same component C1 of the deconvoluted OSL signal was correlated to TL peak 3, based on characteristics of the OSL dose response, for doses between 2 mGy and 4 Gy. The dose of 40 mGy investigated in the present study, falls into this dose range and here the same correlation between the OSL signal and TL peak 3, based on both the step annealing experiment in Fig. 2 and the comparison of bleaching rates for the model with optical attenuation in Table 3 is suggested. Although quite different model functions were used to

analyze the OSL data in the two cited studies and in the present work, the implications regarding correlation between the OSL signal and TL peaks are thus actually the same. The correlation of the OSL signal and TL peak 3 at low doses is also consistent with earlier studies, as was already mentioned previously (Bulur and Göksu, 1998; Bulur and Saraç, 2013; Yukihiro, 2011). Finally, the shift of the dominant contribution to the OSL signal from TL peak 3 at low doses to TL peak 2 at high doses is consistent with the suggestions made by Yukihiro (2020).

4. Conclusion

Analysis of the thermal stability of the OSL signal of BeO at selected doses and of the dose response of TL peak 2 and 3 and the OSL signal after different thermal treatments at a dose of 40 mGy and between 10 and 100 Gy gives direct experimental evidence that at 40 mGy, the OSL signal is strongly correlated only to the traps of TL peak 3 and that at doses of 10 Gy and higher there is an increasing contribution of the traps of TL peak 2 to the OSL signal, which likely dominate at the highest doses. The linear dose response of the OSL signal could then be the result of superposition of saturation effects of the bleachable traps of TL peak 3 and supralinear dose response of traps of TL peak 2 up to a dose of about 40 Gy and the subsequent linear dose response of both peaks for higher doses. The residual intensities of the TL glow peaks were measured after various bleaching times, and model functions, with and without consideration of optical attenuation fitted to determine the bleaching decay rates of individual TL peaks. A similar approach was applied to the OSL curves. When comparing decay rates of TL peaks to the decay rates of the OSL components, it was found that for doses of 10 Gy and higher, both models produced similar consistent results, which supported the

Table 3

Bleaching decay rates, given by the inverse values of the characteristic times τ_i , of TL peaks and OSL component values of BeO using the model with optical attenuation (equations (10) and (14)). An uncertainty of “0.0” means that the uncertainty was smaller than 0.044. As the uncertainty of the attenuation coefficients was not considered in the fitting, the estimated parameter uncertainties likely underestimate the true uncertainties.

Dose/ Gy	TL Peak or OSL	Characteristic times/s		Number of fitted components
		τ_1 (fast)	τ_2 (slow)	
0.04	2	1.3 ± 0.0	49.1 ± 0.1	2
	3	18.8 ± 0.0	-	1
	OSL	17.9 ± 1.0	-	1
10	2	3.9 ± 0.0	40.9 ± 0.0	2
	3	1.2 ± 0.4	40.4 ± 0.0	2
	OSL	7.6 ± 0.0	43.8 ± 0.0	2
20	2	8.5 ± 0.0	38.8 ± 0.0	2
	3	0.5 ± 0.6	48.5 ± 0.0	2
	OSL	6.9 ± 0.0	39.5 ± 1.9	2
40	2	10.8 ± 0.0	48.5 ± 0.0	2
	3	4.4 ± 0.0	57.8 ± 0.0	2
	OSL	10.8 ± 0.0	48.9 ± 0.0	2
60	2	9.5 ± 0.0	47.1 ± 0.0	2
	3	2.7 ± 0.1	55.8 ± 0.0	2
	OSL	8.9 ± 0.0	48.3 ± 0.0	2
80	2	4.2 ± 0.0	49.6 ± 0.1	2
	3	3.3 ± 0.1	57.6 ± 0.0	2
	OSL	8.8 ± 0.0	49.3 ± 0.0	2
100	2	7.0 ± 0.0	43.5 ± 0.1	2
	3	3.5 ± 0.1	50.8 ± 0.0	2
	OSL	6.5 ± 0.0	45.4 ± 0.0	2

expected correlation between TL peaks and the OSL signal. At the same time, only the model that considered optical attenuation supported such a correlation also at a dose of 40 mGy and this implies that optical attenuation effects should be taken into account when describing the OSL curve or the bleaching characteristics of the TL peaks of BeO. The TL peaks 2 and 3 may contain multiple OSL traps, and their contribution to the OSL signal varies with the applied dose. The discussion of bleaching models for BeO highlighted the distinct luminescence mechanisms associated with TL peaks 2 and 3, which have been reported previously. The investigation of R-TL intensities yielded noteworthy results that warrant further exploration. Overall, this study contributes additional support and expands the existing knowledge on BeO.

CRediT authorship contribution statement

Elif Kara: Conceptualization, Data curation, Formal analysis, Funding acquisition, Investigation, Methodology, Software, Validation, Writing – original draft. **Clemens Woda:** Supervision, Writing – review & editing.

Declaration of competing interest

The authors declare that they have no known competing financial interests or personal relationships that could have appeared to influence the work reported in this paper.

Data availability

Data will be made available on request.

Acknowledgements

We would like to express our sincerest appreciation to Mirion Technologies (AWST) GmbH for providing us the BeO dosimeters for recent article. EK gratefully acknowledges the financial support of the Study Abroad Postgraduate Education Scholarship (YLSY) awarded by the Republic of Türkiye Ministry of National Education.

References

Aşlar, E., Meriç, N., Şahiner, E., Erdem, O., Kitis, G., Polymeris, G.S., 2019. A correlation study on the TL, OSL and ESR signals in commercial BeO dosimeters yielding intense transfer effects. *J. Lumin.* 214, 116533 <https://doi.org/10.1016/j.jlumin.2019.116533>.

Berger, G.W., Chen, R., 2011. Error analysis and modelling of double saturating exponential dose response curves from SAR OSL dating. *Ancient TL* 29 (1), 9–14.

Berger, G.W., 2010. Estimating the error in equivalent dose values obtained from SAR. *Ancient TL* 28 (2), 55–66.

Bos, A.J.J., 2001. High sensitivity thermoluminescence dosimetry. *Nucl. Instruments Methods Phys. Res. Sect. B Beam Interact. with Mater. Atoms* 184, 3–28. [https://doi.org/10.1016/S0168-583X\(01\)00717-0](https://doi.org/10.1016/S0168-583X(01)00717-0).

Bulur, E., 2007. Photo-transferred luminescence from BeO ceramics. *Radiat. Meas.* 42, 334–340. <https://doi.org/10.1016/j.radmeas.2007.02.065>.

Bulur, E., Göksu, H.Y., 1998. OSL from BeO ceramics: new observations from an old material. *Radiat. Meas.* 29, 639–650. [https://doi.org/10.1016/S1350-4487\(98\)00084-5](https://doi.org/10.1016/S1350-4487(98)00084-5).

Bulur, E., Saraç, B.E., 2013. Time-resolved OSL studies on BeO ceramics. *Radiat. Meas.* 59, 129–138. <https://doi.org/10.1016/j.radmeas.2013.04.009>.

Bulur, E., Yeltik, A., 2010. Optically stimulated luminescence from BeO ceramics: an LM-OSL study. *Radiat. Meas.* 45, 29–34. <https://doi.org/10.1016/j.radmeas.2009.08.007>.

Chen, R., Hornyak, W.F., Mathur, V.K., 1990. Competition between excitation and bleaching of thermoluminescence. *J. Phys. D Appl. Phys.* 23, 724–728. <https://doi.org/10.1088/0022-3727/23/6/015>.

Cruse, K.W., Gammage, R.B., 1975. Improvements in the use of ceramic BeO for TLD. *Health Phys.* 29, 739–746. <https://doi.org/10.1097/00004032-197511000-00014>.

Dallas, G.I., Polymeris, G.S., Afouxenidis, D., Tsirliganis, N.C., Tsagas, N.F., Kitis, G., 2010. Correlation between TL and OSL signals in KMgF3:Ce 3+: bleaching study of individual glow-peaks. In: *Radiation Measurements*. Pergamon, pp. 537–539. <https://doi.org/10.1016/j.radmeas.2009.11.008>.

Gray, H.J., Mahan, S.A., 2015. Variables and potential models for the bleaching of luminescence signals in fluvial environments. *Quat. Int.* 362, 42–49. <https://doi.org/10.1016/j.quaint.2014.11.007>.

Kitis, G., Vlachos, N.D., 2013. General semi-analytical expressions for TL, OSL and other luminescence stimulation modes derived from the OTOR model using the Lambert W-function. *Radiat. Meas.* 48, 47–54. <https://doi.org/10.1016/j.radmeas.2012.09.006>.

Lembo, L., Pimpinella, M., Mukherjee, B., 1990. Self optical attenuation coefficient of TL glow in BeO detectors. *Radiat. Protect. Dosim.* 33, 43–45. <https://doi.org/10.1093/oxfordjournals.rpd.a080754>.

Levy, P.W., 1982. Thermoluminescence and optical bleaching in minerals exhibiting second order kinetics and other charge retrapping characteristics.

McKeever, S.W.S., 1994. Models for optical bleaching of thermoluminescence in sediments. *Radiat. Meas.* 23, 267–275. [https://doi.org/10.1016/1350-4487\(94\)90051-5](https://doi.org/10.1016/1350-4487(94)90051-5).

McKeever, S.W.S., Chen, R., 1997. Luminescence models. *Radiat. Meas.* 27, 625–661. [https://doi.org/10.1016/S1350-4487\(97\)00203-5](https://doi.org/10.1016/S1350-4487(97)00203-5).

Nikiforov, S.V., Pagonis, V., Merezchnikov, A.S., 2017. Sublinear dose dependence of thermoluminescence as a result of competition between electron and hole trapping centers. *Radiat. Meas.* 105, 54–61.

Pagonis, V., Kitis, G., Chen, R., 2020. A new analytical equation for the dose response of dosimetric materials, based on the Lambert W function. *J. Lumin.* 225, 117333 <https://doi.org/10.1016/j.jlumin.2020.117333>.

Polymeris, G.S., Çoskun, S., Tsoutsoumanos, E., Konstantinidis, P., Aşlar, E., Şahiner, E., Meriç, N., Kitis, G., 2021. Dose response features of quenched and reconstructed, TL and deconvolved OSL signals in BeO. *Results Phys.* 25, 104222 <https://doi.org/10.1016/j.rinp.2021.104222>.

Rhyner, C.R., Miller, W.G., 1970. Radiation dosimetry by optically-stimulated luminescence of BeO. *Health Phys.* 18, 681–684. <https://doi.org/10.1097/00004032-197006000-00010>.

- Sohbati, R., Murray, A., Jain, M., Buylaert, J.-P., Thomsen, K., 2011. Investigating the resetting of OSL signals in rock surfaces. *Geochronometria* 38, 249–258. <https://doi.org/10.2478/s13386-011-0029-2>.
- Sommer, M., Freudenberg, R., Henniger, J., 2007. New aspects of a BeO-based optically stimulated luminescence dosimeter. *Radiat. Meas.* 42, 617–620. <https://doi.org/10.1016/j.radmeas.2007.01.052>.
- Sommer, M., Henniger, J., 2006. Investigation of a BeO-based optically stimulated luminescence dosimeter. *Radiat. Protect. Dosim.* 119, 394–397. <https://doi.org/10.1093/rpd/nci626>.
- Sommer, M., Jahn, A., Henniger, J., 2008. Beryllium oxide as optically stimulated luminescence dosimeter. *Radiat. Meas.* 43, 353–356. <https://doi.org/10.1016/j.radmeas.2007.11.018>.
- Tochilin, E., Goldstein, N., Miller, W.G., 1969. Beryllium oxide as a thermoluminescent dosimeter. *Health Phys.* 16, 1–7. <https://doi.org/10.1097/00004032-196901000-00001>.
- Watanabe, S., Gundu Rao, T.K., Page, P.S., Bhatt, B.C., 2010. TL, OSL and ESR studies on beryllium oxide. *J. Lumin.* 130, 2146–2152. <https://doi.org/10.1016/j.jlumin.2010.06.009>.
- Yukihara, E.G., 2020. A review on the OSL of BeO in light of recent discoveries: the missing piece of the puzzle? *Radiat. Meas.* 134, 106291. <https://doi.org/10.1016/j.radmeas.2020.106291>.
- Yukihara, E.G., 2019. Observation of strong thermally transferred optically stimulated luminescence (TT-OSL) in BeO. *Radiat. Meas.* 121, 103–108. <https://doi.org/10.1016/j.radmeas.2018.12.014>.
- Yukihara, E.G., 2011. Luminescence properties of BeO optically stimulated luminescence (OSL) detectors. *Radiat. Meas.* 46, 580–587. <https://doi.org/10.1016/j.radmeas.2011.04.013>.

References

- Ahmed, S.N., 2007. *Physics and Engineering of Radiation Detection*. Elsevier, USA.
- Aitken, M.J., 1987. *Thermoluminescence Dating*, 1985, Academic Press, Orlando., Geoarchaeology. <https://doi.org/10.1002/gea.3340020110>
- Akselrod, M.S., Bøtter-Jensen, L., McKeever, S.W.S., 2006. Optically stimulated luminescence and its use in medical dosimetry. *Radiat. Meas.* 41. <https://doi.org/10.1016/J.RADMEAS.2007.01.004>
- Aşlar, E., Meriç, N., Şahiner, E., Erdem, O., Kitis, G., Polymeris, G.S., 2019. A correlation study on the TL, OSL and ESR signals in commercial BeO dosimeters yielding intense transfer effects. *J. Lumin.* 214, 116533. <https://doi.org/10.1016/j.jlumin.2019.116533>
- Aşlar, E., Şahiner, E., Polymeris, G.S., Meriç, N., 2020. Feasibility of determining Entrance Surface Dose (ESD) and mean glandular dose (MGD) using OSL signal from BeO dosimeters in mammography. *Radiat. Phys. Chem.* 177, 109151. <https://doi.org/10.1016/J.RADPHYSHEM.2020.109151>
- Azorin Nieto, J., 2016. Present status and future trends in the development of thermoluminescent materials. *Appl. Radiat. Isot.* 117, 135–142. <https://doi.org/10.1016/j.apradiso.2015.11.111>
- Becker, K., Cheka, J.S., Oberhofer, M., 1970. Thermally Stimulated Exoelectron Emission, Thermoluminescence, and Impurities in LiF and BeO. *Health Phys.* 19, 391–403. <https://doi.org/10.1097/00004032-197009000-00002>
- Berger, G.W., Chen, R., 2011. Error analysis and modelling of double saturating exponential dose response curves from SAR OSL dating. *Ancient TL* 29 (1), 9–14. <https://doi.org/10.26034/la.atl.2011.444>
- Berger, G.W., 2010. Estimating the error in equivalent dose values obtained from SAR. *Ancient TL* 28 (2), 55–66.
- Bilski, P., Gieszczyk, W., Obryk, B., Hodyr, K., 2014. Comparison of commercial thermoluminescent readers regarding high-dose high-temperature measurements. *Radiat. Meas.* 65, 8–13. <https://doi.org/10.1016/j.radmeas.2014.04.020>
- Bos, A.J.J., 2006. Theory of thermoluminescence. *Radiat. Meas.* 41, S45–S56. <https://doi.org/10.1016/j.radmeas.2007.01.003>
- Bos, A.J.J., 2001. High sensitivity thermoluminescence dosimetry. *Nucl. Instruments Methods Phys. Res. Sect. B Beam Interact. with Mater. Atoms* 184, 3–28. [https://doi.org/10.1016/S0168-583X\(01\)00717-0](https://doi.org/10.1016/S0168-583X(01)00717-0)
- Bøtter-Jensen, L., 1997. Luminescence techniques: instrumentation and methods. *Radiat. Meas.* 27, 749–768. [https://doi.org/10.1016/S1350-4487\(97\)00206-0](https://doi.org/10.1016/S1350-4487(97)00206-0)
- Bøtter-Jensen, L., Andersen, C.E., Duller, G.A.T., Murray, A.S., 2003. Developments in radiation, stimulation and observation facilities in luminescence measurements. *Radiat. Meas.* 37, 535–541. [https://doi.org/10.1016/S1350-4487\(03\)00020-9](https://doi.org/10.1016/S1350-4487(03)00020-9)
- Bøtter-Jensen, L., Bulur, E., Duller, G.A., Murray, A., 2000. Advances in luminescence instrument systems. *Radiat. Meas.* 32, 523–528. [https://doi.org/10.1016/S1350-4487\(00\)00039-1](https://doi.org/10.1016/S1350-4487(00)00039-1)
- Broadhead, B., Noble, C., Ramachandran, P., 2022. A direct comparison of the optically stimulated luminescent properties of BeO and Al₂O₃ for clinical in-vivo dosimetry. *Phys. Eng. Sci. Med.* 45, 859–866. <https://doi.org/10.1007/s13246-022-01155-x>

-
- Bulur, E., 1996. An alternative technique for optically stimulated luminescence (OSL) experiment. *Radiat. Meas.* 26, 701–709. [https://doi.org/10.1016/S1350-4487\(97\)82884-3](https://doi.org/10.1016/S1350-4487(97)82884-3)
- Bulur, E., 2007. Photo-transferred luminescence from BeO ceramics. *Radiat. Meas.* 42, 334–340. <https://doi.org/10.1016/j.radmeas.2007.02.065>
- Bulur, E., Göksu, H.Y., 1998. OSL from BeO ceramics: New observations from an old material. *Radiat. Meas.* 29, 639–650. [https://doi.org/10.1016/S1350-4487\(98\)00084-5](https://doi.org/10.1016/S1350-4487(98)00084-5)
- Bulur, E., Saraç, B.E., 2013. Time-resolved OSL studies on BeO ceramics. *Radiat. Meas.* 59, 129–138. <https://doi.org/10.1016/j.radmeas.2013.04.009>
- Bulur, E., Yeltik, A., 2010. Optically stimulated luminescence from BeO ceramics: an LMOSL study. *Radiat. Meas.* 45, 29–34. <https://doi.org/10.1016/j.radmeas.2009.08.007>
- Chen, R., Hornyak, W.F., Mathur, V.K., 1990. Competition between excitation and bleaching of thermoluminescence. *J. Phys. D. Appl. Phys.* 23, 724–728. <https://doi.org/10.1088/0022-3727/23/6/015>
- Cruse, K.W., Gammage, R.B., 1975. Improvements in the Use of Ceramic BeO for TLD. *Health Phys.* 29, 739–746. <https://doi.org/10.1097/00004032-197511000-00014>
- Choi J.H. et al., 2006. Luminescence characteristics of quartz from the Southern Kenyan Rift Valley: dose estimation using LM-OSL SAR. *Radiation Measurements.* <https://doi.org/10.1016/j.radmeas.2006.05.003>
- Dallas, G.I., Polymeris, G.S., Afouxenidis, D., Tsirliganis, N.C., Tsagas, N.F., Kitis, G., 2010. Correlation between TL and OSL signals in KMgF₃:Ce³⁺: bleaching study of individual glow-peaks. In: *Radiation Measurements*. Pergamon, pp. 537–539. <https://doi.org/10.1016/j.radmeas.2009.11.008>
- Dhanekar, S., Rangra, K., 2021. Wearable Dosimeters for Medical and Defence Applications: A State of the Art Review. *Adv. Mater. Technol.* 6, 2000895. <https://doi.org/10.1002/admt.202000895>
- Eduardo G Yukihara, S.W.M., 2011. *Optically stimulated luminescence: fundamentals and applications*. John Wiley & Sons.
- G Scarpa, 1970. The dosimetric use of beryllium oxide as a thermoluminescent material: A preliminary study. *Phys. Med. Biol.* 15, 667–672. <https://doi.org/10.1088/0031-9155/15/4/006>
- Gasparian, P.B.R., Vanhavere, F., Yukihara, E.G., 2012. Evaluating the influence of experimental conditions on the photon energy response of Al₂O₃:C optically stimulated luminescence detectors. *Radiat. Meas.* 47, 243–249. <https://doi.org/10.1016/j.radmeas.2012.01.012>
- Geber-Bergstrand, T. (2017). *Optically Stimulated Luminescence for Retrospective Radiation Dosimetry. The Use of Materials Close to Man in Emergency Situations*. [Doctoral Thesis (compilation), Department of Translational Medicine]. Lund University: Faculty of Medicine. <https://lup.lub.lu.se/search/publication/44effcd5-cae7-4819-9f47-ae5462f1f649>
- Gray, H.J., Mahan, S.A., 2015. Variables and potential models for the bleaching of luminescence signals in fluvial environments. *Quat. Int.* 362, 42–49. <https://doi.org/10.1016/j.quaint.2014.11.007>
- Greiter, M. B., Denk, J., & Hoedlmoser, H. (2016). Secondary standard calibration, measurement and irradiation capabilities of the individual monitoring service at the Helmholtz Zentrum Munchen: aspects of uncertainty and automation. *Radiation Protection Dosimetry*, 1-5.
- Guide to the “Risø TL/OSL reader”, 2013. . DTU Denmark.
- Henaish, B.A., Sayed, A.M., Morsy, S.M., 1979. Light influence on thermoluminescent BeO and other TL-phosphors. *Nuclear Instruments and Methods* 163, 511–517.

[https://doi.org/10.1016/0029-554X\(79\)90140-X](https://doi.org/10.1016/0029-554X(79)90140-X)

- Horowitz, Y.S., 2014. Thermoluminescence dosimetry: State-of-the-art and frontiers of future research. *Radiat. Meas.* 71, 2–7. <https://doi.org/10.1016/j.radmeas.2014.01.002>
- Jahn, A., Sommer, M., Ullrich, W., Wickert, M., Henniger, J., 2013. The BeOmax system – Dosimetry using OSL of BeO for several applications. *Radiat. Meas.* 56, 324–327. <https://doi.org/10.1016/j.radmeas.2013.01.069>
- Kara, E., Woda, C., 2023a. Further characterization of BeO detectors for applications in external and medical dosimetry. *Radiat. Meas.* 165, 106950. <https://doi.org/10.1016/j.radmeas.2023.106950>
- Kara, E., Woda, C., 2023b. Correlation between thermoluminescence and optically stimulated luminescence signal in BeO. *Radiat. Meas.* 107049. <https://doi.org/10.1016/j.radmeas.2023.107049>
- Kittel, C., 2013. *Introduction to Solid State Physics.*, 8th ed. John Wiley & Sons., Hoboken, New Jersey.
- Kitis, G., Vlachos, N.D., 2013. General semi-analytical expressions for TL, OSL and other luminescence stimulation modes derived from the OTOR model using the Lambert W-function. *Radiat. Meas.* 48, 47–54. <https://doi.org/10.1016/j.radmeas.2012.09.006>
- Kouroukla, Eftychia (2015). *Luminescence dosimetry with ceramic materials for application to radiological emergencies and other incidents.*, Durham theses, Durham University. Available at Durham E-Theses Online: <http://etheses.dur.ac.uk/11362/>
- Jahn, A., Sommer, M., Henniger, J., 2014. OSL efficiency for BeO OSL dosimeters. *Radiat. Meas.* 71, 104–107. <https://doi.org/10.1016/J.RADMEAS.2014.03.024>
- Jahn, A., Sommer, M., Ullrich, W., Wickert, M. and Henniger, J. 2013. The BeOmax system- Dosimetry using OSL of BeO for several applications. *Radiat. Meas.*, 56, 324-327.
- Lakshmanan, A., 2008. *Luminescence and display phosphors: phenomena and applications.* Nova Science Pub Inc, New York.
- Lembo, L., Pimpinella, M., Mukherjee, B., 1990. Self optical attenuation coefficient of TL glow in BeO detectors. *Radiat. Protect. Dosim.* 33, 43–45. <https://doi.org/10.1093/oxfordjournals.rpd.a080754>
- Levy, P.W., 1982. Thermoluminescence and optical bleaching in minerals exhibiting second order kinetics and other charge re trapping characteristics.
- Malthez, A.L.M.C., Freitas, M.B., Yoshimura, E.M., Button, V.L.S.N., 2014. Experimental photon energy response of different dosimetric materials for a dual detector system combining thermoluminescence and optically stimulated luminescence. *Radiat. Meas.* 71, 133–138. <https://doi.org/10.1016/J.RADMEAS.2014.07.018>
- Mandeville, C.E., Albrecht, H.O., 1954. Luminescence of Beryllium Oxide. *Phys. Rev.* 94, 494–494. <https://doi.org/10.1103/PhysRev.94.494>
- Markey, B.G., Colyott, L.E., McKeever, S.W.S., 1995. Time-resolved optically stimulated luminescence from α -Al₂O₃:C. *Radiat. Meas.* 24, 457–463. [https://doi.org/10.1016/1350-4487\(94\)00119-L](https://doi.org/10.1016/1350-4487(94)00119-L)
- McKeever, S. W.S., Moscovitch, M., & Townsend, P.D., 1995. *Thermoluminescence dosimetry materials: properties and uses.*
- McKeever, S.W.S., 1997. Luminescence Models. *Radiation Measurements*, 625-661.
- McKeever, S.W.S., 1994. Models for optical bleaching of thermoluminescence in sediments.

-
- Radiat. Meas. 23, 267–275. [https://doi.org/10.1016/1350-4487\(94\)90051-5](https://doi.org/10.1016/1350-4487(94)90051-5)
- McKeever, S.W.S., 2002. New millenium frontiers OF of luminescence Dosimetry. Radiat. Prot. Dosimetry 100, 27–32.
- McKeever, S.W.S., 2004. Recent advances in dosimetry using the optically stimulated luminescence of Al₂O₃:C. Radiat. Prot. Dosimetry 109, 269–276. <https://doi.org/10.1093/rpd/nch302>
- McKeever, S.W.S., 2001. Optically stimulated luminescence dosimetry. Nucl. Instruments Methods Phys. Res. Sect. B Beam Interact. with Mater. Atoms 184, 29–54. [https://doi.org/10.1016/S0168-583X\(01\)00588-2](https://doi.org/10.1016/S0168-583X(01)00588-2)
- McKeever, S.W.S., 1985. Thermoluminescence of Solids. Cambridge University Press. <https://doi.org/10.1017/CBO9780511564994>
- McKeever, S.W.S., Akselrod, M.S., 1999. Radiation Dosimetry using Pulsed Optically Stimulated Luminescence of Al₂O₃:C. Radiat. Prot. Dosimetry 84, 317–320. <https://doi.org/10.1093/oxfordjournals.rpd.a032746>
- McKeever, S.W.S., Chen, R., 1997. Luminescence models. Radiat. Meas. 27, 625–661. [https://doi.org/10.1016/S1350-4487\(97\)00203-5](https://doi.org/10.1016/S1350-4487(97)00203-5)
- McKinlay, A.F., 1981. Thermoluminescence dosimetry. United Kingdom.
- Mrčela, I., Bokulić, T., Izewska, J., Budanec, M., Fröbe, A., & Kusić, Z. (2011). Optically stimulated luminescence in vivo dosimetry for radiotherapy: physical characterization and clinical measurements in (60) Co beams. Physics in medicine and biology, 56(18), 6065–6082. <https://doi.org/10.1088/0031-9155/56/18/018>
- Mukherjee, B., 2015. LiBe-14: A novel microdosimeter using LiF and BeO thermoluminescence dosimeter pairs for clinical and aerospace applications. Radiat. Meas. 72, 31–38. <https://doi.org/10.1016/j.radmeas.2014.11.003>
- Murthy, K.V.R., 2013. Thermoluminescence and its Applications: A Review. Defect Diffus. Forum 347, 35–73. <https://doi.org/10.4028/www.scientific.net/DDF.347.35>
- Nasdala, L., Götze, J., Hanchar, J.M., Gaft, M., Krbetschek, M.R., n.d. Luminescence techniques in Earth Sciences, in: Spectroscopic Methods in Mineralogy. Mineralogical Society of Great Britain and Ireland, Germany, pp. 43–91. <https://doi.org/10.1180/EMU-notes.6.2>
- Nikiforov, S.V., Pagonis, V., Merezhnikov, A.S., 2017. Sublinear dose dependence of thermoluminescence as a result of competition between electron and hole trapping centers. Radiat. Meas. 105, 54–61.
- Olko, P., 2010. Advantages and disadvantages of luminescence dosimetry. Radiat. Meas. 45, 506–511. <https://doi.org/10.1016/j.radmeas.2010.01.016>
- Pagonis, V., Kitis, G., Chen, R., 2020. A new analytical equation for the dose response of dosimetric materials, based on the Lambert W function. J. Lumin. 225, 117333. <https://doi.org/10.1016/j.jlumin.2020.117333>.
- Perks, C.A., Roy, G.L., Prugnaud, B., 2006. Introduction of the InLight monitoring service. Radiat. Prot. Dosimetry 125, 220–223. <https://doi.org/10.1093/rpd/ncl126>
- Polymeris, G.S., Çoskun, S., Tsoutsoumanos, E., Konstantinidis, P., Aşlar, E., Şahiner, E., Meriç, N., Kitis, G., 2021. Dose response features of quenched and reconstructed, TL and deconvolved OSL signals in BeO. Results Phys. 25, 104222. <https://doi.org/10.1016/j.rinp.2021.104222>
- Randall, J. T. and Wilkins, M. H. F., 1945. Phosphorescence and electron traps I. The study of

-
- trap distributions. *Proc. Roy. Soc. London*.
- Randall, J.T. and Wilkins, M.H.F. 1945b. Phosphorescence and electron traps: II. The interpretation of long-period phosphorescence. *Proc. R. Soc. London A* , 184, 390–407.
- Reft, C. S., 2009. The energy dependence and dose response of a commercial optically stimulated luminescent detector for kilovoltage photon, megavoltage photon, and electron, proton, and carbon beams. *Med. Phys.* 36, 5. <https://doi.org/10.1118/1.3097283>
- Rhyner, C.R., Miller, W.G., 1970. Radiation dosimetry by optically-stimulated luminescence of BeO. *Health Phys.* 18, 681–684. <https://doi.org/10.1097/00004032-197006000-00010>.
- Rivera-Montalvo, T., 2016. Diagnostic radiology dosimetry: Status and trends. *Appl. Radiat. Isot.* 117, 74–81. <https://doi.org/10.1016/j.apradiso.2016.03.008>
- Rivera, T., 2012. Thermoluminescence in medical dosimetry. *Appl. Radiat. Isot.* 71, 30–34. <https://doi.org/10.1016/J.APRADISO.2012.04.018>
- Rodriguez, M., Yukihiro, E., Ahmad, S., Ruan, C., 2012. MO-F-213CD-04: Characterization of Optically Stimulated Luminescence Detectors for Organ Dose Phantom Measurement in Diagnostic Radiology. *Med. Phys.* 39, 3877–3877. <https://doi.org/10.1118/1.4735829>
- Santos, A.M.C., Mohammadi, M., Afshar V., S., 2015. Evaluation of a real-time BeO ceramic fiber-coupled luminescence dosimetry system for dose verification of high dose rate brachytherapy. *Med. Phys.* 42, 6349–6356. <https://doi.org/10.1118/1.4931968>
- Scarpa, G. 1970. The dosimetric use of beryllium oxide as a thermoluminescent material: a preliminary study. *Phys. Med. Biol.*, 15, 667-672
- Sohbati, R., Murray, A., Jain, M., Buylaert, J.-P., Thomsen, K., 2011. Investigating the resetting of OSL signals in rock surfaces. *Geochronometria* 38, 249–258. <https://doi.org/10.2478/s13386-011-0029-2>.
- Sommer, M., Freudenberg, R., Henniger, J., 2007. New aspects of a BeO-based optically stimulated luminescence dosimeter. *Radiat. Meas.* 42, 617–620. <https://doi.org/10.1016/j.radmeas.2007.01.052>
- Sommer, M., Henniger, J., 2006. Investigation of a BeO-based optically stimulated luminescence dosimeter. *Radiat. Prot. Dosimetry* 119, 394–397. <https://doi.org/10.1093/rpd/nci626>
- Sommer, M., Jahn, A., Henniger, J., 2008. Beryllium oxide as optically stimulated luminescence dosimeter. *Radiat. Meas.* 43, 353–356. <https://doi.org/10.1016/j.radmeas.2007.11.018>
- Souza, L.F., Novais, A.L.F., Antonio, P.L., Caldas, L.V.E., Souza, D.N., 2019. Luminescent properties of MgB₄O₇:Ce,Li to be applied in radiation dosimetry. *Radiat. Phys. Chem.* 164, 108353 <https://doi.org/10.1016/j.radphyschem.2019.108353>.
- Stabin, M.G., 2007. *Radiation Protection and Dosimetry: An Introduction to Health Physics*. Springer, Germany.
- Stoneham, M., 2001. *Theories of defects in solids*. Oxford Classic Texts in the Physical Science
- Sunta, C.M., Ayta, W.E.F., Kulkarni, R.N., PETERS, T.M., Watanabe, S., 1997. General-order kinetics of thermoluminescence and its physical meaning. *J. Phys. D. Appl. Phys.* 30, 1234–1242. <https://doi.org/10.1088/0022-3727/30/8/013>
- Şahin, S., Güneş Tanir, A., Meriç, N., Aydinkarahalıoğlu, E., 2015. Measurement of radiation dose with BeO dosimeters using optically stimulated luminescence technique in radiotherapy applications. *Appl. Radiat. Isot.* 103, 31–36. <https://doi.org/10.1016/J.APRADISO.2015.05.013>

-
- Şahin, S., Şahiner, E., Göksel, F., Meriç, N., 2020. Comprehensive evaluation of electron radiation dose using beryllium oxide dosimeters at breast radiotherapy. *J. Radiother. Pract.* 19, 38–44. <https://doi.org/10.1017/S1460396919000190>
- Tochilin, E., Goldstein, N., Miller, W.G., 1969. Beryllium Oxide As a Thermoluminescent Dosimeter. *Health Phys.* 16, 1–7. <https://doi.org/10.1097/00004032-196901000-00001>
- Thomsen, K. J. (2004). Optically Stimulated Luminescence Techniques in Retrospective Dosimetry using Single Grains of Quartz extracted from Unheated Materials [Doctoral thesis, Risø National Laboratory, Roskilde Denmark]. Risø National Laboratory. <https://vdocuments.mx/documents/kristina-jorkov-thomsen-optically-stimulated-luminescence-techniques.html>
- Trindade N.M., Kahn H., Yoshimura E. M., 2018. Thermoluminescence of natural BeAl₂O₄:Cr³⁺ Brazilian mineral: Preliminary studies. *J. Lumin.* 195, 356. <https://doi.org/10.1016/j.jlumin.2017.11.057>
- Altunal V. et al., 2022. Three newly developed BeO-based OSL dosimeters. *J. Lumin.* <https://doi.org/10.1016/j.jlumin.2021.118528>
- W. S. McKeever, S., 2002. New Millennium Frontiers of Luminescence Dosimetry. *Radiat. Prot. Dosimetry* 100, 27–32. <https://doi.org/10.1093/oxfordjournals.rpd.a005865>
- W. S. McKeever, S., Moscovitch, M., 2003. Topics under Debate - On the advantages and disadvantages of optically stimulated luminescence dosimetry and thermoluminescence dosimetry. *Radiat. Prot. Dosimetry* 104, 263–270. <https://doi.org/10.1093/oxfordjournals.rpd.a006191>
- Watanabe, S., Gundu Rao, T.K., Page, P.S., Bhatt, B.C., 2010. TL, OSL and ESR studies on beryllium oxide. *J. Lumin.* 130, 2146–2152. <https://doi.org/10.1016/j.jlumin.2010.06.009>
- Yagui, A., Malthez, A.L.M.C., Filipov, D., 2020. Dose evaluation in pediatric gastrointestinal fluoroscopy. *Radiat. Phys. Chem.* 167, 108384. <https://doi.org/10.1016/J.RADPHYSICHEM.2019.108384>
- Yukihara, E.G., Andrade, A.B., Eller, S., 2016. BeO optically stimulated luminescence dosimetry using automated research readers. *Radiat. Meas.* 94, 27–34. <https://doi.org/10.1016/j.radmeas.2016.08.008>
- Yukihara, E.G., Gasparian, P.B.R., Sawakuchi, G.O., Ruan, C., Ahmad, S., Kalavagunta, C., Clouse, W.J., Sahoo, N., Titt, U., 2010. Medical applications of optically stimulated luminescence dosimeters (OSLDs). *Radiat. Meas.* 45, 658–662. <https://doi.org/10.1016/J.RADMEAS.2009.12.034>
- Yukihara, E.G., 2020. A review on the OSL of BeO in light of recent discoveries: the missing piece of the puzzle? *Radiat. Meas.* 134, 106291 <https://doi.org/10.1016/j.radmeas.2020.106291>.
- Yukihara, E.G., 2011. Luminescence properties of BeO optically stimulated luminescence (OSL) detectors. *Radiat. Meas.* 46, 580–587. <https://doi.org/10.1016/j.radmeas.2011.04.013>.
- Yukihara, E.G., 2019. Observation of strong thermally transferred optically stimulated luminescence (TT-OSL) in BeO. *Radiat. Meas.* 121, 103–108. <https://doi.org/10.1016/j.radmeas.2018.12.014>.
- Yukihara, E.G., McKeever, S.W.S., 2008. Optically stimulated luminescence (OSL) dosimetry in medicine. *Phys. Med. Biol.* 53, R351–R379. <https://doi.org/10.1088/0031-9155/53/20/R01>
- Yukihara, E.G., McKeever, S.W.S., (2011). Optically stimulated luminescence Fundamentals and

applications. John Wiley & Sons, Ltd.

Yukihara, E.G., McKeever, S.W.S., Akselrod, M.S., 2014. State of art: Optically stimulated luminescence dosimetry – Frontiers of future research. *Radiat. Meas.* 71, 15–24. <https://doi.org/10.1016/j.radmeas.2014.03.023>

Yukihara, E.G., Kron, T., 2020. Applications of optically stimulated in medical dosimetry. *Radiat. Prot. Dosimetry* 192, 122–138. <https://doi.org/10.1093/rpd/ncaa213>

Zhang C. X., Tang Q., Lin L. B., Luo D. L., Thermoluminescence glow curves and optical stimulated luminescence of undoped α -Al₂O₃ crystals, *Radiation Protection Dosimetry*, Volume 119, Issue 1-4, September 2006, Pages 402–407, <https://doi.org/10.1093/rpd/nci579>

Appendix A: CT application

Pediatric patients are more sensitive to the harmful effects of ionizing radiation compared to adults. Due to their highly proliferating cells and longer remaining life expectancy children have a higher risk of developing cancer following radiation exposure. As for adults it is, thus, necessary to calculate and track the radiation dose delivered to children undergoing medical examinations. Both LiF:Mg,Ti TLDs and BeO OSLDs are passive dosimeters and applicable candidates for dose measurement in medical applications due to their tissue equivalence, small size, high sensitivity, and commercial availability (Bos, 2001; Malthez et al., 2014). In this study, the radiation dose delivered to a pediatric anthropomorphic phantom representing a one-year-old in a Computed Tomography (CT) examination was measured, using these dosimeters placed in the phantom's organs.

Materials and Methods

Calibration and CT irradiations were conducted at the Federal Office for Radiation Protection (BfS), with luminescence readings performed at Helmholtz Zentrum Munich, both situated in Neuherberg, Germany.

Thermoluminescence Dosimeter (LiF:Mg,Ti)

For the TLD measurements of the phantom's organs, the rod type TLDs (TLD-100, Thermo Fischer Scientific, Waltham, Massachusetts, USA) were used with the dimensions of 1 x 1 x 6 mm. Table 1 shows reading protocols for TL and OSL dosimeters.

Optically Stimulated Luminescence Dosimeter (BeO)

Commercially available disk-shaped BeO ceramics (Thermalox TM 995, Brush Wellman Inc., USA) with a diameter of 4 mm and a thickness of ~0.5 mm was used in this study. A total number of 150 BeO dosimeters randomly selected from the same batch were used.

Table 1. The OSL and TL readout protocol for BeO OSLDs and LiF:Mg,Ti TLDs.

Protocol	BeO	LiF:Mg,Ti
Annealing	700 °C for 5 min	400 °C for 20 min
<i>Irradiation CT</i>		
Preheating	160 °C for 10 s	100°C for 10 min
Luminescence Reading	300 s Optical stimulation	Up to 350°C Thermal stimulation

Calibration of Dosimeters

To ensure accurate calibration, each type dosimeters underwent individual calibration by irradiation using an X-ray tube (COMET AG, Flamatt, Switzerland) with the same radiation qualities employed in the experiments. The calibration dose (dose in water, *DW*) was determined using a stem chamber (M2331, PTW, Freiburg, Germany) and an electrometer (UNIDOS E, PTW, Freiburg, Germany). Prior to irradiation, corrections for temperature and pressure were applied to the chamber, along with a radiation quality correction of the measured dose using the chamber's radiation quality correction term (*k_q*), which was interpolated for the specific tube voltages

required. The calibration measurement followed the same readout protocol as the experimental measurement at the CT scanner.

The CT Application

Irradiations were performed at BfS in Neuherberg, Germany with a CT scanner (Brightspeed 16, GE Healthcare, Milwaukee, Wisconsin, USA). Table 2 shows the scan parameters. This procedure was repeated three times.

Table 2. Scan parameters for CT irradiations.

CT data	
CTDIvol [mGy]	9.64
Tube current [mA]	300
Voltage [kV]	100
Slice thickness [mm]	1.25

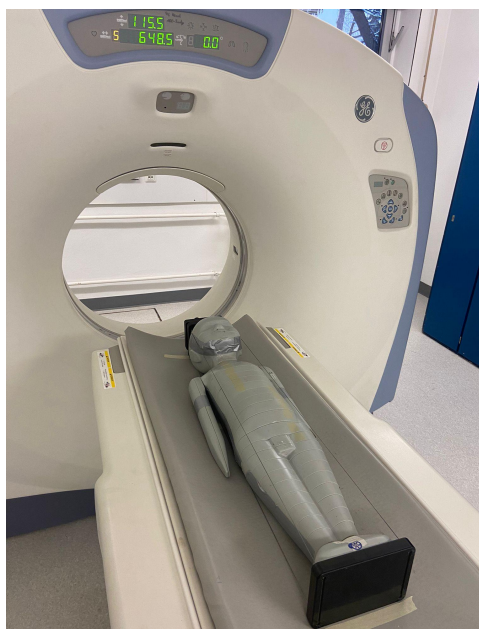


Figure 1. Irradiation set-up at the Federal Office for Radiation Protection (BfS) and the pediatric anthropomorphic phantom of one-year-old ATOM/CIRS.

ATOM Phantom (1 year)

A reference anthropomorphic pediatric phantom (ATOM® Phantom Family, SUN NUCLEAR, Norfolk, Virginia, USA) corresponding to the body of a one-year-old infant was used. It is composed of tissue-equivalent materials and consists of 28 slices with 2.5 cm in thickness. These slides contain holes (\varnothing 5 mm) in different anatomical regions, allowing for the positioning of dosimeters such as OSLDs to measure organ doses. Irradiation set-up and a slice of the pediatric anthropomorphic phantom can be seen in Figure 1 and 2, respectively.

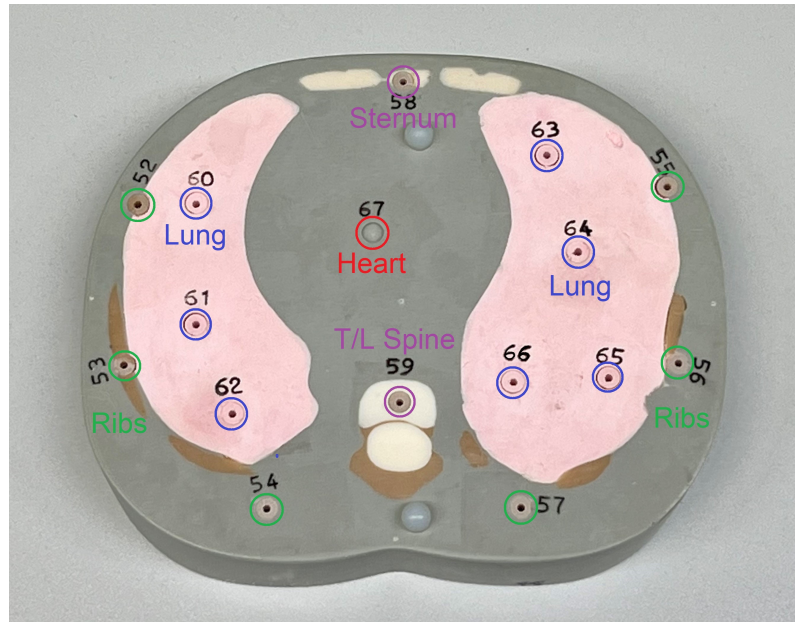


Figure 2. A slice (11) of the ATOM phantom available at the Federal Office for Radiation Protection (BfS) with the locations of the associated organs.

Previous studies (Crane and Gammage, 1975; Henaish et al., 1979; Yukihiro et al., 2016) have noted that BeO dosimeters are sensitive to light. Therefore, dosimeters were protected from light during the calibration, phantom irradiations, and reading processes to ensure accurate measurements. Markers were used to ensure reproducibility of the phantom's position.

Results

Organ Dose Measurements

The absorbed organ doses shown in Table 3 represent average values with the corresponding standard deviations. Given results are the average of three irradiations with the standard deviation. The thyroid, located within the examination field, received the highest absorbed organ doses recorded at 30.8 mGy and 28.8 mGy for LiF:Mg,Ti TLDs and BeO OSLDs, respectively. Conversely, the brain demonstrated the lowest dose among all organs, with measurements of 19.5 mGy and 18.5 mGy using LiF:Mg,Ti TLDs and BeO OSLDs, respectively. The agreement within the measured organ doses by LiF:Mg,Ti TL and BeO OSL dosimeters ranged widely from ~1.2 % to ~6.9 %. The mean standard deviation for all measured organ doses using LiF:Mg,Ti TL, and BeO OSL dosimeters were within $\pm 4\%$, except for the lungs. For lung doses measured using BeO dosimeters, the standard deviation was $\pm 5.2\%$, with a recorded dose of 24.2 ± 1.3 mGy.

Table 3. Measured organ doses for one-year-old phantom exposed to CT scan. Results are the mean values and standard deviations for measured organ doses by OSLDs within each organ. Results on LiF:Mg,Ti (TLD): Iris Wölvitsch, BfS, private communication.

Organ	LiF:Mg,Ti (TLD)	BeO (OSL)	Difference	Number of TLDs or OSLDs	Slice Number
	mGy	mGy	%		
Brain	19,5 ± 0,6	18,5 ± 0,6	-5,1	9	2, 3, 4
Bone surface	19,6 ± 0,6	20,5 ± 0,5	4,6	54	4, 6-13**, 15, 17-20, 22, 23, 25, 28
Uterus	22,6 ± 0,7	21,9 ± 0,4	-3,1	1	17
Salvary glands	22,7 ± 0,7	22,0 ± 0,6	-3,1	3	3,6
Oral mucosa	22,7 ± 0,7	22,0 ± 0,6	-3,2	3	6
RBM	22,3 ± 0,7	21,1 ± 0,5	-5,4	49	4, 6-13, 15, 17-20, 25, 28
Adrenals	21,3 ± 0,7	22,5 ± 0,4	5,6	2	13
Kidney	22,2 ± 0,7	23,2 ± 0,8	4,5	8	14, 15
Urinary bladder	25,0 ± 0,8	24,3 ± 0,7	-2,8	6	18, 19
Pancreas	25,1 ± 0,8	24,8 ± 0,5	-1,2	3	13
Colon	25,3 ± 0,8	24,3 ± 0,9	-4	12	15-18
Liver	25,3 ± 0,8	24,4 ± 0,7	-3,5	12	15-18
Small intestine	25,3 ± 0,8	24,3 ± 0,9	-3,9	7	13-15
Spleen	24,6 ± 0,8	25,3 ± 0,5	2,8	4	13, 14
Gallbladder	24,0 ± 0,8	22,9 ± 0,1	-4,6	2	14, 15
Gonades	26,1 ± 0,8	25,4 ± 0,8	-2,7	4	17, 20
Oesophagus	26,2 ± 0,8	25,6 ± 0,3	-2,3	3	8, 10, 12
Stomach	25,3 ± 0,8	23,6 ± 0,6	-6,7	5	12, 13
Lung	26,0 ± 0,8	24,2 ± 1,3	-6,9	23	9,12
Heart	23,2 ± 0,8	22,3 ± 0,3	-3,9	2	10, 11
Thymus	27,5 ± 0,8	26,4 ± 0,6	-4	2	9
Prostate	24,5 ± 0,8	24,0 ± 0,2	-2	1	19
Endothelin	26,7 ± 0,8	25,9 ± 0,5	-3	6	6,8
Breast	28,5 ± 0,9	27,1 ± 0,2	-4,9	2	10
Thyroid	30,8 ± 1	28,8 ± 0,5	-6,5	2	7

*RBM indicates the red bone marrow.

** The "-" symbol between the numbers indicates the specified phantom slices and the other slice(s) that lies between these.

Conclusion

Absorbed organ doses were determined using tissue equivalent BeO OSL and LiF:Mg,Ti TL dosimeters, after a total body scan in a one-year-old pediatric phantom. The consistency of the irradiation protocol and the phantom and dosimeter placement enabled reliable comparisons between the absorbed dose measurements from each exposure. Although the results of BeO OSLDs are compatible with those of LiF:Mg,Ti TLDs, the TLDs tended to yield higher dose values than OSLDs in most organs. The thyroid received the highest absorbed organ doses of 30.8 mGy and 28.8 mGy for while the brain exhibited the lowest dose among all organs, measuring 19.5 mGy and 18.5 mGy with LiF:Mg,Ti TLDs and BeO OSLDs, respectively. The observed discrepancy in the dose measurements between the two types of dosimeters can be attributed to the energy dependence of these dosimeters, given that a typical CT spectrum encompasses a range of photon energies. The calculated organ doses exhibited varying uncertainties. These variations in standard deviations could be attributed to multiple factors, including the number of dosimeters per organ, dosimeter impurities, and the depth of the dosimeter position from the phantom surface.

These results indicate that BeO OSLDs are compatible in medical applications. Additional research is required to comprehensively examine the energy dependence demonstrated by both types of dosimeters in different clinical settings in order to account for variations in dose measurements between these dosimeters.

Acknowledgements

I am really excited to be about to get a PhD degree at LMU from the same university as Max Planck, who is my favorite physicist for his intelligence and most of all for his human personality.

I would like to express my gratitude to Prof. Dr. Werner Ruehm who contributed significantly to my Ph.D. journey as a role model for a young Ph.D. student with his precious presence and analytical approach.

I experienced that even in the international academic environment in a civilized European country, unfortunately, not everything can be perfect. I would like to thank Dr. Amudha Brugger and Dr. Melanie Waldenberger for ensuring more equal and safer working conditions.

Many thanks to colleagues from The Federal Office for Radiation Protection (BfS), Dr. Helmut Schlatt and Iris Wölwitsch, for letting me conduct a CT study and making it possible for me to do research there.

I would like to express my gratitude to Prof. Dr. Siamak Haghdooost and Prof. Dr. Pr. Jacques Balosso for proton therapy courses at the University of Caen Normandy. Their expertise and dedication have not only enriched my understanding but have also left an indelible mark on my academic journey. I would like to express my deepest appreciation for the radiation biology meetings and his support to young researchers to Dr. Omid Azimzadeh.

I wish to express my sincere gratitude to Dr. Smith Drupa and Dr. Jillian Newmyer from the Health Physics Society of America (HPS) for awarding me the scholarship to attend the HPS 2022 and 2023. Their support has been invaluable to my academic and professional development. I would also like to extend my heartfelt thanks to my friends Ridhita, Emmanuel, Dimitri, and Andrew for their friendship and encouragement throughout this journey.

My doctorate was completed through courses offered by the Helmholtz Zentrum München and with great coffee breaks with my colleagues Zeynep, Suhayra, Alvaro and Nicholas. I owe special thanks to Niko and Isabel for being an extremely understanding and supportive roommates. And all my friends in Munich for making my life here so colourful especially Anna, Despina, Hjørdis, Louie, and Miriam.

A special thank you to my valuable friend Umut. Your support has been a cornerstone of my success, and I am profoundly grateful.

Türkiye Cumhuriyeti Milli Eğitim Bakanlığı'na yurt dışı lisansüstü eğitim bursu için ve Münih ile Berlin Eğitim ataşeliklerine teşekkür ederim.

I have embraced and incorporated his principles, diligent work ethic, and profound love for our country into every aspect of my life. The Founder of the Republic of Türkiye is the hope of endless hope, love, intelligence, freedom, virtue, courage, determination, hard work, resistance, science and Mustafa Kemal Atatürk is the name of art.

Sen hiç eğilmediğin için biz halen dik durabiliyoruz.

With endless love, endless respect, and endless gratitude...

Curriculum vitae

Elif Kara

Publications

1. Kara, E., Woda, C., Correlation between thermoluminescence and optically stimulated luminescence signal in BeO, 2023, Radiation Measurements.
2. Kara, E., Woda, C., Further characterization of BeO detectors for applications in external and medical dosimetry, 2023, Radiation Measurements.
3. Kara, E., Kayahan E., Optical System Design of Thermal Imaging Camera in MWIR Band (3-5 μ m), 2017, Acta Materialia.

In preparation

- Wöhlwitsch I., Kara E., Schlatt H., A one-year-old anthropomorphic phantom organ dose assessment using LiF: Mg, Ti TLDs and BeO OSLDs in computed tomography.
- Woda C., Kara E., Thermoluminescence and optically stimulated luminescence spectrums of BeO.

Conferences Contributions

- Further characterization of BeO detectors for applications in external and medical dosimetry. Elif Kara, Clemens Woda, The Health Physics Society (HPS), Spokane, USA, 2022.
- A one-year-old anthropomorphic phantom organ dose assessment using BeO OSLDs in computed tomography. Elif Kara, Clemens Woda, The Health Physics Society (HPS), Maryland, USA, 2023.
- Correlation between Thermoluminescence and Optically Stimulated Luminescence in BeO. Elif Kara, Clemens Woda, The International Symposium on the System of Radiological Protection (ICRP), Tokyo, Japan, 2023.
- Enhancing the efficiency of Optically Stimulated Luminescence readers through optical design, Elif Kara, The Health Physics Society (HPS), Florida, USA, 2024.
- Dose Re-Estimation in Total-Body Computed Tomography (CT) Scans: A Comparison of TT-OSL and PTTL Techniques with BeO OSL Dosimeters. Elif Kara, The Health Physics Society (HPS), Florida, USA, 2024.